Metallosupramolecular studies of the ambivergent ligand N-(2-pyridyl)-4-amino-4-oxobutanoic acid.

A thesis submitted in partial fulfilment of the requirements for the degree of Masters of Science in Chemistry.

Mark Ewen Russell

University of Canterbury

2012

Table of Contents

Acknowledgements

First and foremost I would like to express my deepest gratitude to my supervisor Associate Professor Paul Kruger for being enthusiastic with great ideas and being supportive throughout my masters project. I cannot express my thanks enough to Dr Chris Hawes, Dr Matt Polson, Dr Chris Fitchett and other members of the department for the extreme effort they have put in to supporting me through this project and to Matt especially for all the work he put in to helping with my crystal structures and any other problem that arose throughout the past two years. I would like to thank Dr Marie Squire for her prowess with NMR and mass spectrometry as well as listening to me and supporting me when I needed it. Also thank you to Dr Meike Holzenkaempfer for all the mass spectrometry she has done for me throughout the past couple of months. To the guys at Monash University, Boujemaa Moubaraki, Professor Keith Murray and Nicholas Chilton, who did the magnetic characterisations of the clusters, thank you very much for your help and ingeniousness. Thanks to the Kruger group, past and present, especially Alan and Rosanna for all of your expertise and advice throughout the write up and experiment process of the project as well as the 832 office mates, past and present. I also would like to express my thanks to Alan for the proof reading and advice on magnetism he has given to me. I would also like to acknowledge the Fitchett and Steel groups for all their support, particularly Jayne and Robbie, and the Fez group for allowing me to work in their lab and Andrew for the organic chemistry advice.

To my family, Mum, Dad, Ian, Nana and Melissa, thank you for all the support you guys have given to me throughout the past three years. To all my friends in Melbourne and around New Zealand, with special mention to Ayla and Harriet, thank you so much for all the long conversations and support and keeping me on the right track throughout the project and writing process. Last but not least I cannot thank my best friend, Emma, enough for all of her support throughout the past three years and constantly believing in me and giving me many a pep talk to help me finish my masters.

Abbreviations:

NMR: Nuclear Magnetic Resonance

COSY: Correlation Spectroscopy

IR: Infrared

MP: Melting Point

ESMS: Electrospray Mass Spectrometry

MOF: Metal Organic Framework

TGA: Thermogravimetric Analysis

EPR: Electron Paramagnetic Resonance

IR: Infrared

Infrared Abbreviations:

S: Strong

M: Medium,

W: Weak

Br: Broad

Atom colour scheme:

Black: Carbon

White: Hydrogen

Red: Oxygen

Light Blue: Nitrogen

Green: Chlorine

Dark Blue: Cobalt

Gold: Copper

Dark Yellow: Iron

Light Green: Nickel

Abstract

Eight mononuclear complexes were prepared from the N-(2-pyridyl)-4-amino-4-oxobutanoic acid (**H_2L1**) ligand. **H_2L1** chelated to cobalt(II), nickel(II) and copper(II) through the pyridine and amido nitrogen atoms while the carboxylic acids did not coordinate. 1D and 3D hydrogen bonding networks were formed through interactions between non coordinated solvent molecules and anions within the crystal lattices along with carboxylic acid interaction to the metal centres.

One 1D and two 2D coordination polymers were formed with cobalt(II) and nickel(II) under solvothermal conditions. The **H_2L1** ligand again chelated to the metal ions through the same mode seen in the mononuclear complexes. The two 2D coordination polymers were isostructural to each other and were formed with cobalt(II) and nickel(II). The carboxylate functional groups formed from the deprotonation of the carboxylic acids on the **H_2L1** ligand bridged two symmetry equivalent metal ions forming a [4,4] 2D coordination polymer.

Multinuclear discrete complexes were formed with **H_2L1** and cobalt(II), copper(II) and iron(II/III) metal ions. An octanuclear cobalt metal cluster formed through slow evaporation of copper perchlorate, **H_2L1** in a methanol solution and the addition of triethylamine to deprotonate the carboxylic acid groups. A pentanuclear iron metal cluster with two Fe(II) centres and three Fe(II) centres was also prepared. Within this metal cluster an iron carboxylate triangle motif formed between the three Fe(II) centres with a bridging μ_3-O at the centre. The **H_2L1** ligand coordinated to the metal ions through the pyridine nitrogen and amido oxygen atoms along with the carboxylate oxygen atoms. Magnetic characterisation of both metal clusters showed dominant antiferromagnetic interactions. A hexanuclear Cu(II) metal cluster was prepared using the **H_2L1** ligand and copper acetate. An *in situ* oxidation of the α methylene carbon adjacent to the amide functional group in the **H_2L1** ligand formed **H_2L1A**. The hexanuclear complex has four square pyramidal Cu(II) ions and two square planar Cu(II) ions. Chelation to the Cu(II) centres occurred through the pyridine and amido nitrogen atoms which was not seen in any other complexes prepared in the study. The carboxylate groups bridged two Cu(II) ions. Magnetic characterisation of the metal cluster showed dominant ferromagnetic interactions between the Cu(II) metal centres.

Chapter 1

Introduction

1.1 *Preamble and scope.*

The basis for this project was to investigate the coordination chemistry of the 2-(N-pyridyl)-4-amino)-4-oxobutanic acid, 3-(N-pyridyl)-4-amino)-4-oxobutanic acid and 4-(N-pyridyl)-4-amino)-4-oxobutanic acid ligands to transition metal ions from the 1st row to prepare supramolecular complexes. The ligand has key motifs such as the 2-pyridyl-amido and carboxylate groups that have been shown in the literature to coordinate to metal ions. Key complexes were targeted during the research study which included: discrete mononuclear complexes, polynuclear metal cluster complexes and coordination polymers. Studies of the structures, intermolecular interactions and magnetic properties for these complexes were to be investigated.

A brief overview of pertinent supramolecular chemistry is described below. Due to the enormous magnitude of supramolecular, it is not possible to do justice to all of the significant results or all of the key supramolecular chemists in the area. However, core areas of the subject are covered briefly and specific examples for supramolecular molecules, polynuclear discrete complexes, coordination polymers and metal clusters will be described to provide scope to the present study.

Supramolecular chemistry deals with the study of weak interactions between molecules. These interactions may include hydrogen bonds, π–π stacking interactions, halogen bonding, cation–π interactions, metal–metal interactions and van der Waal forces. These forces aid synthesis of large supramolecular complexes that have specific properties which lead to a range of potential applications. Again due to the size of the subject area there is no way to do it justice to it in this thesis. For anyone unfamiliar with the subject area there exists numerous resources which outline the area of supramolecular chemistry in great detail.[1-3]

1.2 *Supramolecular and metallosupramolecular chemistry.*

Supramolecular chemistry is the study of the intermolecular bond or the chemistry of non-covalent interactions[1], as described by Lehn. This type of chemistry looks into the forces which attract or repel two chemical species together.[1] In molecular chemistry the covalent bond is key, whereas here weaker intermolecular reactions will be discussed and are involved with the formation of supramolecules from smaller chemical species.[1] The field of supramolecular chemistry and the intermolecular interactions can span many disciplines including biological processes; where proteins or enzymes recognise substrates though receptors that bind them through intermolecular forces.[2] From this supramolecules can be designed to recognise particular substrates and bind to them through intermolecular bonds. The principle of supramolecular chemistry is not to build a molecule one atom at a time but to combine structures so they self assemble into supramolecular structures.[3-4]

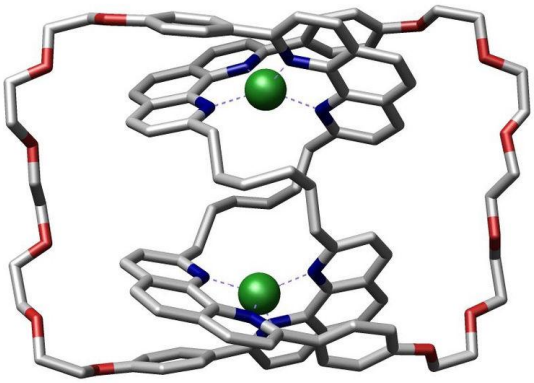

Figure 1.1 *A molecular trefoil knot*[5] *reported by Sauvage.*[6]

Figure 1.1 shows a molecular trefoil knot reported by Sauvage in 1989. Two Cu(I) ions are used to template the molecular trefoil knot and are coordinated to four nitrogen atoms on two ligands.[6] Coordination bonds are also considered part of supramolecular chemistry and give rise to metallosupramolecular chemistry.[3]

1.3 *Metallosupramolecular chemistry.*

In addition to the intermolecular interactions bringing chemical species together into larger supramolecules, coordination bonds between metal ions and ligands can also be involved.[3, 7] When the coordination bond between a metal ion and a ligand is involved in the formation of supramolecules the term metallosupramolecular chemistry is used.[3] Usually transition metal ions are used in metallosupramolecular chemistry.[7] Transition metals have the information required to direct self assembly built into them depending on the metal ion.[7] Particular geometries are formed when certain transition metal ions are used, such as Zn(II) and Cu(I) ions which form tetrahedral and square planar geometries. Co(II), Ni(II) and Fe(II) or Fe(III) may assume octahedral geometries. However, many geometries exist and are shown in Figure 1.2 and a formed by numerous transition metal ions.

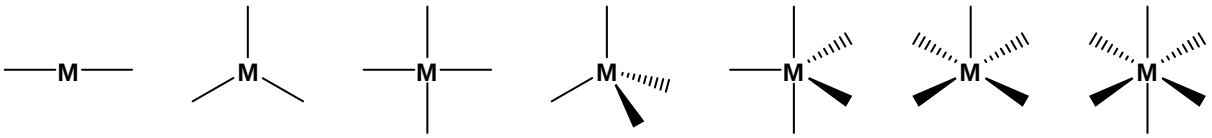

Figure 1.2 *Commonly encountered geometries of transition metal ion complexes. From left to right; linear, trigonal planar, square planar, tetrahderal, trigonal bipyramidal, square pyramidal and octahedral.*

In order to form metallosupramolecular assemblies from these transition metal ion geometries all that is needed are ligands to coordinate to them. These can be divergent ligands to give coordination polymers or convergent ligands to give discrete metallosupramolecules.[3] These ligands

possess hetero atoms such as oxygen atoms and nitrogen atoms which readily form coordination bonds with transition metal ions. With this information programmed into the metal ions and ligands, spontaneous self assembly can occur.[7] The terms synthon and tecton can be used to describe coordination bonds and intermolecular interactions within metallosupramolecular chemistry. Intermolecular interactions are generally termed synthons, while the metal ions and ligands which make up a complex are termed tectons. [8-9]

1.4 *Intermolecular interactions in supramolecular chemistry.*

The area of supramolecular chemistry involves investigating the intermolecular interactions that occur between molecules.[1] These interactions range from strong to weak and include hydrogen bonds,[10-11] halogen bonds,[12] π–π interactions,[13] metal-metal attractions[14-16] and other weak forces. Generally, intermolecular interactions take place between electron density rich sites to electron density poor sites.

Hydrogen bonding is the is the most common of the non covalent intermolecular interactions and is considered a synthon in the area of supramolecular chemistry.[3] Hydrogen atoms are the most common electron acceptor sites.[12] In hydrogen bonds common donor atoms are nitrogen and oxygen atoms in the form of N–H and O–H; however, C–H moieties can also act as donors especially where the carbon atom is in an electron poor environment.[17] Table 1.1 shows the parameters for strong, moderate and weak hydrogen bonds that are used in the scope of this thesis.[11] However numerical values are only a guide and all hydrogen bonds should be evaluated individually.

Table 1.1 *Hydrogen bond values used in the scope of this thesis as suggested by Jeffery.*[10-11]

	Strong	Moderate	Weak
Interaction Type	strongly covalent	mostly electrostatic	electrostatic/dispersive
bond lengths H···A [Å]	1.2-1.5	1.5-2.2	> 2.2
lengthening of X−H[Å]	0.08-0.25	0.02-0.08	<0.02
X−H versus H···A	X–H ≈ H···A	X–H < H···A	X–H << H···A
X···A[Å]	2.2-2.5	2.5-3.2	>3.2
directionality	strong	moderate	weak
bond angles[°]	170-180	> 130	>90
bond energy [kcal mol^{-1}]	15-40	4-15	<4
relat. IR shift $\Delta\tilde{\upsilon}_{HX}$ [cm^{-1}]	25%	10-25%	< 10%
^{1}H NMR downfield shift (δ)	14-22	< 14	

Another form of tecton that exists in supramolecular chemistry are between aromatic moieties.[18-20] Several π–π interactions exist which include face–to–face interactions, offset face–to–face interactions, which can have the aromatic rings parallel to each other and displaced or have a slight angle between them and be displaced, and edge–to–face interactions.[13, 18] All of these interactions play a role in the formation of supramolecular structures. These interactions typically have energies of 2 kJ mol^{-1}, a general distance range of 3.3 - 3.8 Å and an angle of ~20°.[13] Many aromatic rings can form interactions and together form other π interactions such as a parallel fourfold aryl embrace.[18-20] Figure 1.3 shows graphical representations of the π–π stacking interactions.

Figure 1.3 From left to right: Face–Face π–π stacking interaction, offset face–to–face π–π stacking interaction and edge–to–face π–π stacking interaction.[21]

1.5 *Mononuclear complexes in supramolecular chemistry.*

Mononuclear discrete complexes are common in the area of metallosupramolecular chemistry, or more commonly, coordination chemistry. Discrete mononuclear complexes can act as building blocks in the formation of larger supramolecular structures through intermolecular interactions such as hydrogen bonds and other interactions stated above.[22-23] Some mononuclear discrete complexes have unique properties such as anion binding, reactivity through electrochemistry which also gives rise to molecular level devices.[22] In the scope of the study the hydrogen bonding between mononuclear complexes, non coordination solvent molecules and anions are discussed. Other applications of mononuclear complexes allow the supramolecular chemist to gauge the dimensions of a particular ligand and show what coordination modes are favoured by the metal ions. Mononuclear complexes also help indicate what coordination mode is favoured by a ligand.

1.6 *Polynuclear complexes in supramolecular chemistry.*

Within the area of supramolecular chemistry many multinuclear complexes are reported. These include but are not limited to; Coordination polymers, helicates, catenanes, rotaxanes, knots, cages and clusters.[24] Below is a brief outline of the forms of multinuclear complexes reported in the scope of this project.

1.6.1 *Coordination polymers.*

Batten described a coordination polymer as an infinite array that has metal ions linked together by coordinated ligands.[3] To be a coordination polymer the bonds linking these metal ions and ligands must be coordination bonds. If weaker interactions such as hydrogen bonding and π–π stacking interactions form the infinite net then it is not considered a coordination polymer. Coordination polymers are also typically formed from transition metal ions or lanthanoid ions.[3] Although coordination polymers are readily made from metal ions and ligands they can also contain guest molecules and counter ions. Transition metals such as the first row elements and Zn, Cd, Hg and Ag are used in the preparation of coordination polymers. These are generally used due to their predictability when it comes to the complex geometries formed. However, lanthanoid ions are becoming popular due to their ability have a high connectivity as well as luminesent properties.[3] Typically divergent ligands are used that have pyridyl, imidazole, nitrile or carboxylate functional groups, to name a few, built into them. 1D, 2D and 3D coordination polymers can be prepared depending on the metal ion and ligands which are used.

The first coordination polymer reported was Prussian blue which was first synthesised by accident in the early 18th century by Diesbach.[3, 25-26] Prussian blue was in fact the first synthetic coordination complex.[3] The crystal structure of Prussian blue was not reported until the 1977 by Buser.[27] Further structures of coordination polymers were solved during the 20th century. These included the structure of $Zn(CN)_2$, and $Cd(CN)_2$, the Hofman clathrate, $[Cu(adiponitrile)]NO_3$ which had six interpenetrating networks and various other examples.[3, 28-29]

In 1989 and 1990 landmark papers by Robson showed a new approach to the design of new coordination polymers through the network approach with the node and spacer concept.[30-31] Through this concept new coordination polymers could be designed which had interesting properties. Robson also reported the design of new coordination polymers using metal ions with tetrahedral geometries such as Zn(II), Cd(II) and Cu(I) when reacted with divergent ligands such as cyanide. One significant coordination polymer or metal organic framework reported was MOF-5 by Yaghi.[32] A graphical representation of MOF-5 is shown in Figure 1.4. MOF-5 is constructed from 1,4-benzoic acid. In the Figure 1.4 a large void space seen in the coordination polymer and is represented by a yellow sphere.

Getting larger and larger void spaces and larger surface areas can lead to certain applications for coordination polymers such as absorption of gases.[33]

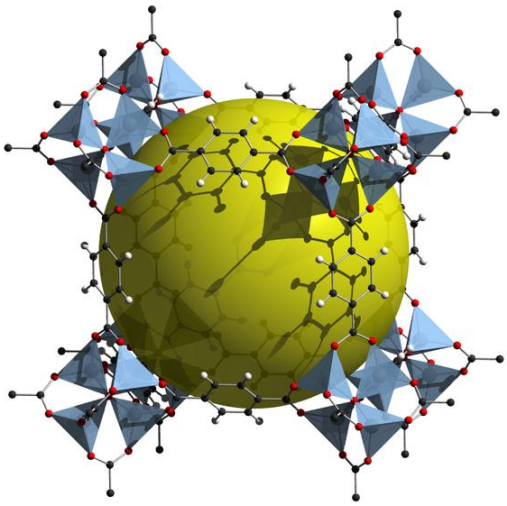

Figure 1.4 *The coordination polymer MOF-5.*[34]

Aside from large porosity and surface areas, coordination polymers have many more potential applications. These involve applications of magnetism, ion/guest exchange, non-linear optical activity, chiral networks, reactive networks, heterogeneous catalysis, luminescence, multifunctional materials and others.[3] Many contributions to the field of coordination polymers have been made during the 90s and 2000's by Yaghi, Kitigawa and Ferey to name just a few.[35-43]

1.6.2 *Networks and Topology.*

The structure of a solid can be described as a network or net.[3, 44] The first instance of using networks to describe and design coordination polymers was by Robson and Hoskins.[30-31, 36]. Robson discussed the use of the node and spacer concept when describing and designing coordination polymers. An example is the use of metal ions, acting as nodes, which prefer the tetrahedral geometry such as Zn(II), Cd(II) and Cu(I) with ligands, acting as the spacers, such as cyanide or 4,4',4",4'"-tetracyanotetraphenylmethane respectively to construct a diamond-related network.[30-31, 36] This type of diamond-related network is shown below in Figure 1.5 and has tetrahedral nodes.

Determining topologies of coordination polymers has been extensively covered by Batten.[3] Coordination polymers can be described as nets, where a net is a polymeric collection of interlinked nodes. A node is defined to be connected to three or more other nodes and a link is connected to two nodes. A repeating pattern must also be present in the crystal structure of the coordination polymer in order for it to be assigned a network topology. Shown in Figure 1.5 is a [4,4] sheet formed from a

square planar four connected node. It must be noted that the networks in Figure 1.5 both have four connected nodes but the nodes, due to their geometries, favour different nets.

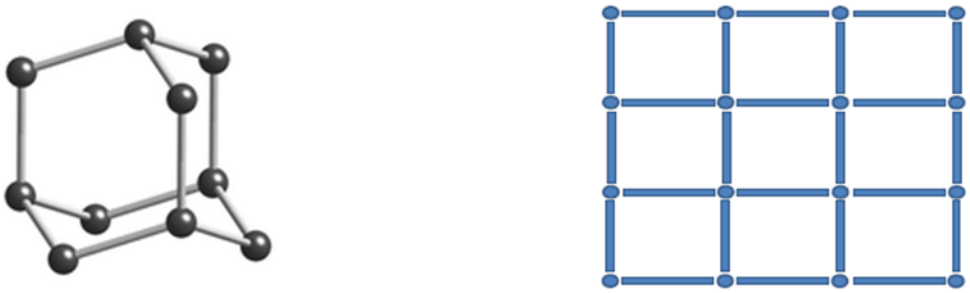

Figure 1.5 *From left to right: Diamond-related network which is produced by reaction of Cu(I) with 4,4',4'',4'''-tetracyanotetraphenylmethane.*[45] *A graphical representation of a [4,4] sheet preferred by a 4-connected square planar node.*[46]

1.6.3 *Polynuclear discrete complexes.*

Discrete assemblies in supramolecular chemistry include: helicates,[47-48] catenanes,[49-51] rotaxanes,[52-53] knots,[54-56] cages[57-61] and clusters.[62-70] Both cages and clusters are discussed further below. In 1996, Lehn reported the metal directed self assembly of a circular double helicate prepared with Fe(II) and a convergent ligand[71] and is shown in Figure 1.6.

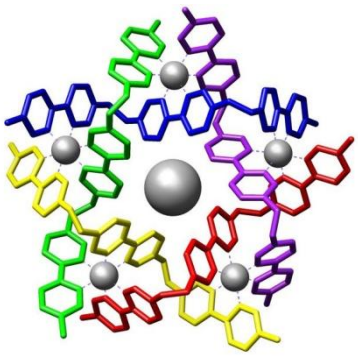

Figure 1.6 *Graphical representation of the metal directed circular double helicate*[72] *reported by Lehn.*[71]

Further examples of polynuclear discrete complexes are complexes that involve host guest chemistry. These discrete assemblies are cages which can accept guest molecules into them. As discussed by Lehn this sort of supramolecular assembly involves the receptor and substrate concept.[1] Here cages and other supramolecules recognise and encapsulate anions and other chemical species in them. These types of supramolecules could have applications in biological areas where concentrations of substrates are low as well as many more.[73-76] Shown in Figure 1.7 is an examples of an encapsulating cage from the literature reported by Nitschke.[77]

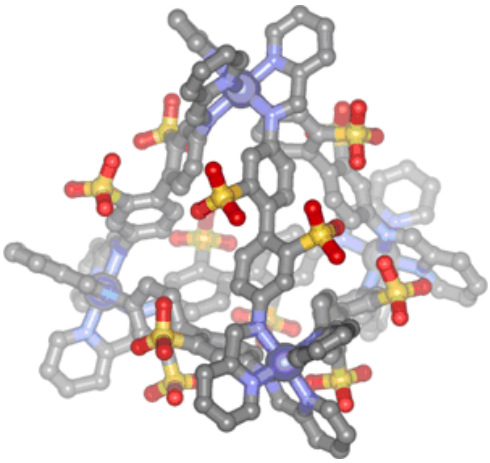

Figure 1.7 *The supramolecular polynuclear[78] cage reported by Nitschke.[77]*

This cage can encapsulate white phosphorus and allows it to be stable in air.[77] Reversibility is also seen within the cage where the white phosphorus can be extracted by using the a competing chemical species such as benzene. Although this is just one example of a molecular cage many more examples are reported by Batten, Fujita and Rebek among others[57-61], however the scope of this introduction cannot do justice to the scale of this area of supramolecular chemistry. Another type of discrete polynuclear complexes are clusters which are discussed below.

1.6.4 *Cluster Chemistry.*

Metal clusters or coordination clusters can be prepared from d-block transition metal ions and have a wide range of applications.[62] Metal clusters are prepared to mimic bioinorganic sites in proteins, for their magnetic properties and potential for being a single-molecule magnet and catalysis.[62] These metal clusters are prepared from d-block transition metals.[62] The metal ions in the metal clusters are generally bridged by two or more ligands. These ligands can be organic or inorganic ligands and have varying terminal ligands which can coordinate via monodentate binding or chelation. They also have a variety of solvate molecules in the structures.

The copper acetate monohydrate complex has been studied since 1823 by Brooke and many more who have described the crystallography of the cluster.[79] The X-ray crystallography was reported on the copper acetate structure in 1953.[79-80] The crystal structure of the copper acetate monohydrate cluster is shown below in Figure 1.8. It shows a dinuclear copper cluster with four acetate groups bridging each metal ion. A coordinated water molecule is coordinated to each Cu(II) ion.

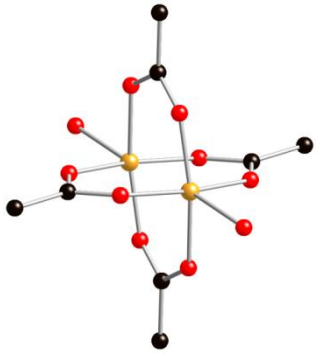

Figure 1.8 *The crystal structure of copper acetate monohydrate cluster.*[79]

A significant metal cluster was the Mn_{12} cluster first reported by Novak[69-70] as shown in Figure 1.9. The manganese cluster has a general formula of $[Mn_{12}(O_2CR)_{16}(H_2O)_4]$, where R is either a methyl or phenyl group. The cluster has twelve manganese metal ions, eight are Mn(III) ions and four are Mn(IV) ions. The metal ions are bridged by sixteen carboxylate groups and has four coordinated water molecules.[69-70] The magnetic characteristics of this metal cluster was the first reported instance of single molecule magnet behaviour.[62] Metal clusters have been reported using V(III), Fe(II), Fe(III), Co(II), Ni(II) metal ions and even lanthanide metal ions such as Ln(II) have been used.[63-68] These metal clusters have also shown SMM behaviour.[62] Single molecule magnets have potential to store information due to their magnetic characteristics.[62] Due to this SMMs have a potential application in quantum computing devices.

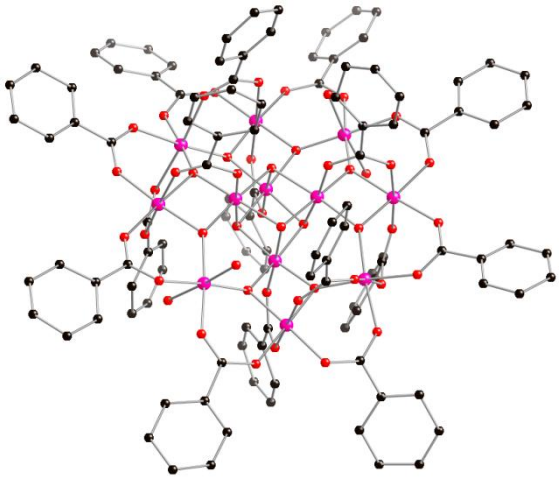

Figure 1.9 *Crystal structure of* $[Mn_{12}(O_2CPh)_{16}(H_2O)_4]$.[69]

There are many examples of polynuclear metal clusters reported in the literature with many types of transition metals and carboxylate function groups involved in bridging the metal ions. For the scope of this study only cobalt metal clusters, copper metal clusters and iron metal clusters were looked into further. Examples with all three transition metals have been reported in the literature with

ferromagnetic and antiferromagnetic properties.[81-83] Figure 1.10 shows reported metal clusters prepared from Co(II), Cu(II) and Fe(II) ions.[81-83]

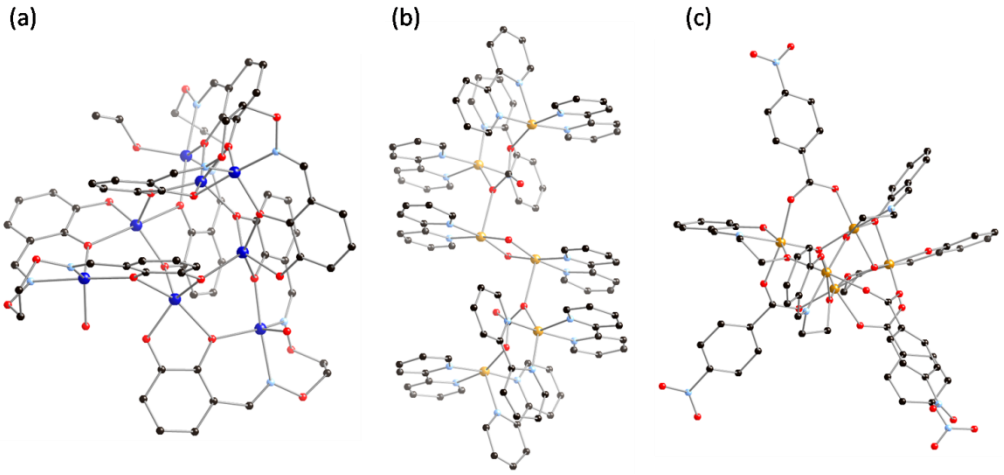

Figure 1.10 *(a) Octanuclear Co(II) ion metal cluster.*[81] *(b) Hexanuclear Cu(II) ion metal cluster.*[82] *(c) Pentanuclear Fe(II) ion metal cluster.*[84]

1.6.5 *A brief background to magnetism.*

Magnetisation is the induction of a magnetic dipole within a solid material. In this case the crystal of a cluster complex. Magnetism is characterised by **M** which is defined as the magnetic dipole moment per unit volume when a magnetic field is applied to the molecule. The basic magnetism equation is stated in (A).[85]

$$M = \mu_0^{-1}\chi_M B \qquad (A)$$

In equation (A) the μ_0 value is the vacuum permeability, χ_M is the magnetic susceptibility and B is the applied magnetic field. Further to this the Curie Law is stated in equation (B).[85]

$$\chi_M = C / T \qquad (B)$$

Again as above the χ_M is the magnetic susceptibility of a particular molecule. C is the Curie constant and is characteristic of the type of molecular species being measured, while T is the temperature. The Curie Law states that the magnetic susceptibility is inverse to the temperature.

1.6.5.1 *Diamagnetism and paramagnetism.*

Diamagnetism is when individual atoms or molecules have paired magnetic dipole moments. When diamagnetism is present within an atom or molecule the magnetic moment is directed against

the external magnetic field generated. In contrast paramagnetism is when an atom or molecule has unpaired magnetic dipole moments. Here each atom or molecule has a permanent magnet dipole moment. Diamagnetism is not dependant on temperature or applied magnetic field, where as paramagnetism is dependent on temperature but not the applied magnetic field.[85-86]

1.6.5.2 *Antiferromagnetism and ferromagnetism.*

Antiferromagnetism arises when the magnetic dipole moments in neighbouring molecules in a solid form an antiparallel arrangement with each other. On the other hand, a ferromagnetic solid has the magnetic dipole moments arranged parallel to one another in neighbouring molecules. Both examples are shown in Figure 1.11. The magnetic susceptibility as shown by the Curie Law (B) and is a straight line when plotted as χ_M vs temperature when no magnetic field is applied. However, when a magnetic field is applied the magnetic susceptibility for the specific solid would rise if the solid was ferromagnetic and fall if the solid was antiferromagnetic based off the Curie Law. Both ferromagnetism and antiferromagnetism are dependent on both temperature and applied magnetic field.[85-86]

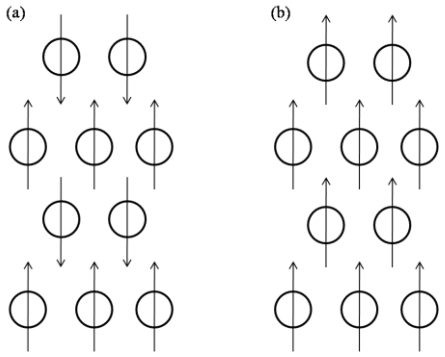

Figure 1.11 *(a) Magnetic dipoles arranged antiparallel in an antiferromagnetic solid. (b) Magnetic dipoles arranged parallel in a ferromagnetic solid.*

The copper acetate monohydrate metal cluster shown in Figure 1.8 is a significant molecule in the study of magnetic behaviour in metal clusters.[80] The magnetic susceptibility of the copper acetate cluster was first reported by Guha.[87] The cluster itself shows two interacting Cu(II) ions bridged by acetate ligands. Further studies such as EPR were reported by Bleaney and Bowers to understand the full magnetic behaviour of the cluster.[88] There have been countless more studies of the copper acetate cluster reported since.[80, 89-90]

Ferromagnetism is the type of magnetism looked for in metal clusters. Intermolecular interactions outlined above can influence the magnetic properties of a solid and can also be considered

to be the origin of hysteresis in transition compounds.[91] The magnetic characterisation of the multinuclear metal clusters prepared were studied in full.

1.7 *Introduction to the ligand.*

Coordination to metal ions by the 2-(N-pyridyl)-4-amino)-4-oxobutanic acid can occur through the specific functional groups that are outlined below. Examples of the coordination modes of the functional groups present in the ligand are described with reference to relevant literature examples. A comprehensive literature search has outlined where the ligand has been used and what anaylsis has been performed and are described in the following sections. Shown in Figure 1.12 is the structure of the N-(2-pyridyl)-4-amino-4-oxobutanoic acid ligand (**H_2L1**) used in the research study. The **H_2L1** ligand is ambivergent and can act as either a convergent or divergent ligand.[92]

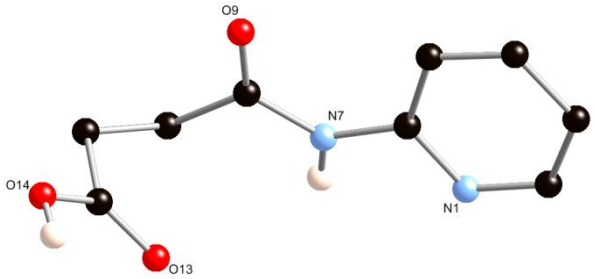

Figure 1.12 *Structure of the **H_2L1** ligand.*

1.7.1 *The pyridyl-amido motif in coordination complexes.*

The 2-pyridyl-amido motif has been built into ligands and are common in coordination complexes such as mononuclear and multinuclear complexes.[93-99] There are three atoms where coordination to metal ions can take place in this motif. These are through the nitrogen atom in the pyridine ring as well as the nitrogen and oxygen atoms in the amido moiety. The four common types of coordination modes for this motif are shown in Figure 1.13. Most common of the coordination modes is the bidentate coordination mode with the oxygen atom in the amido group and the nitrogen atom in the pyridine group both chelating to the same metal ion in the complex.[93-96] A less common coordination mode is also through both nitrogen atoms in the pyridine ring and amido group.[97] There are also cases where ligands with this motif built in can bridge two metals in a complex, through the two nitrogen atoms in the pyridyl and amido groups shown in Figure 1.13.[97-98] Bridging between three metals is possible with this motif through the two nitrogen atoms and one oxygen atom and is shown in Figure 1.13,[99] however, there is also the possibility of two types of coordination modes in the same complex.[99] This example shows a bis-amido pyridyl ligand coordinating to three metal ions.

Two metal ions are coordinated to the amido nitrogen atom and the amido oxygen atom represented as the coordination mode (c) shown in Figure 1.13. The third metal ion is coordinated to the nitrogen atom in the pyridine ring and the oxygen atom on a second amido group or the coordination mode (a) in Figure 1.13. The final coordination mode of the motif is where the pyridyl nitrogen atom and amido oxygen atom coordinate to the same metal ion and the amido nitrogen coordinates to a separate metal ion.[100]

The 3-pyridyl-amido and 4-pyridyl-amido motifs are also common in the literature. The 3-pyridyl-amido motif has two coordination modes, one through the pyridine nitrogen and the other bridging through both the pyridine nitrogen and amido nitrogen atoms.[35, 101] It is used in a range of complexes from discrete to coordination polymers.[35, 102-104] The 4-pyridyl-amido motif is most commonly used in ligands in coordination polymers and commonly only coordinates through the nitrogen atom in the pyridine ring. However, there are examples of it bridging metal ions through the pyridine nitrogen and the amido oxygen atom.[105-107]

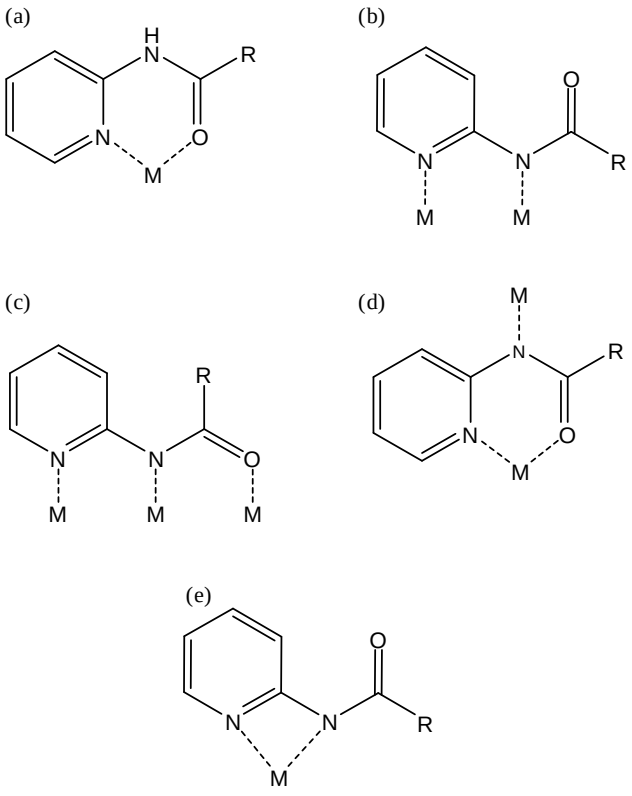

Figure 1.13 *Coordination modes of the pyridyl-amido motif reported in the literature. (a) Chelating (η^1) mode, (b) Bridging (μ_2-η^1, η^1) mode, (c) Bridging (μ_3-η^1, η^1, η^1) mode, (d) Chelating bridging (μ_2-η^1 η^1) mode. (e) Chelating (η^1) mode.*

1.7.2 *Carboxylic acid and carboxylate functional groups in coordination complexes.*

Another common functional group used in supramolecular chemistry is the carboxylic acid group. While the carboxylic acid group itself can coordinate to metal ions, the deprotonated form, the

carboxylate functional group can also coordinate to metal ions. Shown in Figure 1.14 are the common coordination modes of the carboxylate and carboxylic acid groups.

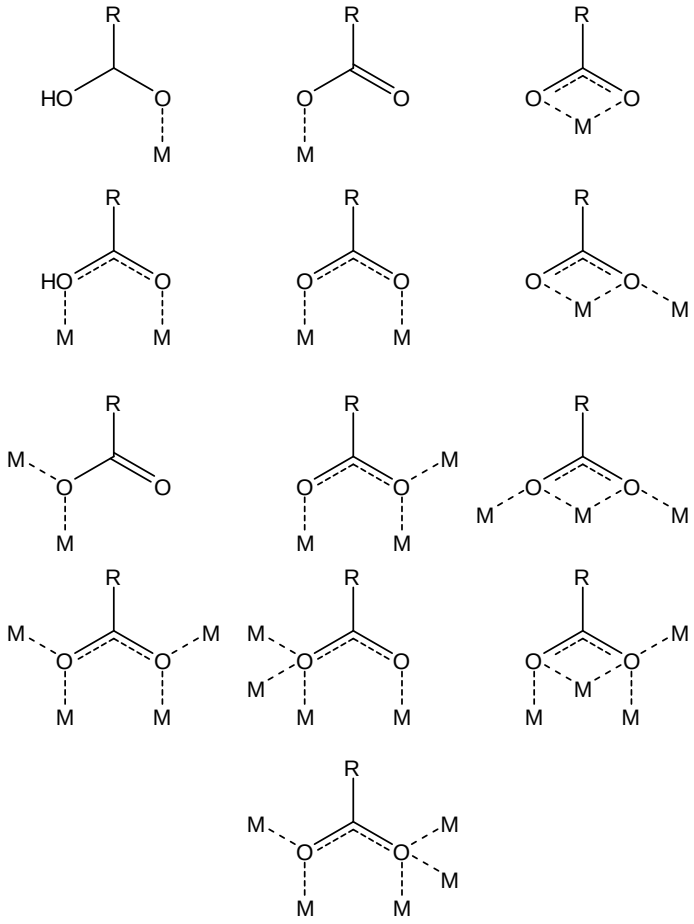

Figure 1.14 Coordination modes of the carboxylic acid and carboxylate groups reported in the literature. From top left to bottom right; (η^1) mode,[108] (η^1) mode,[109] chelating (η^2) mode,[109] bridging (μ_2-η^1, η^1) mode,[110] bridging (μ_2-η^1, η^1) mode,[109] chelating bridging (μ_2-η^2, η^1) mode,[109] bridging (μ_2-η^2) mode,[109] Chelating bridging (μ_3-η^1, η^2) mode,[109] chelating bridging (μ_3-η^1, η^2 ,η^1) mode,[109] chelating bridging (μ_4-η^2, η^2) mode,[109] chelating bridging mode (μ_4-η^3, η^1) mode,[111] chelating bridging (μ_4-η^1, η^2, η^2) mode[112] and chelating bridging (μ_5-η^2, η^3) mode.[113]

Carboxylic acids and carboxylate groups have a wide range of coordination modes making them suitable for ligands used in the preparation of coordination complexes. Due to the variety of coordination modes there is an abundance of ligands with carboxylic acid and carboxylate function groups.[3, 109] The functional groups are common in many discrete and multinuclear complexes, with multinuclear complexes being coordination polymers and cluster complexes.[114] Carboxylic acids and carboxylate functional groups coupled with the pyridyl amido complexes shown in Figure 1.14 provide an excellent building block for ligands to produce metal complexes.

1.7.3 *Previous work with N-(2-pyridyl)-4-amino-4-oxobutanoic acid (**H_2L1**) and related ligands.*

The crystal structure of the **H_2L1** ligand has recently been reported by Wang[115] and is shown in Figure 1.15. The ligand was prepared with succinic anhydride and 2-aminopyridine in dimethylformamide. Further preparations of the ligand are also reported in the literature where different conditions are used.[116-117]

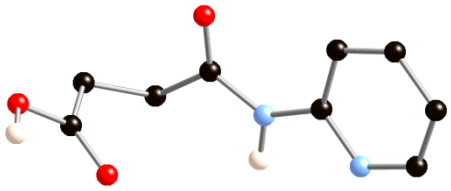

Figure 1.15 *The crystal structure of **H_2L1** by Wang.[115]*

Studies involving the use of the **H_2L1** ligand appear in the literature and a Scifinder search on the 29th of October 2012 returned 31 references involving the **H_2L1** ligand. Although the **H_2L1** is not a novel ligand it has only been reported in biological studies[118-121] and supramolecular hydrogels.[122-123] A few papers have reported spectral studies on transition metal complexes with the N-(2-pyridyl)-4-amino)-4-oxobutonic acid ligand coordinated to form mononuclear discrete complexes. These spectral studies included , such as, infrared spectroscopy, magnetic moments and electrochemical studies. The complexes involved transition metals such as Cu(II) and Ni(II) ions.[124-128] Although the spectral studies were carried out no crystal structures of the complexes were reported.

An example of the N-(2-pyridyl)-4-amino)-4-oxobutanic acid ligand used in conjunction with manganese and 1, 10-phenanthroline to form a mononuclear discrete structure with the crystal structure reported by Shen.[129] A further preparation for the N-(2-pyridyl)-4-amino)-4-oxobutanic acid ligand is also reported. A slow evaporation crystallisation was used to crystallise the complex shown in Figure 1.16.

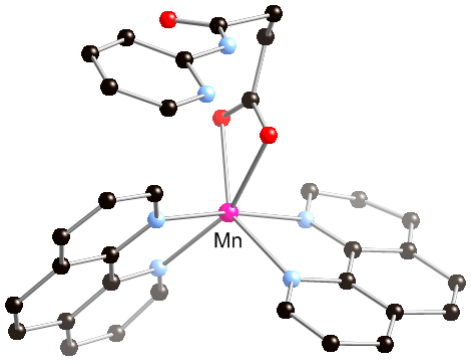

Figure 1.16 *The crystal structure of $[MnL(phen)]^+$ as reported by Shen.[129]*

The ligand itself is coordinated to the Mn(II) ion through the carboxylate group moiety. The carboxylate is chelating the metal between the two oxygen atoms O1 and O1. Spectral studies , magnetic and EPR characterisation were carried out on the discrete Mn(II) complex.[129]

The N-(3-pyridyl)-4-amino)-4-oxobutanic acid (**H_2L2**) and N-(4-pyridyl)-4-amino)-4-oxobutanic acid (**H_2L3**) ligands are not unprecedented in the literature. Like N-(2-pyridyl)-4-amino)-4-oxobutanic acid, both ligands have been prepared in several ways and are used in biological studies and supramolecular hydrogels.[116, 119] No crystal structures or hydrogen bonding characterisations of either ligands are reported in the literature.

1.8 *The present study.*

The three ligands **H_2L1**, **H_2L2** and **H_2L3** will be used to prepare mononuclear and multinuclear complexes. The ligands themselves are not novel with biological studies, formations of hydrogels and spectral studies being carried out on the ligand and complexes prepared from the ligand which have been outlined above. However, only one crystal structure of a transition metal complex has been reported with the **H_2L1** ligand. Due to this a the structural properties of the ligands will be investigated with 1st row transition metals, using single crystal X-ray diffraction. Various synthetic techniques will be investigated such as bench top crystallisation methods and solvothermal synthesis techniques. The coordination modes of the 2, 3 and 4-pyridyl-amido motifs will be investigated when bound to first row transition metals to see how they compare to those reported in the literature. Further work will be to investigate if multinuclear complexes such as coordination polymers and clusters can be prepared by extending the coordination mode of all three ligands through the carboxylic acid functional groups. In addition, the coordination modes of the carboxylic acid and carboxylate functional groups will be investigated and compared to those already reported in the literature. When deemed suitable, the complexes prepared will be characterised magnetically to see if there are antiferromagnetic or ferromagnetic interactions.

Chapter 2

Results and Discussion

2.1 *Results and Discussion*

2.1.1 *Introduction*

In order to prepare discrete and multinuclear compounds, certain factors were taken into account when choosing a family of ligands which were best suited for the needs of this project. These factors include the rigidity of the ligand, types of donor atoms in the ligand, and what particular functional groups the ligand had that could coordinate with transition metals such as cobalt, manganese, nickel, copper and iron.

H_2L1, **H_2L2** and **H_2L3** were considered to be ideal ligands as they had a number of functional groups of interest capable of coordinating to transition metal ions. These ligands all have a nitrogen donor atom in the pyridine ring, an amide group with the possibility of coordination through the nitrogen or the oxygen atoms, and a carboxylic acid functional group which can coordinate through two oxygen atoms in a variety of ways. In the compounds that follow the ligands coordinate with two or more of these functional groups to transition metal ions to form discrete, polymeric and cluster compounds.

2.1.2 *Synthesis of **H_2L1**, **H_2L2** and **H_2L3**.*

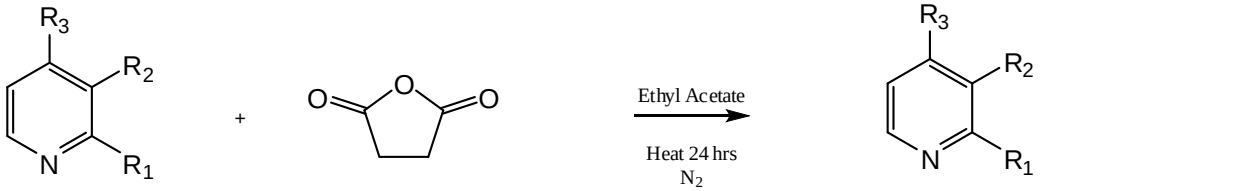

H_2L1; $R_1 = NH_2$ $R_2, R_3 = H$
H_2L2; $R_2 = NH_2$ $R_1, R_3 = H$
H_2L3; $R_3 = NH_2$ $R_1, R_2 = H$

H_2L1; $R_1 =$ 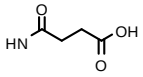 $R_2, R_3 = H$
H_2L2; $R_2 =$ 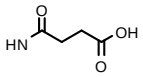 $R_1, R_3 = H$
H_2L3; $R_3 =$ 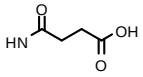 $R_1, R_2 = H$

Figure 2.11 *General reaction scheme for the preparation of **H_2L1**, **H_2L2** and **H_2L3**.*

All three ligands were prepared from a modified literature preparation[117] or from preparations from previous Kruger group members. Succinic anhydride and the respective aminopyridine in either ethyl acetate, for **H_2L1** and **H_2L2**, or dry THF under a N_2 flow for **H_2L3**, were heated to reflux temperature. After several hours a white precipitate was seen to form and heating was continued for 24 hours. After which time all three were filtered hot and washed with hot ethyl acetate or water and hot ethyl acetate for **H_2L1**, **H_2L2** and **H_2L3** respectively. The resulting white precipitates were

recrystallised with yields of 13% - 39% and characterised via several analytical and spectroscopic methods.

2.1.3 *Characterisation of* ***H_2L1***, ***H_2L2*** *and* ***H_2L3.***

The ^{1}H NMR spectra of **H_2L1** - **H_2L3** were consistent with the proposed structures. Two methylene proton signals were in the region of 2 - 3 ppm and all aromatic proton signals of the pyridine ring appeared in the region of 7 - 8 ppm. All signals were confirmed with the use of ^{1}H,^{1}H COSY NMR spectra. Below in Figure 2.1 is the ^{1}H NMR spectrum for **H_2L1**, which is representative.

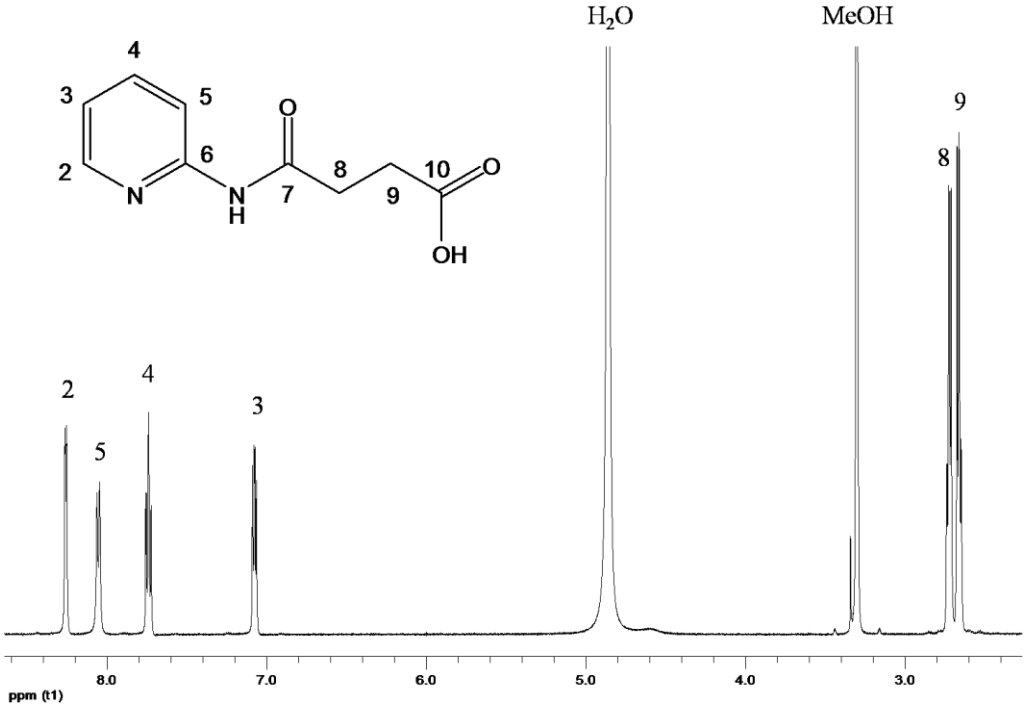

Figure 2.1 *^{1}H NMR spectrum showing all proton signals for* ***H_2L1*** *run in CD_3OD. (Note: Amido proton is exchanging with the solvent and is unseen in the ^{1}H NMR spectrum)*

The ^{13}C NMR spectra for **H_2L1** - **H_2L3** were also consistent with the proposed structures. All methylene carbon atom peaks were within the region of 28 - 31 ppm and the pyridine ring carbon atoms for all ligands were within the range of 113 - 151 ppm which is consistent for aromatic carbon atoms. The two amido and carboxylic acid quaternary carbon atoms signals for **H_2L1** - **H_2L3** were within the range of 171 - 175 ppm which is indicative of carbonyl carbon atom signals in ^{13}C spectra. Mass spectrometry on ligands **H_2L1** - **H_2L3** returned high resolution masses consistent with the parent ion of $[M+H]^+$ which has a calculated mass of 195.0764 g mol^{-1}. All infrared spectra for the ligands **H_2L1**, **H_2L2** and **H_2L3** displayed the expected absorbance profiles. With carboxylic acids coming in the range of 1725 - 1700 cm^{-1} and 3000 - 2500 cm^{-1}. Amide functional groups were shown in the ranges of 1680 - 1630cm^{-1} and 1570 - 1515 cm^{-1} and carboxylate functional groups were seen in the ranges of 1610 - 1550cm^{-1} and 1420 - 1300 cm^{-1}.[130]

2.1.4 *Single crystal X-ray diffraction of* ***H_2L1****,* ***H_2L2*** *and* ***H_2L3****.*

Colourless needle crystals of **H_2L1,** block crystals of **H_2L3,** suitable for single crystal X-ray crystallography were grown in a methanol solution that was allowed to stand for two days. While colourless block crystals of **H_2L2** grew from a 50:50 solution of methanol and acetonitrile after standing covered for four days.

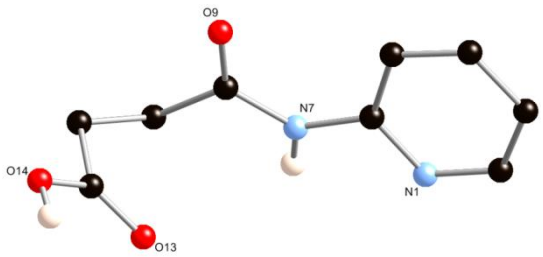

Figure 2.2 *Crystal structure of* ***H_2L1*** *with hetero atoms labelled and all non hydrogen bonding hydrogen atoms omitted for clarity.*

Shown above in Figure 2.2 is the crystal structure of **H_2L1** which crystallised in the space group $P2_1/n$ and refined with an R1 factor of 5.13% . The angle between the atoms of the pyridyl ring and the amido group plane is 7.61(1)° showing they are relatively planar with each other. Hetero atoms such as the nitrogen atoms N1 and N2 and oxygen atoms O2 and O3 are sites for hydrogen bonding throughout the crystal lattice.

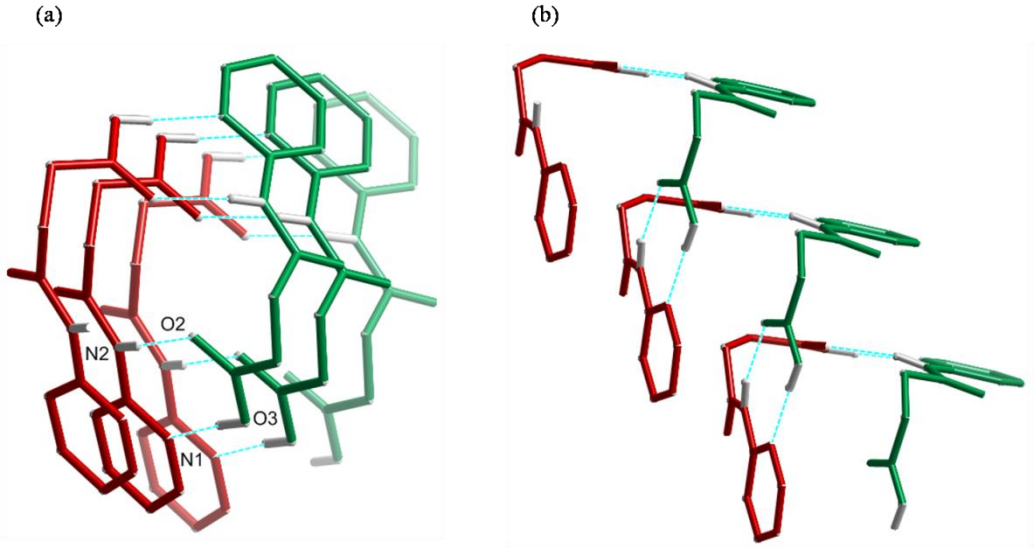

Figure 2.3 *(a) A view of* ***H_2L1*** *looking down the right handed helix formed by hydrogen bonding. (b) The right handed helix formed by hydrogen bonding* ***H_2L1*** *molecules as viewed from the side of the right handed helix. All non hydrogen bonding hydrogen atoms omitted for clarity.*

H_2L1 forms helices via hydrogen bonding between molecules as shown in Figure 2.3. Right and left handed helices are formed via a head to tail configuration of the **H_2L1** molecules to form

hydrogen bonds between the carboxylic acid proton and pyridine and the amide proton and the carboxylic acid oxygen atom which are denoted as O3−H3···N1 and N2−H2···O2, respectively. Specific parameters of these hydrogen bonds are outlined in Table 2.1. For simplicity only the right handed helix has been shown in Figure 2.3.

Table 2.1 *Parameters for hydrogen bonds in ligands* ***H_2L1****,* ***H_2L2*** *and* ***H_2L3****.*

D–H···A	D–H/Å	*d*(H···A)/Å	*d*(D···A)/Å	<(DH···A)/°	Symmetry codes
H_2L1					i = 3/2-x,-1/2+y,1/2-z
O3–H3···N1^{i}	0.854(17)	1.837(18)	2.687(3)	173(3)	ii = 3/2-x,1/2+y,1/2-z
N2–H2···O2^{ii}	0.855(17	1.978(17)	2.833(3)	166	
H_2L2					iii = 3/2-x,-1/2+y,3/2-z
N2–H2···O2^{iii}	0.854(12)	2.002(13)	2.8539(14)	175.4(14)	iv = 1/2+x,1/2-y,-1/2+z
O3–H3···N1^{iv}	0.924(13)	1.705(14)	2.6188(14)	169.1(16)	
H_2L3					v = -1-x,-y,-z
N2–H2···O2^{v}	0.865(13)	1.965(14)	2.8217(16)	170.0(15)	vi = -2-x,-1-y,-z
O3–H3···O3^{vi}	0.861(18)	1.601(18)	2.453(2)	170(5)	vii = 2-x,1-y,1-z
N1–H1···N1^{vii}	0.877(17)	1.778(17)	2.654(2)	177(4)	

H_2L2 shown here in Figure 2.4, like **H_2L1**, crystallised in the *P*21/*n* space group and refined with an R1 factor of 2.86%. In the case of **H_2L2** the amide nitrogen atom N2 is bound to the meta position of the pyridine ring. The plane to plane angle of the pyridyl atoms to the amido atoms is 7.89(5)° making both groups relatively planar with each other. **H_2L2** also has the same hetero atoms available for hydrogen bonding as **H_2L1** and are explored further in figure 2.5.

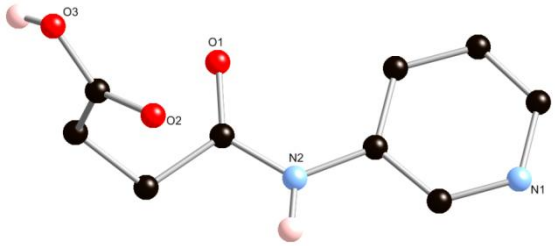

Figure 2.4 *Crystal structure of* ***H_2L2*** *with hetero atoms labelled and all non hydrogen bonding hydrogen atoms omitted for clarity.*

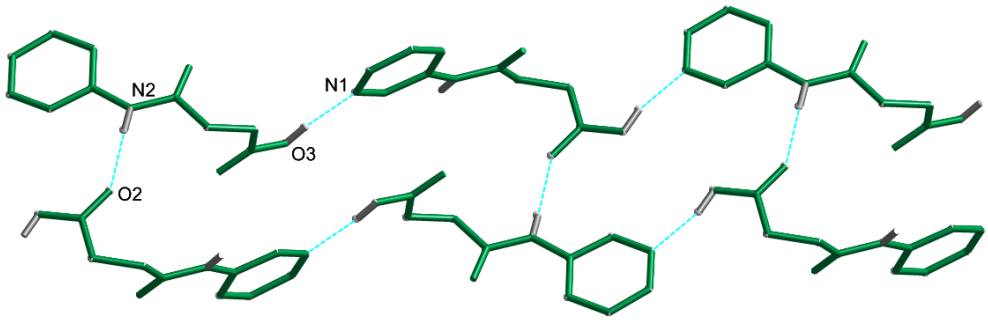

Figure 2.5 *Hydrogen bonding depicting the right handed helix of* ***H_2L2****, all hydrogen atoms not involved in hydrogen bonding removed for clarity.*

Figure 2.5 shows the hydrogen bonding linking ligand **H_2L2** into strands. The hydrogen bond O3-H3···N1 which binds **H_2L2** via head-to-tail conformation through the carboxylic acid oxygen O3 on one moiety and the pyridine nitrogen atom on another. In order for it to form a head to tail hydrogen bonding strand every other molecule is rotated 180°. One strand is then linked to another going in the opposite direction by the hydrogen bond N2–H2···O2 from the amide nitrogen atom to the carboxylic acid oxygen atom. Table 2.1 lists parameters for both of these hydrogen bonds depicted in Figure 2.5. A further hydrogen bond shown in Figure 2.6 shows **H_2L2** strands forming a 3D hydrogen bonding network.

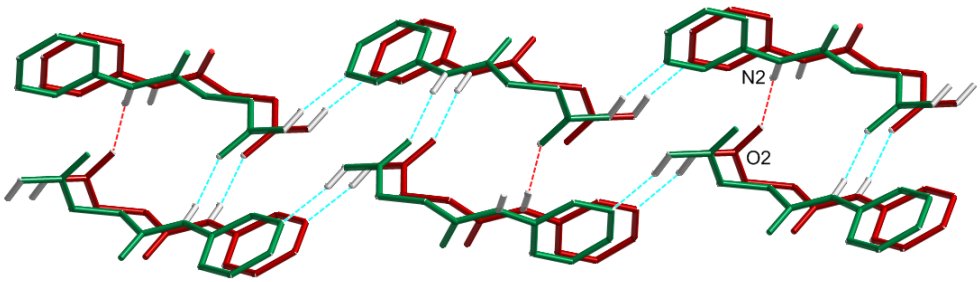

Figure 2.6 *Hydrogen bonding in the* ***H_2L2*** *lattice between different helices. Hydrogen atoms not involved in hydrogen bonding omitted for clarity.*

Unlike **H_2L1** which only hydrogen bonds to two other **H_2L1** molecules, each **H_2L2** molecule hydrogen bonds to four others as shown in Figure 2.6 to form a 3D hydrogen bonding network. Two via the hydrogen bonds shown in Figure 2.5 and two via inter strand hydrogen bonds. Depicted in Figure 2.6 is two different strands linked together via hydrogen bonds between the amide nitrogen atoms and the carboxylic acid oxygen atoms denoted as N2–H2···O2 on each strand indicated by the red dashed hydrogen bonds. The parameters of the hydrogen bond depicted in Figure 2.6 can be found in Table 2.1.

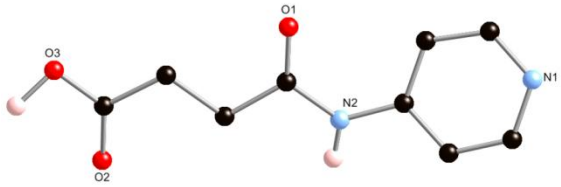

Figure 2.7 *Crystal structure of* ***H_2L3*** *with both N1 and O3 protonated at half occupancy. All non hydrogen bonding hydrogen atoms have been omitted for clarity.*

H_2L3, shown in Figure 2.7, crystallised in the $P\bar{1}$ space group and refined with a R1 factor of 3.26%. In this example the amide group is attached to the para position of the pyridine ring. The angle between the pyridyl and amido atom's planes is 11.98(6)° which makes them relatively planar with each other, but less so than **H_2L1** and **H_2L2**. As shown in Figure 2.7, both nitrogen atom N1 and oxygen atom O3 are protonated, both of these hydrogen atoms have a chemical occupancy of a half. Like **H_2L1** and **H_2L2**, **H_2L3** also hydrogen bonds to itself to form a 2D hydrogen bonding sheet.

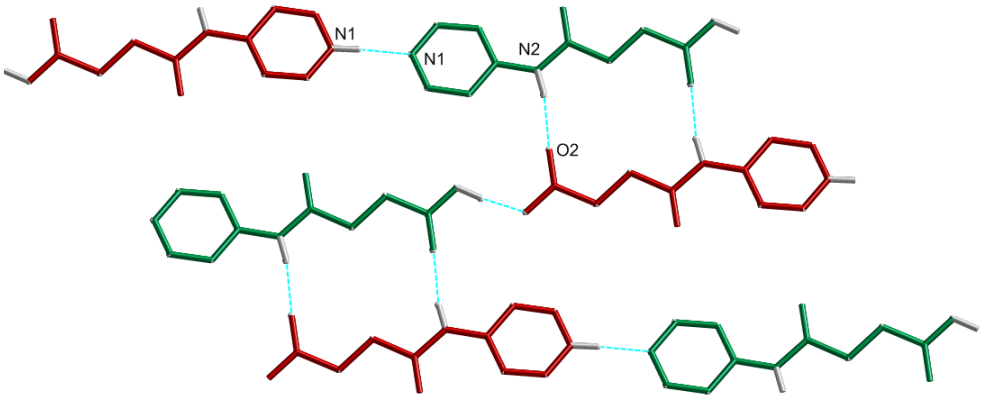

Figure 2.8 *Hydrogen bonding between molecules of* ***H_2L3****. All non hydrogen bonding hydrogen atoms omitted for clarity.*

Figure 2.8 shows the 2D hydrogen bonding sheet formed by **H_2L3** through three different hydrogen bonds. **H_2L3** binds to three different **H_2L3** molecules, one in the same strand and one in strand opposite. Linking between moieties into a strand is via the hydrogen bond N1−H1···N1 in a head to head configuration between pyridine rings and a tail to tail configuration by the hydrogen bond O3−H3···O3 between two carboxylic acid groups on different moieties. Although these atoms are all protonated only 50% of the time allowing these hydrogen bonds to form, this has been shown above in Figure 2.8. Parameters explaining both of these hydrogen bonds are in Table 2.1. Not only does **H_2L3** form strands, these strands then inter link via the hydrogen bond N2-H2···O2 between the amide nitrogen atom and the carboxylic acid oxygen atom, forming a 2D hydrogen bonding sheet again parameters for this bond can be found above in Table 2.1.

Unfortunately both **H_2L2** and **H_2L3** yielded no mononuclear or multinuclear complexes. A variety of metal salts and conditions were used to prepare complexes with both **H_2L2** and **H_2L3** and several crystallisation methods were employed. Attempts were made with slow diffusions, slow evaporations and solvothermal crystallisation techniques to produce crystals, however, when either ligand was mixed with a metal salt a precipitate would form straight away or during the crystallisation process a precipitate would form. Attempts to synthesise complexes with both ligands were abandoned and only work with the **H_2L1** is reported below.

2.2.1 *Introduction to discrete mononuclear complexes prepared from* ***H_2L1***

Ligand **H_2L1** was combined with a variety of metal salts to yield eight discrete metal complexes. In all complexes, the one metal ion is coordinated to two **H_2L1** ligands with solvent molecules or coordinating anions completing the octahedral coordination sphere of the metal ion. The complexes exhibit the same coordination mode through the amido oxygen atom and pyridine nitrogen atom of the two **H_2L1** ligands but have varying axial ligands. Coordinating solvent molecules, anions and the orientations of the carboxylic acid functional groups on both the **H_2L1** ligands enable hydrogen bonding within the crystal lattice of each complex.

2.2.2 *General synthesis and characterisation of discrete complexes* ***1 - 8****.*

Eight discrete complexes were isolated by either solvothermal synthesis, vapour diffusion or slow evaporation. A range of solvents and, anti solvents, were used to prepare the complexes. Each complex was fully characterised via elemental analysis, infrared spectroscopy, single crystal X-ray diffraction and X-ray powder diffraction. Although mass spectroscopy was carried out on complexes **1 - 8** no peaks matching the complexes or fragments of the complexes were seen in the spectra. The spectra only showed a mass for the **H_2L1** ligand.

2.2.3 *Description of complexes* ***1 - 8.***

2.2.3.1 *Discrete complexes prepared from vapour diffusion and slow evaporation.*

Complex **1** was prepared from **H_2L1** and cobalt perchlorate in acetonitrile solution, using diisopropyl ether as the anti solvent in a slow diffusion crystallisation. After one week orange block crystals formed in 11% yield and were isolated directly by filtration. The crystals were suitable for single crystal X-ray diffraction.

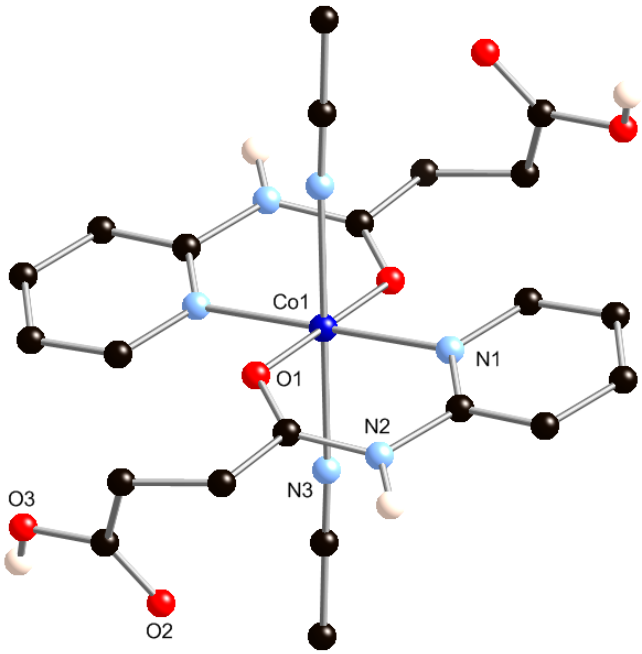

Figure 2.9 *Crystal structure of complex **1** with anions and all non hydrogen bonding hydrogen atoms omitted for clarity.*

Figure 2.9 shows the crystal structure of complex **1** which crystallised in to the $P2_1/c$ space group and refined with a R1 factor of 5.78%. The unit cell contains two molecules of complex **1** and four perchlorate anions. Two **H_2L1** ligands chelate to a Co(II) ion via the nitrogen atom N1 in the pyridine ring and an oxygen atom O1 from the amido group. Two acetonitrile molecules occupy the axial sites of the Co(II) ion to give a pseudo octahedral geometry. Both the carboxylic acid groups from the **H_2L1** ligands remain protonated and do not coordinate to the metal centre.

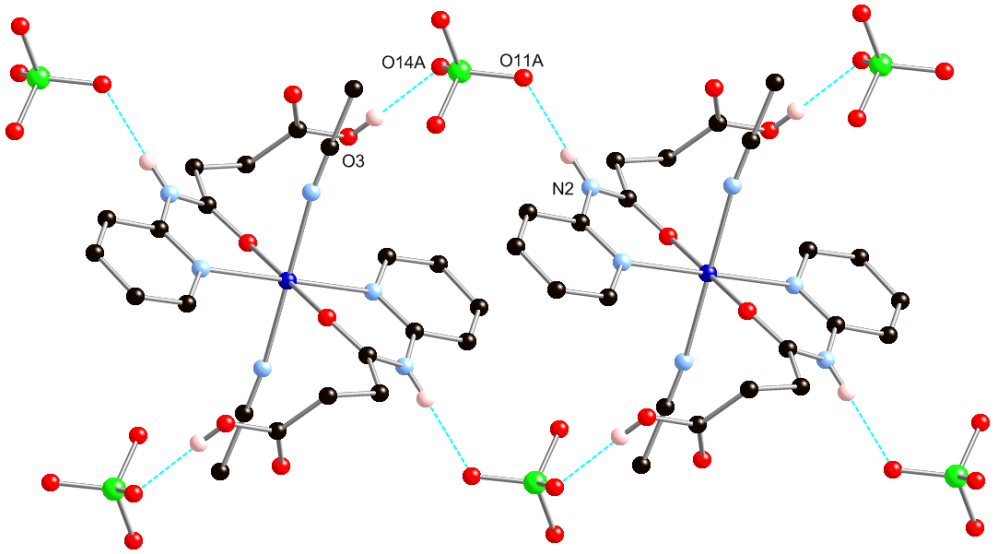

Figure 2.10 *Hydrogen bonding of complex **1** between perchlorate anions and nitrogen and oxygen atoms N2 and O3. All non hydrogen bonding hydrogen atoms have been omitted for clarity.*

However, the carboxylic acid groups and the perchlorate anions participate in hydrogen bonding within the crystal lattice shown in Figure 2.10. The hydrogen bonds N2-H2···O11A and O3-H3···O14A link the amido group and carboxylic acid to two different oxygen atoms on the perchlorate anion. Bond lengths and angles for all of the hydrogen bonds in complex **1** are presented in Table 2.2.

Table 2.2 *Parameters for hydrogen bonds in complex **1**.*

D–H···A	D–H/Å	*d*(H···A)/Å	*d*(D···A)/Å	<(DH···A)/°	Symmetry Codes
N2–H2···O11A^{i}	0.87(2)	2.07(3)	2.910(6)	163(6)	i = -1+*x*,+*y*,+*z*
O3–H2···O14A	0.85(2)	1.86(2)	2.709(6)	172(7)	

Complex **2** was prepared from **H_2L1** and nickel perchlorate in nitromethane solution, using diisopropyl ether as the anti solvent in slow diffusion crystallisation. Small blue block crystals formed after one week in 14% yield and were isolated directly by filtration. The crystals of complex **2** were suitable for single crystal X-ray diffraction.

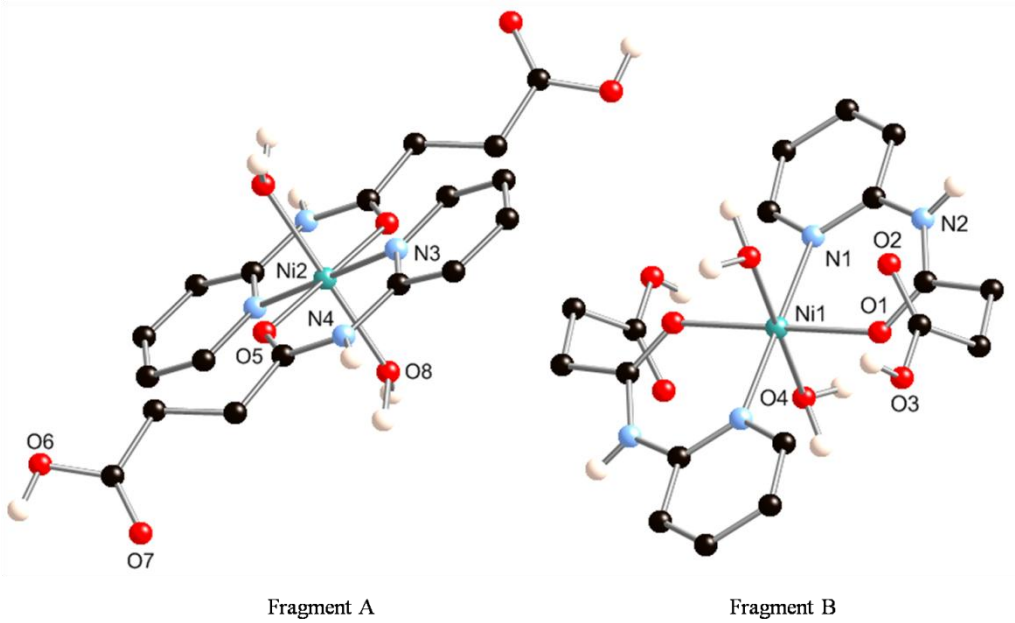

Figure 2.11 *Crystal structure of complex **2** with fragments **A** and **B** shown as they are orientated in the same crystal. Anions and non hydrogen bonding hydrogen atoms omitted for clarity.*

Complex **2** shown in Figure 2.11, crystallised in the $P2_1/c$ space group and refined with a R1 factor of 3.70%. In the unit cell, there are two complex molecules and four perchlorate anions. Within the perchlorate anion three of the oxygen atoms are disordered over two sites. The two fragments, **A** and **B**, of complex **2** are shown in Figure 2.11. In fragment **A** the carboxylic acid groups are guache to the plane of the pyridine rings, while in fragment **B** the carboxylic acid groups are anti to the plane of

the pyridine rings. Complex **2** has two **H_2L1** ligands chelating to a Ni(II) via the nitrogen atom N1 in the pyridine ring and the oxygen atom O1 in the amide group. The axial ligands in this case are two water molecules O4 and O8 which again, like the cobalt species, makes the Ni(II) metal ion in both fragments pseudo octahedral geometry.

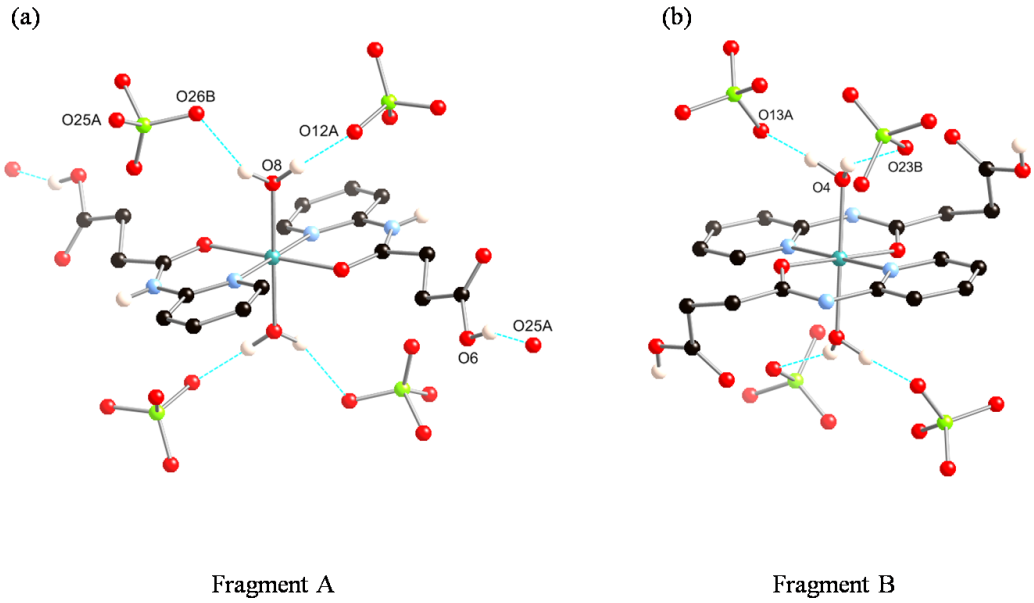

Figure 2.12 *(a) Hydrogen bonding between perchlorate anions and fragment **A** in the crystal structure of complex **2**. (b) Hydrogen bonding between perchlorate anions and fragment **B** in the crystal structure of complex **2**. All non hydrogen bonding hydrogen atoms omitted for clarity.*

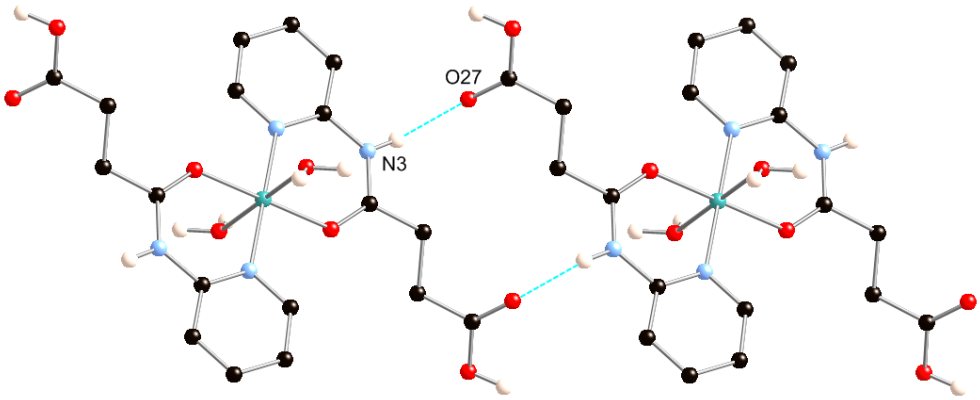

Figure 2.13 *Hydrogen bonding between neighbouring fragments of **A** in complex **2**. All non hydrogen bonding hydrogen atoms omitted for clarity.*

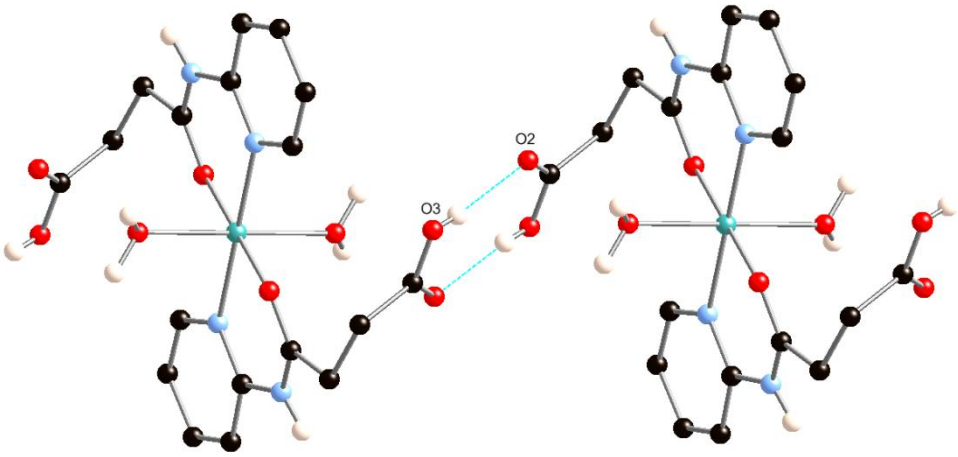

Figure 2.14 *Hydrogen bonding between neighbouring fragment **B** molecules. All non hydrogen bonding hydrogen atoms omitted for clarity.*

The two fragments of complex **2** hydrogen bond to themselves and one another. Fragment **A** hydrogen bonds to neighbouring molecules to form 1D hydrogen bonding chains via the hydrogen bond N4−H4···O7 between the nitrogen atom on the amido moiety and the carboxylic acid group oxygen atom on a neighbouring molecule as shown in Figure 2.13. Through hydrogen bonds O6−H6···O25A and O8−H8B···O26B two neighbouring fragment **A** chains link together via a perchlorate anion and the carboxylic acid group on one fragment **A** molecule and the axial water ligand on another. A 1D hydrogen bonding chain is formed between neighbouring fragment **B** molecules when the hydrogen bond O3−H3···O2 is formed shown in Figure 2.14. Chains of fragment **A** and **B** link together to form a 3D hydrogen bonding network. Three unique hydrogen bonds O8−H8A···O12A, O4−H4B···O13A and O4−H4C···O23B between the perchlorate anions and axial water ligands on both fragments link the chains together shown in Figure 2.12. The parameters for all hydrogen bonds are listed in Table 2.3.

Table 2.3 *Parameters for hydrogen bonds in complex* ***2****.*

D–H···A	D–H/Å	*d*(H···A)/Å	*d*(D···A)/Å	<(DH···A)/°	Symmetry codes
O3–H3···O2^{i}	0.811(18)	1.856(19)	2.663(3)	173(3)	i = 1+*x*,+*y*,+*z*
N4–H4···O7^{ii}	0.848(18)	2.054(4)	2.889(3)	168(3)	ii = -1+*x*,-1+*y*,+*z*
O8–H8A···O12A^{iii}	0.850(19)	1.93(2)	2.769(3)	168(4)	iii = 1-*x*,-*y*,-*z*
O4–H4B···O13A^{iv}	0.823(19)	2.20(3)	2.939(3)	150(4)	iv = -*x*,-1-*y*,1-*z*
O4–H4C···O23B	0.819(19)	2.10(3)	2.795(5)	143(4)	
O8–H8B···O26B^{iii}	0.834(19)	2.09(3)	2.818(6)	145(4)	
O6–H6···O25A	0.852(19)	1.97(2)	2.792(3)	161(4)	

As in complex **1**, complex **3** was formed by reacting **H_2L1** with a cobalt perchlorate. However, a nitromethane solution was used instead of acetonitrile solution. Toluene was used as the anti solvent in a vapour diffusion, and small block pink crystals formed within one week in 24% yield, which were suitable for single crystal X-ray diffraction.

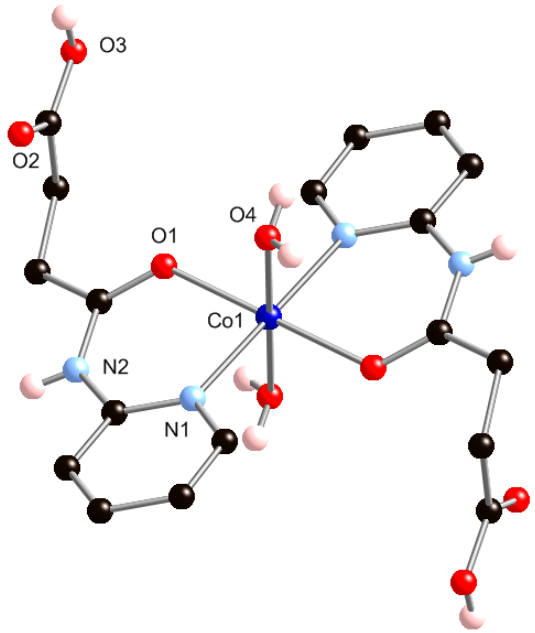

Figure 2.15 *Crystal structure of complex* ***3*** *with all perchlorate anions and nitromethane molecules removed for clarity. All non hydrogen bonding hydrogen atoms also removed for clarity.*

Complex **3**, shown in Figure 2.15, crystallised in the $P\bar{1}$ space group and refined with a R1 factor of 2.55% and shows similar features to complex **1**. One molecule of complex **3**, two perchlorate molecules and two nitromethane molecules comprise the unit cell. However instead of acetonitrile

axial ligands seen in complex **1**, water is coordinated in the axial positions of the Co(II) metal. This gives the metal ion a pseudo octahedral geometry.

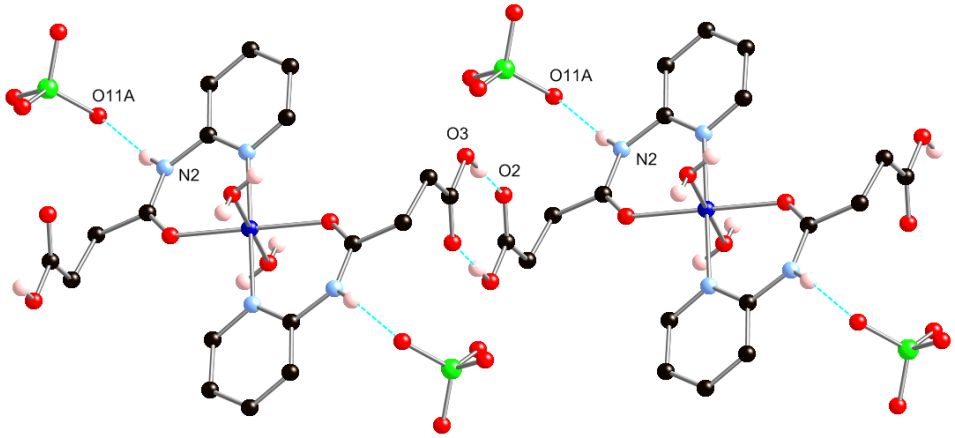

Figure 2.16 *Hydrogen bonds within the crystal structure of complex **3** between the carboxylic acid groups of two neighbouring complex **3** molecules. All non hydrogen bonding hydrogen atoms omitted for clarity.*

The axial water ligands and the anti configuration of the carboxylic acid groups combined with the perchlorate anions form a hydrogen bonding network. Complex **3** forms a 1D hydrogen bonding chain via the carboxylic acid functional groups as shown in Figure 2.16. Two neighbouring complex **3** molecules link to one another through the carboxylic acid groups, forming the hydrogen bond O3−H3···O2. In addition there is a hydrogen bond between the N2−H2 in the amido moiety and a perchlorate anion, N2−H2···O11A as shown in Figure 2.16. This hydrogen bond links the chains to four neighbouring chains. Parameters describing both these hydrogen bonds are listed in Table 2.4.

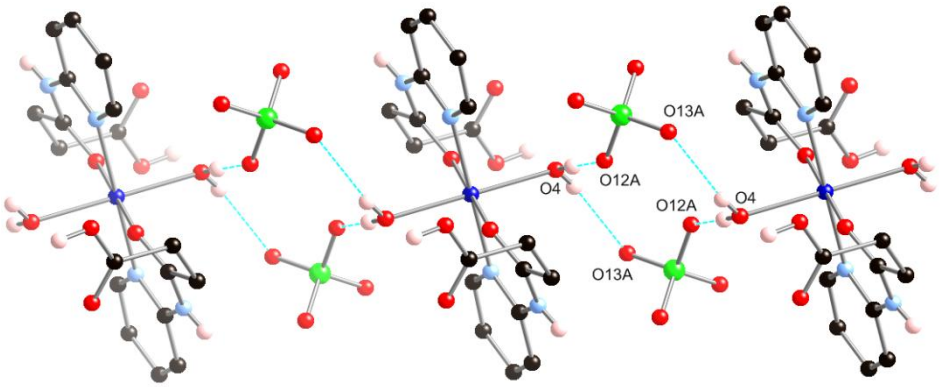

Figure 2.17 *Hydrogen bonding between the perchlorate anion and complex **3**. All non hydrogen bonding hydrogen atoms omitted for clarity.*

Further hydrogen bonding through the perchlorate anions allows complex **3** to link to further molecules. Figure 2.17 shows how the perchlorate anions link the 1D hydrogen bond chains together

to form a 3D hydrogen bonding network. The axial water ligands O4 link neighbouring chains through two separate oxygen atoms on the perchlorate anion. These hydrogen bonds are O4−H4B···O13A and O4−H4A···O12A with parameters for both listed in Table 2.4. Overall one chain hydrogen bonds to eight neighbouring chains via the described hydrogen bonds.

Table 2.4 *Parameters for hydrogen bonds in complex* ***3****.*

D–H···A	D–H/Å	*d*(H···A)/Å	*d*(D···A)/Å	<(DH···A)/°	Symmetry codes
N2–H2···O11A^{i}	0.824(15)	2.103(16)	2.9177(19)	170.1(19)	i = -*x*,1-*y*,1-*z*
O3–H3···O2^{ii}	0.830(16)	1.824(17)	2.6528(18)	176(2)	ii = 1-*x*,1-*y*,-*z*
O4–H4B···O13A^{iii}	0.798(16)	2.099(17)	2.8599(18)	159(2)	iii = 1-*x*,-*y*,1-*z*
O4–H4A···O12A	0.818(15)	2.029(16)	2.8419(19)	173(2)	

Copper perchlorate and **H_2L1** in acetone was used to prepare complex **4**. Using a slow diffusion crystallisation with diethyl ether as the anti solvent, blue needle crystals formed after one day in 14% yield, which were suitable for single crystal X-ray diffraction.

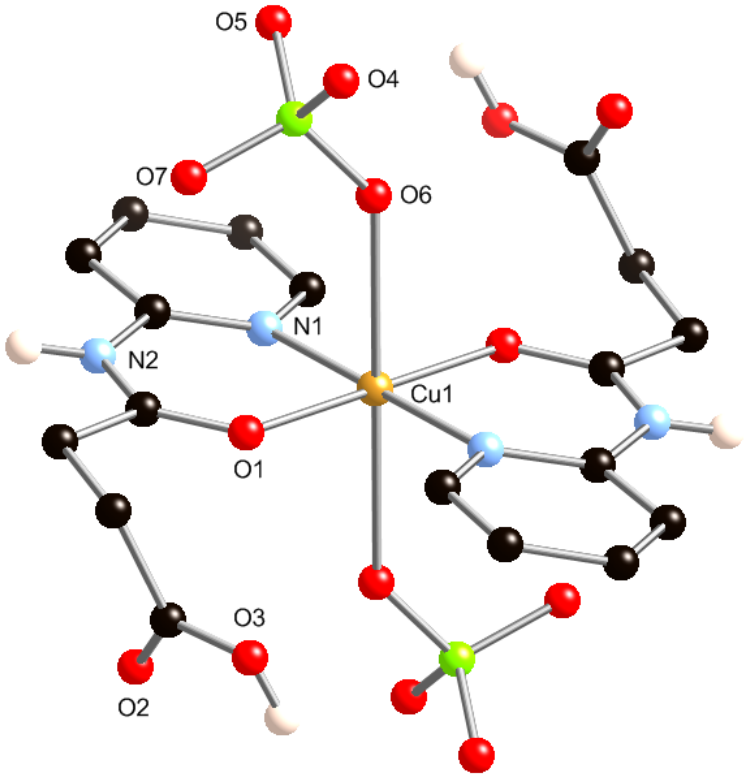

Figure 2.18 *Crystal structure of complex* ***4****. Solvent and non hydrogen bonding hydrogen atoms omitted for clarity.*

Complex **4** crystallised in the $P2_1/c$ space group, refined with a R1 factor of 2.75% and is shown in Figure 2.18. The unit cell is comprised of two complex **4** molecules and two acetone solvent molecules. Complex **4** shows similarities with complexes already discussed, with two **H_2L1** ligands chelated to a Cu(II) metal ion through the nitrogen atom N1 and oxygen atom O1. Again the carboxylic acid functional groups are anti to each other. Perchlorate anions coordinate to the Cu(II) ion as axial ligands with bond lengths of 2.4566(13) Å, giving a distorted pseudo octahedral geometry. This distortion is caused by the Jahn - Teller effect.[131-132]

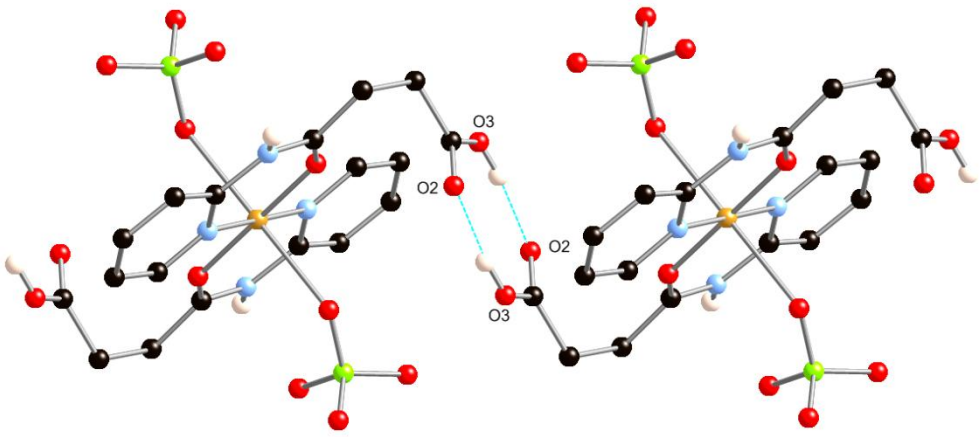

Figure 2.19 *Hydrogen bonding between molecules of complex **4**. Solvent and hydrogen atoms omitted for clarity.*

Figure 2.19 shows the hydrogen bonding between complex **4** molecules. These are between carboxylic acid groups. Neighbouring complex **4** molecules link to form 1D hydrogen bonding chains through the carboxylic acid function groups via the hydrogen bond O3–H3···O2. The parameters for the hydrogen bond are in Table 2.5.

Table 2.5 *Parameters for hydrogen bonds in complex **4**.*

D–H···A	**D–H/Å**	***d*(H···A)/Å**	***d*(D···A)/Å**	**<(DH···A)/°**	**Symmetry codes**
O3–H3···O2^{i}	0.73(3)	1.89(3)	2.6193(18)	173(3)	i = *-x,-y,1-z*

2.2.3.2. *Discrete complexes prepared from solvothermal synthesis.*

Complex **5** was prepared from nickel nitrate in acetonitrile solution under solvothermal conditions. The solution was heated at 100 °C for 36 hours and cooled to room temperature at 2 °C per hour. Small blue block crystals were isolated directly via filtration in 40% yield. The crystals were suitable for single crystal X-ray diffraction.

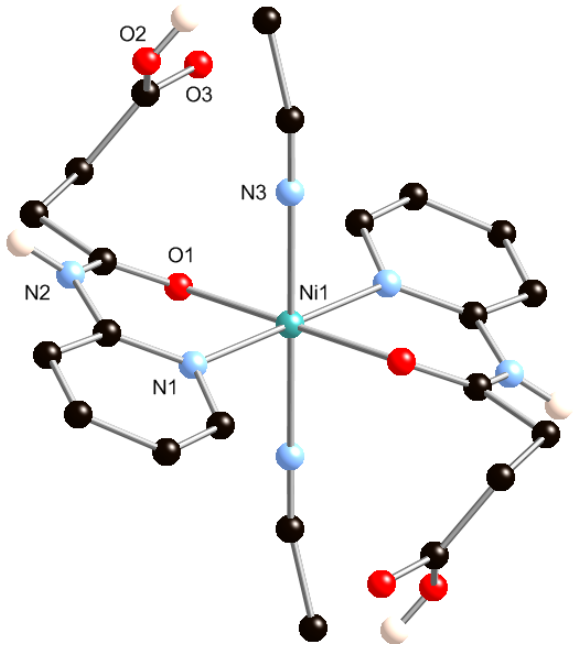

Figure 2.20 *Crystal structure of complex* ***5****. All anions, disorder in the acetonitrile axial ligands and non hydrogen bonding hydrogen atoms omitted for clarity.*

Complex **5** crystallised in the $P\overline{1}$ space group and refined with a R1 factor of 4.80%, is shown in Figure 2.20. Two complex **5** molecules and four disordered nitrate anions comprise the unit cell. The nitrate anion oxygen atoms are all disordered over two sites, each with half occupancy, and the nitrogen atom is in the same position. Like the previous complexes, two **H_2L1** ligands are coordinated to a Ni(II) ion with two axial ligands, in this case acetonitrile, giving the metal ion a pseudo octahedral geometry. Again there is disorder in the acetonitrile axial ligand with both carbon atoms disordered over two sites at half occupancy. The carboxylic acid functional groups are out of the plane of the rest of the ligand. The electron density confirmed the oxygen atoms O2 and O3 were with half occupancy hydrogen atoms confirmed by the bond lengths of carboxylic acid group oxygen atoms O2 and O3 which were both 1.2574(12) Å.

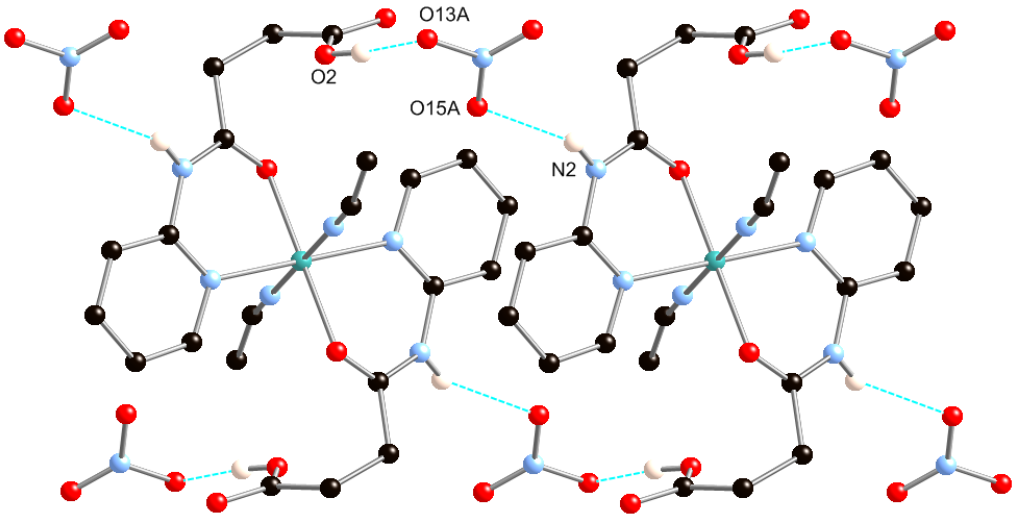

Figure 2.21 *Hydrogen bonding molecules of complex **5** and nitrate anions within the crystal lattice. All non hydrogen bonding hydrogen atoms omitted for clarity.*

A 1D hydrogen bonding chain is formed between neighbouring molecules of complex **5** shown in Figure 2.21. Nitrate anions hydrogen bond to two neighbouring complex **5** molecules. These hydrogen bonds are between the amido nitrogen atom and the oxygen atom, N2−H2B···O15A. The second hydrogen bond is between the nitrate anion oxygen atom to the oxygen atom on the carboxylate group, O2−H3···O13A. Parameters for both hydrogen bonds are in Table 2.6.

Table 2.6 *Parameters for hydrogen bonds in complex **5**.*

D–H···A	**D–H/Å**	***d*(H···A)/Å**	***d*(D···A)/Å**	**<(DH···A)/°**	**Symmetry codes**
O2–H3···O13A	0.863(8)	1.822(13)	2.6287(16)	154.9(18)	i = -1+*x*,+*y*,+*z*
N2–H2B···O15A^{i}	0.851(6)	2.081(6)	2.9095(15)	164.1(7)	

Complex **6** was prepared from crystals of the coordination polymer complex **10** which is described later in the coordination polymer section. Water was added to complex **10** crystals and allowed to stand overnight. Blue block crystals of complex **6** formed in 17% yield and were isolated directly by filtration. The crystals of complex **6** were suitable for single crystal X-ray diffraction.

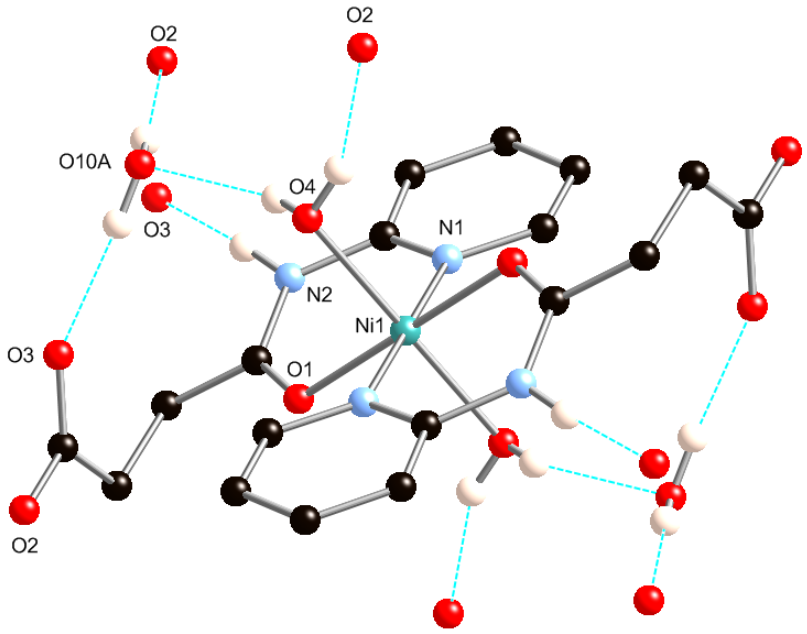

Figure 2.22 *The crystal structure of complex* ***6****. All non hydrogen bonding hydrogen atoms removed for clarity.*

Complex **6** shown in Figure 2.22, crystallised in the $P2_1/n$ space group and refined with a R1 factor of 4.12%. The unit cell comprises of two molecules of complex **6** and four solvent water molecules. Similar structural features of the previous complexes are evident in complex **6**. These include a pseudo octahedral geometry around the Ni(II) metal ion and two axial water ligands. Both carboxylic acid groups have deprotonated to form carboxylate groups, which are anti to the pyridine rings in complex **6**. There are five unique hydrogen bonds in the crystal lattice of complex **6** shown in Figure 2.22. Six neighbouring complex **6** molecules hydrogen bond together forming a 3D hydrogen bonding network. Two hydrogen bonds O4−H4A···O10A and O4−H4B···O2 link the solvent water molecule to the axial water ligands and carboxylate groups respectively, in the same molecule. Two hydrogen bonds from the solvent water molecule, O10A−H10A···O3 and O10A−H10B···O2 link to carboxylic acid oxygen atoms on two neighbouring complex **6** molecules. In addition the amido nitrogen atoms on **HL1** hydrogen bond to the carboxylic acids on two different molecules via the bond N2−H2···O3 with the parameters for this bond and four previous listed in Table 2.7.

Table 2.7 *Parameters for hydrogen bonds in complex* ***6****.*

D–H···A	D–H/Å	*d*(H···A)/Å	*d*(D···A)/Å	<(DH···A)/°	Symmetry codes
N2–H2···O3^{i}	0.863(17)	1.854(18)	2.715(3)	174(3)	i = 1/2-*x*,1/2+*y*,1/2-*z*
O4–H4A···O10A^{ii}	0.83(4)	1.91(4)	2.729(3)	169(3)	ii = 1/2-*x*,-1/2+*y*,1/2-*z*
O4–H4B···O2^{iii}	0.87(4)	1.91(4)	2.768(3)	169(3)	iii = -1+*x*,+*y*,+*z*
O10A–H10A···O3^{i}	0.81(4)	2.01(4)	2.807(3)	166(3)	iv = +*x*,1+*y*,+*z*
O10A–H10B···O2^{iv}	0.76(3)	2.01(4)	2.771(3)	173(4)	

Complex **7** was prepared from **H_2L1** and cobalt nitrate in acetonitrile solution via solvothermal synthesis. The solution was heated to 100 °C for 36 hours and cooled to room temperature at 2 °C per hour. Orange block crystals of complex **7** formed in 10% yield after allowing the red solution to stand covered for one day and were suitable for single crystal X-ray diffraction.

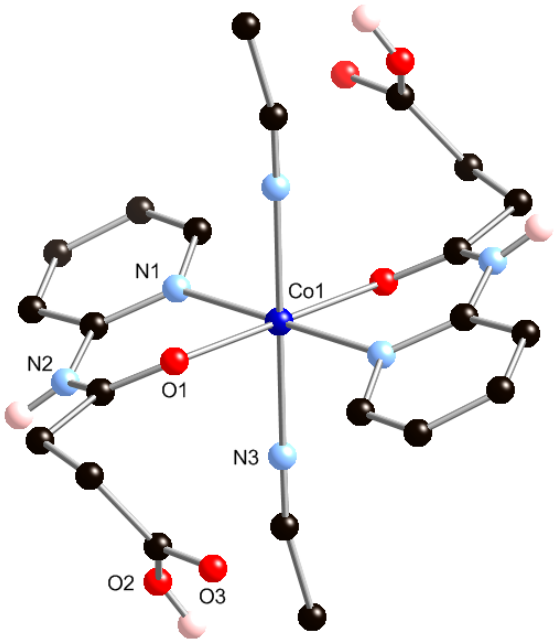

Figure 2.24 *Crystal structure of complex* ***7****. All anions and all non hydrogen bonding hydrogen atoms omitted for clarity.*

Figure 2.24 shows the crystal structure of complex **7** which crystallised into the $P2_1/c$ space group and refined with a R1 factor of 5.25%. It is similar in structure to complex **1**. The unit cell contains two complex **7** molecules and four nitrate anions. **H_2L1** chelates to the Co(II) metal ion via the pyridyl nitrogen atom N1 and amido oxygen atom O1. The Co(II) metal ion is again in pseudo octahedral geometry. The nitrate anions are disordered with the oxygen atoms evenly split over two sites. The two axial acetonitrile ligands are disordered over two sites with the end carbon atoms in half

occupancy although the disorder has been omitted for clarity from Figure 2.24. Electron density indicated that the proton of the carboxylic acid group was disordered over two oxygen atoms O2 and O3. This was confirmed by the carbon to oxygen bond lengths in the carboxylic acid group which were both 1.263(5)Å.

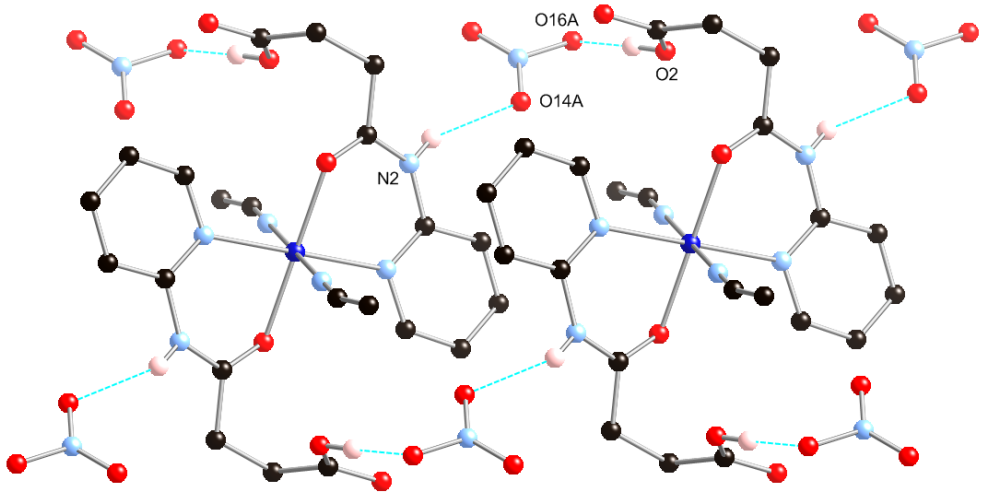

Figure 2.25 *Hydrogen bonding in the complex **7** crystal structure. All non hydrogen bonding hydrogen atoms omitted for clarity.*

Two important hydrogen bonds are shown in Figure 2.25, between neighbouring molecules and the nitrate anions. Two oxygen atoms in the nitrate anion link to the nitrogen atom in the amido group and the oxygen atom in the carboxylic acid. The hydrogen bonds are N2−H2B···O16A and O2−H2···O14A and form a 1D hydrogen bonding chain between neighbouring molecules. Parameters for the selected hydrogen bonds are listed in Table 2.8

Table 2.8 *Parameters for hydrogen bonds in complex **7**.*

D–H···A	D–H/Å	*d*(H···A)/Å	*d*(D···A)/Å	<(DH···A)/°	Symmetry codes
O2–H2···O16A	0.861(8)	1.756(8)	2.6159(19)	176.4(12)	i = 1+*x*,+*y*,+*z*
N2–H2B···O14A^{i}	0.856(7)	2.036(7)	2.8853(18)	172.0(9)	

While cobalt perchlorate gave two complexes, **1** and **3**, cobalt chloride in acetonitrile solution produced a discrete complex with **H_2L1** via solvothermal synthesis. The solution was heated to 100 °C for 24 hours and was cooled to room temperature at 4 °C per hour. Purple block crystals of complex **8** formed in 3% yield and were isolated directly by filtration. The crystals of complex **8** were suitable for single crystal X-ray diffraction.

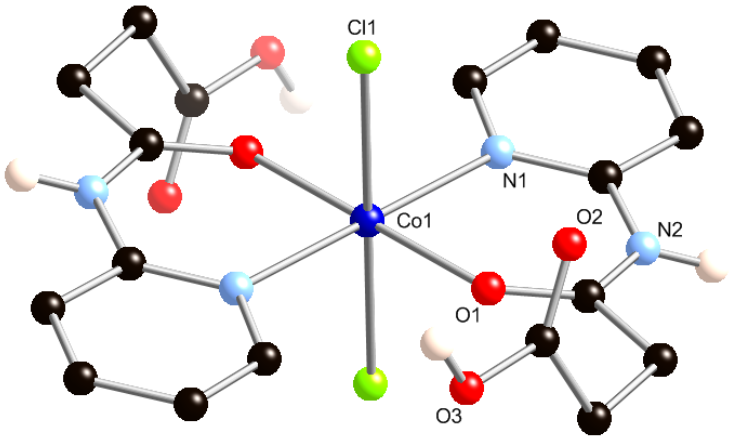

Figure 2.26 *Crystal structure of Complex **8**. Solvent, anions and non hydrogen bonding hydrogen atoms omitted for clarity.*

Complex **8** which crystallised in the $P\overline{1}$ space group and refined with a R1 factor of 3.13% is shown in Figure 2.26. A single molecule of complex **8** and two water molecules are in the unit cell. Bond lengths between the metal ion and the coordinated ligand atoms N1, O1 and Cl1 indicate the cobalt metal ion is in the +2 oxidation state. These were calculated due to the purple colour of the crystal potentially indicating a Co(III) metal complex. Like the previous cobalt complexes, complex **8** has two **H_2L1** ligands chelated to the Co(II) metal ion through the nitrogen atom N1 and oxygen atom O1, with two chloride atoms coordinated to the axial positions giving the metal ion a pseudo octahedral geometry. In addition the carboxylic acid groups are protonated and anti to the plane of the pyridine rings to each other.

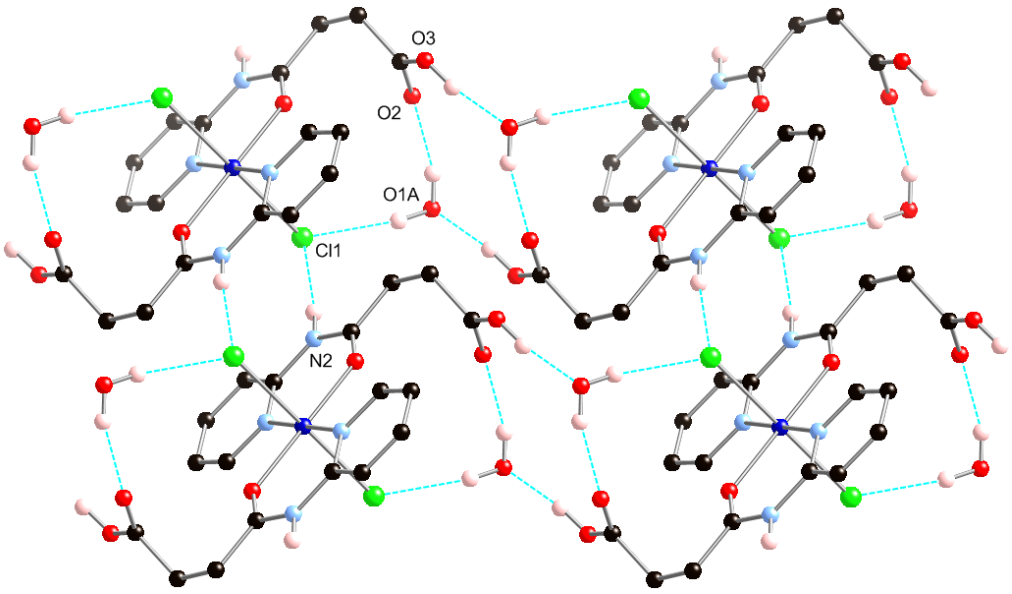

Figure 2.27 *Hydrogen bonding between complex **8** molecules. All non hydrogen bonding hydrogen atoms have been omitted for clarity.*

There is a significant amount of hydrogen bonding within the crystal lattice via the carboxylic acid functional groups, the water molecules and the bound chloride atoms. The chlorine atom Cl1 and carboxylic acid oxygen atom O2 act as the acceptor atoms while the water molecule acts as both an acceptor and donor atom for intermolecular hydrogen bonding shown in Figure 2.27. A 1D hydrogen bonding network is formed by the hydrogen bond N2−H2···Cl1 between the chlorine atom on one molecule and the amido nitrogen atom on another. The water molecule links to the chlorine atom and carboxylic acid through O1A−H1AA···Cl1 and O1A−H1AB···O2 on the same molecule. The 1D hydrogen network chains formed by complex **8** are linked together through the water molecule and the protonated carboxylic acid group on a neighbouring chain to form the hydrogen bond O3−H2···O1A. These two hydrogen bonds link different chains of complex **8** to give a 2D hydrogen bonding network. Parameters for the hydrogen bonds described in Figure 2.27 are in detailed in Table 2.10.

Table 2.10 *Parameters for hydrogen bonds in complex **8**.*

D–H···A	**D–H/Å**	***d*(H···A)/Å**	***d*(D···A)/Å**	**<(DH···A)/°**	**Symmetry codes**
O1A–H1AA···O2	0.846(14)	1.919(15)	2.7414(17)	163(2)	i = 1+*x*,+*y*,+*z*
O1A–H1AB···Cl1	0.847(12)	2.331(13)	3.1733(12)	173(2)	ii = -*x*,1-*y*,-*z*
N2–H2···Cl1^{i}	0.853(11)	2.3333(13)	3.1747(11)	168.9(15)	
O3–H3···O1A^{ii}	0.86(2)	1.73(2)	2.5767(17)	170.5(17)	

2.2.4. *Summary of mononuclear discrete complexes **1** - **8**.*

Eight mononuclear discrete complexes were prepared from the **H_2L1** ligand. Slow vapour diffusions with anti solvents or solvothermal techniques were used to crystallise the complexes **1** - **8**. Complexes **1** - **8** have carboxylic acids groups except for complex **6**. In complex **6** the carboxylic acids are deprotonated and forming a carboxylate group. Each discrete complex has two ligands coordinated in the same mode to a metal ion through the pyridine nitrogen atoms and amido oxygen atoms.

Where the axial ligands on a complex are coordinated water molecules a high degree of hydrogen bonding is seen in the crystal lattice. This is true for complexes **2**, **3** and **6**. A high degree of hydrogen bonding is also seen in complex **8** where the axial ligands are chloride ions. All four of these complexes form 3D hydrogen bonding networks and apart from complex **2** and **3** have non coordinated water molecules. Complexes with coordinated acetonitrile molecules as the axial ligands only form 1D hydrogen bonding polymers through the carboxylate groups and the counter ions in the crystal lattice. Complex **4** is the only discrete complex to have anions bound in the axial positions on the metal ion. Both complex **4** and complex **2** form 1D chains through hydrogen bonding between

carboxylic acid groups or between the carboxylic acid group and the amide nitrogen atom on neighbouring complexes.

2.2.5 *General synthesis and characterisation of coordination polymers complex **9** - **11**.*

Three coordination polymers were prepared from cobalt nitrate, cobalt chloride and nickel nitrate salts with **H_2L1** in acetonitrile under solvothermal conditions using a Teflon lined stainless steel acid digestion bomb. Once prepared the coordination polymers were characterised by several methods including; infrared spectroscopy, thermo gravimetric analysis, micro analysis, single crystal X-ray diffraction and X-ray powder diffraction. A description of all crystal structures, hydrogen bonding and π–π interactions, are discussed below. All complexes were fully characterised by elemental analysis and infrared spectroscopy. No mass spectra were obtained for complexes **9** - **11**. They were insoluble in all appropriate solvents.

2.2.6 *Description of structures for complexes **9** - **11***

2.2.6.1 *Coordination polymers prepared from solvothermal synthesis.*

Complex **9** was prepared from cobalt nitrate and ligand **H_2L1** in acetonitrile under solvothermal conditions, where the solution was heated to 100 °C for 36 hours and cooled to room temperature at 2 °C per hour. Small pink block crystals of complex **9** formed in 17% yield and were isolated directly through filtration. The crystals of complex **9** were suitable for single crystal X-ray diffraction.

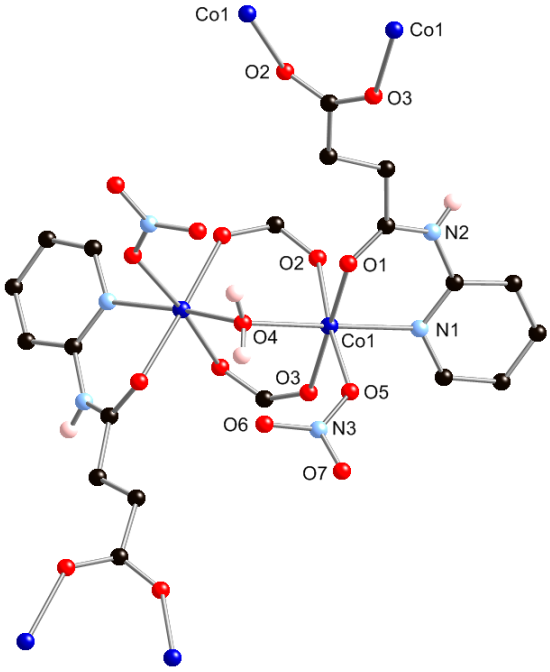

Figure 2.29 *The repeat structure of complex **9**. All non hydrogen bonding hydrogen atoms omitted for clarity.*

Complex **9**, shown in Figure 2.29, crystallised in the *C*2/*c* space group and refined with a R1 factor of 2.44%. The unit cell comprises eight asymmetric units of complex **9**. The carboxylic acid

functional group has deprotonated to form the **HL1** ligand. **HL1** is chelated to a Co(II) metal ion through the pyridine nitrogen atom N1 and amide oxygen atom O1 as was observed in the discrete complexes. Each carboxylate group bridges two equivalent cobalt atoms via two oxygen atoms O2 and O3, which extends the coordination polymer in two dimensions. In addition, a nitrate anion also coordinates through the oxygen atom O5 to the Co(II) metal ion. A pseudo octahedral geometry is formed by a half occupancy water molecule O4 coordinating to the Co(II) metal ion. Two equivalent cobalt metal ions are bridged by the water molecule O4 which lies on a special position and has a twofold rotation axis through it, forming the structure shown in Figure 2.29. The metal to bridging water molecule bond length is 2.1271(11) Å.

Planes formed by the pyridine ring atoms in the two **HL1** ligands are at a 57.20(9)° angle to each other while the metal to metal distance between symmetry equivalent Co(II) metal ions is 3.4821(7) Å. Like the discrete complexes, complex **9** has intermolecular interactions between pyridine rings on separate two dimensional sheets. These interactions are face to face π–π stacking interactions with the pyridine rings parallel to one another. The ring centroid to ring centroid distance in the pyridine ring atoms is 3.5242(15) Å. There are two unique hydrogen bonds in complex **9**. These hydrogen bonds are formed between two oxygen atoms on the nitrate anions, the bridging water molecule O4 and the amide nitrogen atom N2. The hydrogen bonds are N2−H2···O7 and O4−H4···O6 with the parameters for both detailed in Table 2.11. All of these hydrogen bonds are intermolecular just like those in shown in the discrete complexes.

Table 2.11 *Parameters for hydrogen bonds in complex **9**.*

D–H···A	**D–H/Å**	***d*(H···A)/Å**	***d*(D···A)/Å**	**<(DH···A)/°**	**Symmetry codes**
N2–H2···O7^{ii}	0.851(15)	2.051(17)	2.843(2)	155(2)	i = 1-*x*,+*y*,1/2-*z*
O4–H4···O6^{i}	0.845(15)	1.839(16)	2.6531(16)	161(2)	ii = 1/2+*x*,1/2+*y*,+*z*

Complex **10** was prepared from nickel nitrate with **H_2L1** in acetonitrile under solvothermal conditions. The solution was heated to 100 °C for 36 hours and cooled to room temperature at 2 °C per hour. Small green crystals formed in 21% yield and isolated directly via filtration and were suitable for single crystal X-ray diffraction.

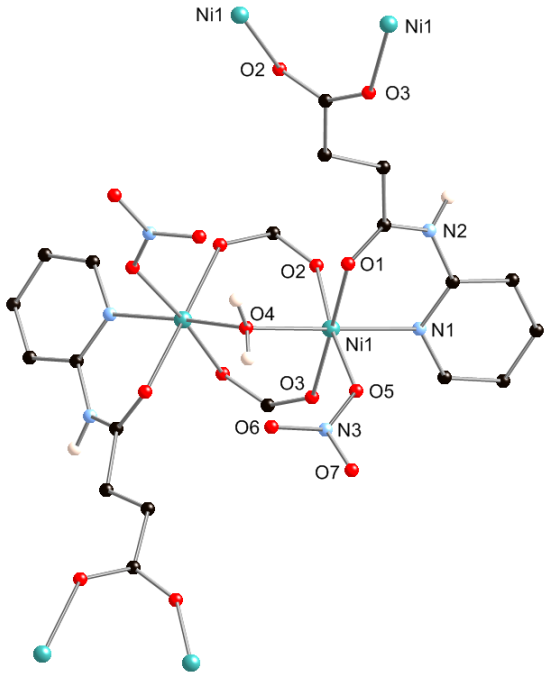

Figure 2.30 *The repeat structure of complex **10**. All hydrogen atoms omitted for clarity.*

Complex **10** is isostructural to complex **9** with a Ni(II) metal ion in a pseudo octahedral geometry. It crystallised in the C_2/c space group and refined with a R1 factor of 3.69%. The unit cell again comprises eight asymmetric units. Like complex **9**, the nickel metal ions are symmetry equivalent to each other and form a 2D coordination polymer. The metal to metal distance is 3.4546(10)Å, while the angle between the planes made up by the two pyridine rings is 56.22(10)° shown in Figure 2.30. Both the angle between pyridine rings and the metal to metal distance are shorter than those in the isostructural complex **9** which are 3.4821(7) Å and 57.20(9)° respectively. In addition the nickel metal ion to bridging water molecule bond length is 2.0650(12) Å compared to that of complex **9** where the bond length is 2.1271(11) Å.

Complex **10** exhibits similar hydrogen bonding, and π–π stacking interactions to complex **9**, however, variations in angles and bond distances for the hydrogen bonds are shown in Table 2.12. The ring centroid to ring centroid distance for the pyridine rings for the π–π stacking interaction varies to that of complex **9** which has a distance of 3.5242(15) Å, and is 3.5140(19) Å for complex **10.** Again the pyridine rings are parallel to each other.

Table 2.12 *Parameters for selected hydrogen bonds for complex **10**.*

D–H···A	D–H/Å	*d*(H···A)/Å	*d*(D···A)/Å	<(DH···A)/°	Symmetry codes
N2–H2···O7^{ii}	0.869(13)	2.059(19)	2.839(2)	149(2)	i = 1-*x*,+*y*,1/2-*z*
O4–H4···O6^{i}	0.839(15)	1.821(15)	2.640(2)	164.9(19)	ii = 1/2+*x*,1/2+*y*,+*z*

Both complex **9** and complex **10** exhibit the same topology. In order to determine the topology of complexes **9** and **10** nodes and links need to be defined. Battern suggested a link is something that links two nodes together and a node is something that is linked to three or more nodes.[3] The crystal structure or network must have a repeating pattern and because of this a finite number of unique nodes and links.[3] In the case of complex **9** and **10**, only nodes are defined, and the bridging water molecules between the two symmetry equivalent metal ions are considered to be the nodes of the network. Both nodes form a square geometry and link to four other nodes in the network. The node to node distances were 8.991(2)Å and 8.9430(9)Å for complex **9** and complex **10,** respectively. It was determined the topology for both coordination polymers was a [4,4] sheet, which is favoured by square planar nodes and both are shown in Figure 2.31.[3]

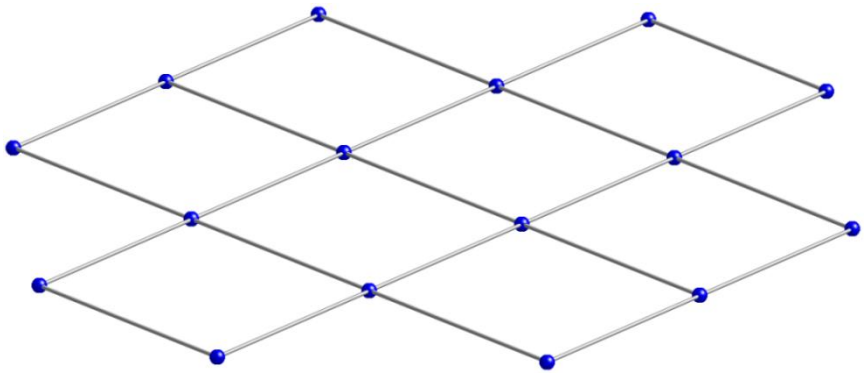

Figure 2.31 *Topology of the coordination polymer complexes **9** and **11** with the bridging water molecules assigned as nodes.*

Complex **11** was prepared from cobalt chloride and **H_2L1** in acetonitrile under solvothermal conditions, where the solution was heated to 100 °C for 48 hours and cooled to room temperature at 4 °C per hour. Pink needle crystals of complex **11** formed in 10% yield and were isolated directly through filtration. The crystals of complex **11** were suitable for single crystal X-ray diffraction.

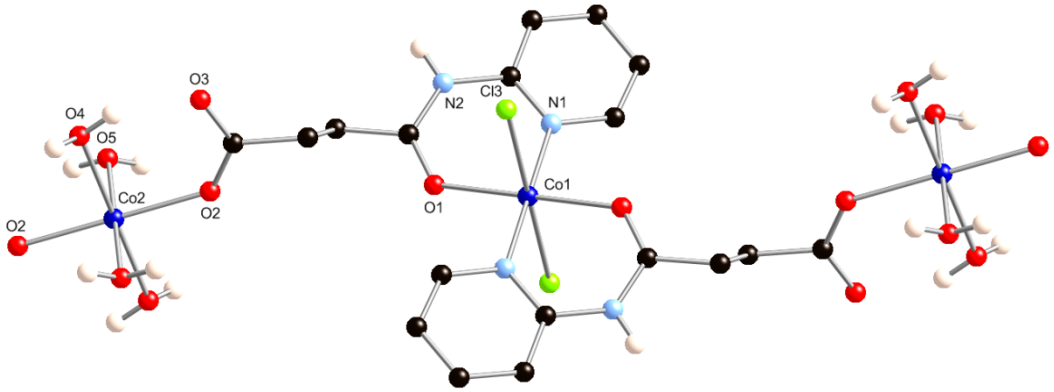

Figure 2.32 *Crystal structure of complex **11** with all solvent and non hydrogen bonding hydrogen atoms omitted for clarity.*

Complex **11** crystallised in the $P\bar{1}$ space group and refined with an R1 factor of 2.72% and is shown in Figure 2.32. Comprising the unit cell are two non-equivalent Co(II) metal ions, two **HL1** ligands, two chloride anions, four coordinated water molecules and two non-coordinating water molecules. Both Co1 and Co2 are Co(II) metal ions and both have pseudo-octahedral geometries. The carboxylate groups on the **H_2L1** ligands are deprotonated forming the **HL1** ligand, which chelates to the metal ion Co1, through the pyridyl nitrogen atom N1 and amido oxygen atom O1, while the carboxylate group oxygen atom O2 coordinates to the Co2 metal ion. Two chloride anions complete the coordination sphere of Co1 while four water molecules complete the coordination sphere of Co2. With **HL1** coordinating to both cobalt metal ions a 1D coordination polymer is formed.

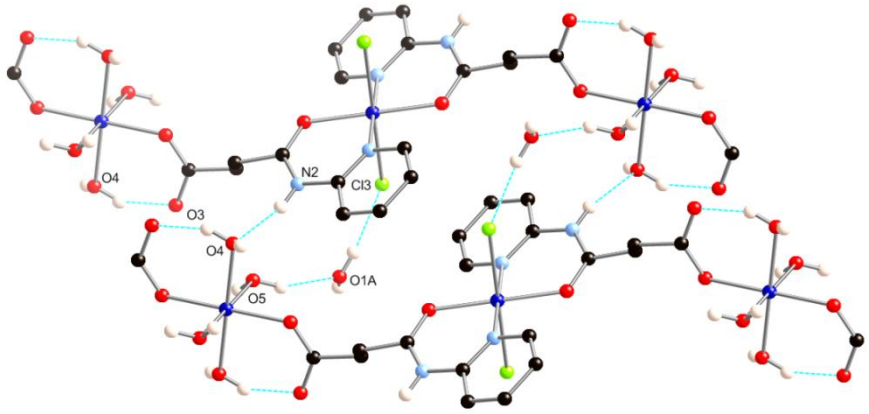

Figure 2.33 *Hydrogen bonding in complex **11** joining chains side by side. All non hydrogen bonding hydrogen atoms omitted for clarity.*

The non-coordinating water molecules, coordinating water molecule and chloride anions are available for hydrogen bonding. Shown in Figures 2.33 are the hydrogen bonds that are present in the crystal structure of complex **11**. There are seven unique hydrogen bonds which connect one chain to six neighbouring chains. There is one intramolecular hydrogen bond O4–H4A···O3 while the remaining six are intermolecular hydrogen bonds which links one complex **11** strand to six neighbouring strands. The parameters for the hydrogen bonds in complex **11** are listed in Table 2.13. A 3D hydrogen bonding network is formed between chains of complex **11**.

Table 2.13 *Parameters for hydrogen bonds for complex **11**.*

D–H···A	D–H/Å	*d*(H···A)/Å	*d*(D···A)/Å	<(DH···A)/°	Symmetry codes
O5–H5A···O1A^{i}	0.761(13)	2.046(7)	2.771(2)	159.2(18)	i = +*x*,1+*y*,+*z*
O5–H5B···O1A^{ii}	0.911(9)	1.833(9)	2.689(2)	155.7(2)	ii = 1-*x*,2-*y*,1-*z*
O4–H4A···O3	0.885(5)	1.753(10)	2.605(2)	160.7(15)	iii = +*x*,1+*y*,-1+*z*
O4–H4B···Cl3^{iii}	0.864(7)	2.269(10)	3.1244(15)	170.4(15)	iv = +*x*,-1+*y*,+*z*
O1A–H1AA···O4^{iv}	0.849(17)	1.825(18)	2.664(2)	169(3)	v = +*x*,+*y*,-1+*z*
O1A–H1AB···Cl3^{v}	0.837(17)	2.268(18)	3.0790(16)	164(2)	vi = -*x*,2-*y*,1-*z*
N2–H2···O4^{vi}	0.832(15)	2.238(10)	2.995(2)	151.4(9)	

2.2.6.2. *Thermogravimetric analysis for complexes **9** - **11**.*

Shown in Figure 2.34 are the thermogravimetric analyses (TGA) plots which show the thermal behaviour of complexes **9** to **10**. Complexes **9** and **10** show losses of 2.91% and 2.81%, respectively, which were consistent with the loss of the bridging water molecules calculated as 2.79% and 2.81% for complex **9** and **10**. These losses occurred at 122 °C < T < 140 °C for complex **9** and 147 °C < T < 168 °C. The difference in temperatures where the loss of the bridging water molecules occurs is because the different sizes of the metal ions and the relative bond strengths leads to a change in bond lengths between the bridging water molecule and the metal ions. Both complex **9** and **10** are stable up until 250 °C and 288 °C, respectively, before decomposition occurs. Full decomposition of both complex **9** and **10** is complete by 550 °C and 490 °C, respectively.

The thermal behaviour of complex **11** was also studied via TGA, shown in Figure 2.34. A weight loss of 15.60% was seen over 91 °C < T < 112 °C which was consistent with the four coordinated water molecules on Co2 and two non coordinating water molecules being lost calculated at 15.80%. Slow decomposition of complex **11** occurred from 112 °C until the complex was fully decomposed by 620°C.

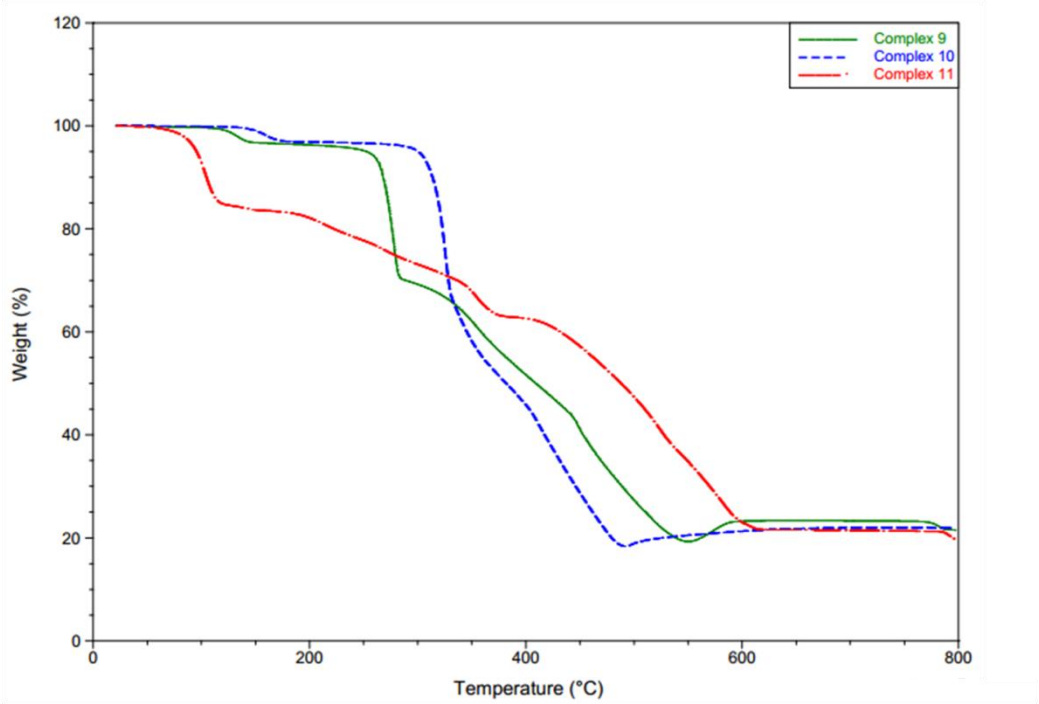

Figure 2.34 *Thermogravimetric analysis (TGA) plots for complexes **9** to **11**.*

2.2.7 *Summary of coordination polymers, complexes **9** - **11**.*

Through solvothermal techniques three coordination polymers were prepared with the **H_2L1** ligand in acetonitrile solutions. Both complex **9** and **10** were prepared with cobalt nitrate and nickel nitrate, respectively, which produced isostructural coordination polymers. For both complexes two symmetry equivalent metal(II) ions were bridged by a coordinated water molecule. The symmetry equivalent metal ions had octahedral geometries and were bridged by carboxylate groups from the **HL1** ligand. This formed [4,4] 2D coordination polymers. Two intermolecular hydrogen bonds were seen within complexes **9** and **10**. Thermogravimetric analysis was run on both structures which showed similar loss of the coordinated bridging water molecule and decomposition of the coordination polymers.

In the case of complex **11** cobalt chloride was used with the **H_2L1** ligand in acetonitrile solution with 1 mL of water. This complex showed two crystallographically different Co(II) ions. One with two **HL1** ligands and two chloride axial ligands coordinated and another with carboxylate oxygen atoms from the **HL1** ligands and four coordinated water molecules. The overall structure was a 1D coordination polymer. The presence of water in the preparation meant non-coordinated water solvent molecules were present in the crystal lattice. This coupled with the chloride axial ligands and the coordinated water molecules on one of the Co(II) ions allowed for significant hydrogen bonding in the

crystal lattice. Thermogravimetric analysis was run on complex **11** which showed the loss of the four coordinated water molecules and the non-coordinated water molecules.

2.2.8 *Synthesis and characterisation of complexes **12** - **14**.*

Four metal clusters were isolated from slow evaporation crystallisations. Methanol and acetonitrile were used to prepare each metal organic cluster. All metal clusters were fully characterised by micro analysis, infrared spectroscopy, X-ray powder diffraction and single crystal X-ray diffraction. Magnetic susceptibility of all metal organic clusters is also reported. No mass spectra were obtained for complexes **12** - **14**. All complexes appeared to break down into the ligand and no fragments of the complexes were seen in the spectra.

2.2.9 *Description of structures of complexes **12** - **14**.*

2.2.9.1 *Single crystal X-ray diffraction and discussion of complex **12**.*

The metal organic cluster complex **12** was synthesised from cobalt perchlorate with **H_2L1** in methanol with triethylamine as the base. The solution was allowed to stand and evaporate, after one week pink block crystals of complex **12** formed in only 1% yield and were isolated by filtration. The crystals were suitable for single crystal X-ray diffraction. Further crops of crystals formed in the filtrate over time, however, this was not required for full characterisation of complex **12**.

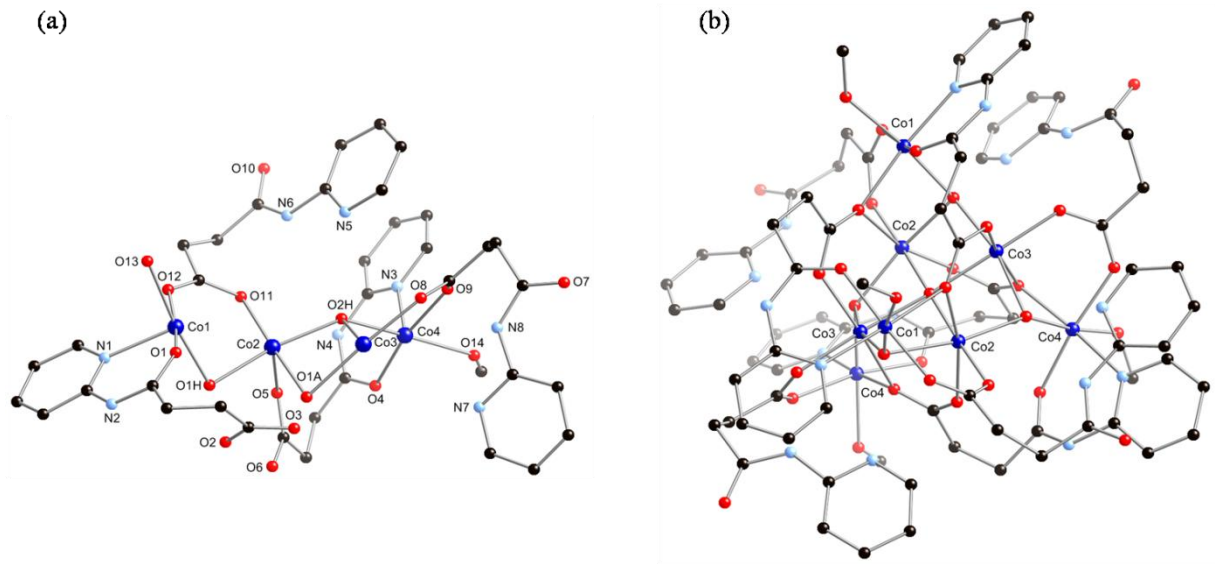

Figure 2.35 *(a) Crystal structure of the asymmetric unit of metal cluster complex **12**. (b) Full structure of metal cluster complex **12**. All anion molecules, solvent molecules omitted for clarity.*

Complex **12** crystallised in the *C*2/*c* space group, refined with a R1 factor of 5.30% and is shown in Figure 2.35. The full crystal structure of complex **12** is complicated due to the large amount of atoms that make up the metal cluster and hence the asymmetric unit for complex **12** is also shown for clarity. The unit cell of complex **12** comprises four complex **12** molecules, twelve perchlorate anions, twenty methanol and eight water solvent molecules. Complex **12** is a octanuclear cobalt cluster which contains eight **HL1** ligands, one μ_4-OH moiety, four μ_3-OH moieties and four methanol axial ligands on four of the cobalt metal ions. There is disorder in one of the perchlorate anions where the chlorine atom in half occupancy over two sites. Two oxygen atoms also on the same perchlorate anion are in half occupancy over two sites. The axial ligand on the cobalt metal ion Co1 is disordered with 60% of the time it being a coordinated water ligand and 40% of the time it being a coordinated methanol ligand.

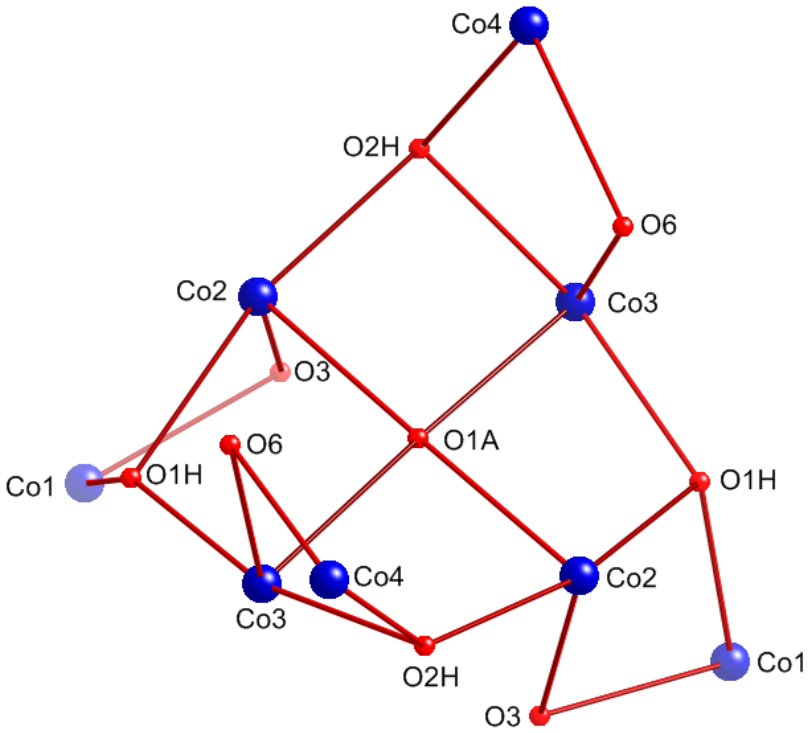

Figure 2.36 *The bridging oxygen atoms between the octanuclear core of complex **12**. All other atoms omitted for clarity.*

There are four crystallographic independent cobalt metal ions, all of which are Co(II). The Co(II) metal ions exhibit pseudo octahedral geometry. Figure 2.36 shows the bridging oxygen atoms involved in the core of complex **12**. There is one μ_4-OH, oxygen atom O1A, which is protonated indicated by the calculated valence state. However, the proton was not refined in the crystal structure but the thermal ellipsoids of O1A are elongated most probably indicating the presence of the hydroxide proton. O1A bridges between two Co2 and two Co3 atoms forming a square and has a -1 valence state. While four μ_3-O hydroxide moieties, two O1H and two O2H oxygen, bridge three

different cobalt metal ions and have a valence state of -1. The μ_3-OH moieties bridge both a Co2 and Co3 cobalt metal ion and either a Co1 or Co4 cobalt metal ion. The oxygen atoms from the carboxylate groups in **HL1**, O3 and O6 bridge the Cu1 and Cu4 atoms to Co2 and Co3 atoms, respectively. The metal core in the cluster complex **12** is not unique and is seen in octanuclear cobalt clusters such as that reported by Akine.[81] A discussion of the differences and similarities between the two metal clusters is in the magnetic section for complex **12**.[62, 81]

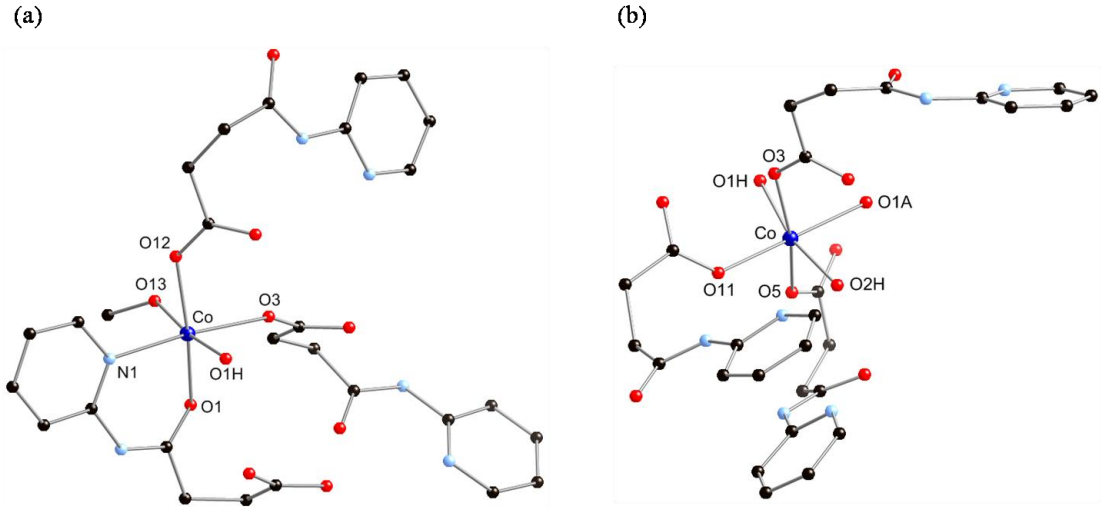

Figure 2.37 *(a) Coordination mode of cobalt metal ions Co1 and Co4. (b) Coordination mode of cobalt metal ions Co2 and Co3. All anions, solvent and hydrogen atoms omitted for clarity.*

There are two different coordination modes of the cobalt metal ions shown in Figure 2.37. The coordination sphere of the cobalt metal ions Co1 and Co4 have three **HL1** ligands coordinated to them through the amido group and carboxylate group oxygen atoms and pyridyl nitrogen atoms. The two remaining sites in the coordination sphere are occupied by a methanol ligand for Co4 and a methanol 40% of the time and a water molecule 60% of the time for Co1 due to disorder in the axial ligand.

The coordination mode of Co2 and Co3 atoms involve the coordination of three **HL1** ligands and is also shown in Figure 2.37. The **HL1** ligands coordinate to the two non-equivalent Co(II) metal ions through one oxygen atom from each carboxylate group of the **HL1** ligands. Two bridging μ_3-OH moieties and one μ_4-OH moiety complete the coordination spheres of the cobalt metal ions Co2 and Co3. The Co-O bond lengths, including the μ_4-OH and μ_3-OH oxygen atoms, are in the range of 2.0378(1) Å to 2.1789(2) Å. While the Co-N bond lengths range from 2.1360(1) Å to 2.1512(1) Å between the pyridyl nitrogen atoms and the Co2 and Co3 atoms.

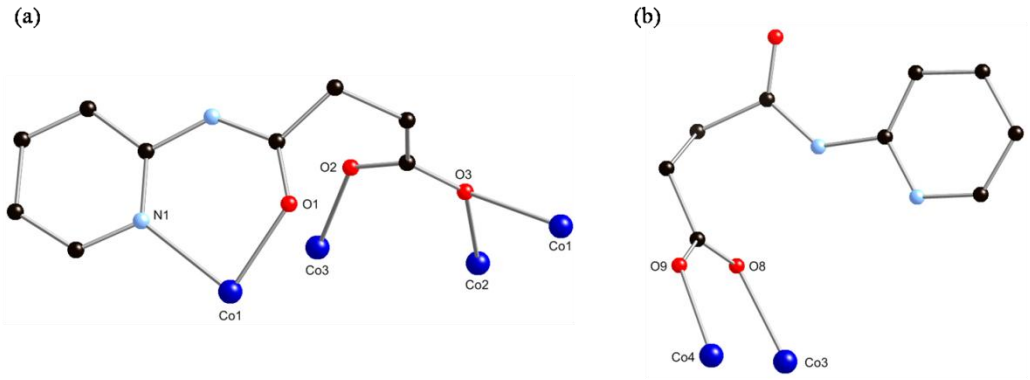

Figure 2.38. *(a) Coordination mode of the **HL1** ligands coordinated through the carboxylate, amido and pyridine moieties in complex **12**. (b) Coordination mode of the **HL1** ligands coordinated through the carboxylate moiety in complex **12.***

The **HL1** ligands in complex **12** have two different coordination modes shown in Figure 2.38. The outer ligands coordinate through the carboxylate group oxygen atoms and bridge two non-equivalent cobalt metal ions. These are either a Co1 or Co4 cobalt metal ion and either a Co2 or Co3 cobalt metal ion. While the inner ligands coordinate to four cobalt anions, three of which are non-equivalent to each other. The pyridine ring nitrogen atom and the amido oxygen atom chelate to either Co1 or Co4 cobalt metal ions. In addition the carboxylate group bridges three cobalt metal ions. One oxygen atom coordinates to either Co2 or Co3 and the other to a symmetry equivalent cobalt metal ion Co1 or Co4 and either Co2 or Co3.

2.2.9.2 *Magnetic susceptibility Measurements for complex **12**.*

Magnetic susceptibility measurements were carried out on complex **12** shown in Figure 2.39. Complex **12** has a $\chi_M T$ value of 18 cm^3 mol^{-1} K at 300 K , which is consistent with 8 uncoupled S = 3/2 Co(II) ions with a g value of 2.19. The $\chi_M T$ value of gradually decreases with decreasing temperature to a value of 0.8 cm^{-3} mol^{-1} K at 2 K. This decrease in $\chi_M T$ with decreasing temperature indicates dominant antiferromagnetic interactions between the Co(II) ions in complex **12**.

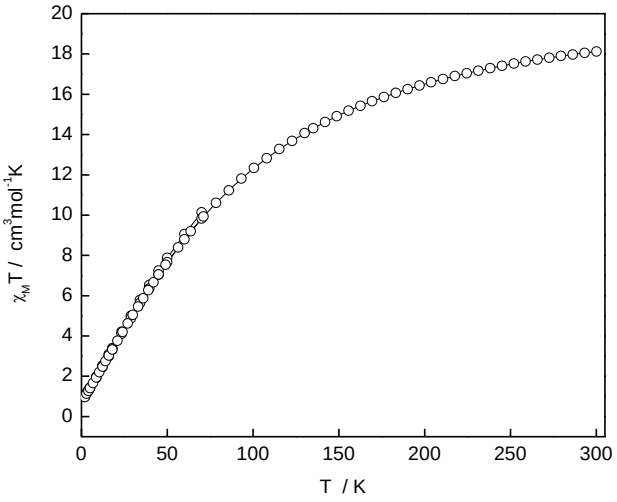

Figure 2.39 *The plot of $\chi_M T$ vs T with an applied dc field of 1 T for the metal cluster complex **12**.*

The magnetisation (M) isotherms shown in Figure 2.40 were run using dc fields ranging from 0 to 50,000 Oe (5 T) and temperatures ranging from 2 to 20K. As shown the M values do not become saturated but show that complex **12** has a small non-zero spin ground state. These plots confirm that antiferromagnetic interactions dominate within complex **12**. Modelling the magnetic data are difficult with in Co(II) systems due to crystal field effects and the strong orbital moment present. Due to eight Co(II) metal ions being in complex **12** quantifying the magnetic data are difficult.

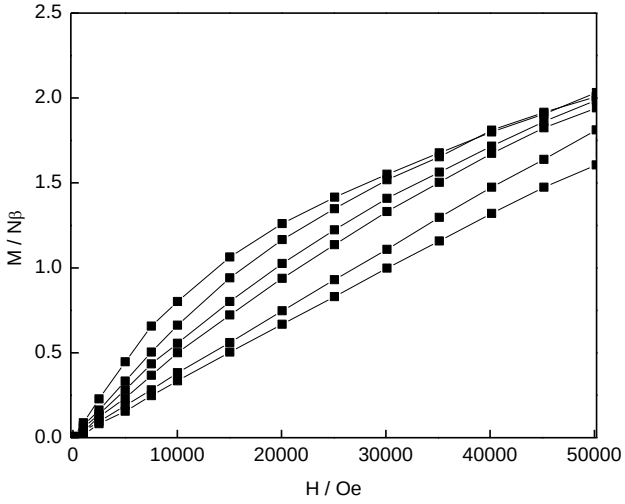

Figure 2.40 *The magnetisation (M) isotherm plots of complex **12**. The temperatures 2K (top) 3K, 4K, 5.6K, 10K and 20K (bottom) are plotted for complex **12**.*

Antiferromagnetic interactions are common in Co(II) ion clusters reported in the literature.[81, 133-135] An octanuclear Co(II) cluster prepared by Akine[81] shows similar magnetic behaviour shown in complex **12**. The cluster has a similar core to that of complex **12**; however does not have a bridging μ_4-OH moiety and the Co(II) ions are in trigonal bipyramidal geometry compared to the pseudo octahedral geometry of the Co(II) ions in complex **12**. They reported a $\chi_M T$ value of 17.6 cm^3 mol^{-1} K at 300 K which compares to the $\chi_M T$ value of complex **12**. The $\chi_M T$ value of the cluster decreased gradually over temperature to 2.41 cm^3 mol^{-1} K at 1.8 K. This suggests the dominant interactions are antiferromagnetic in the complex which is also the case in complex **12**. An example of ferromagnetic interactions in an octanuclear Co(II) ion cluster with 2,2'-biphenol ligands is reported by Jones.[136] The $\chi_M T$ value at 300K is 20.76 cm^3 mol^{-1} K, $\chi_M T$ gradually rises as the temperature approaches 50K. $\chi_M T$ rises rapidly to reach a maximum value of ~33 cm^3 mol^{-1} K at 5K. This is indicative of ferromagnetic interactions.

2.2.9.3 *Single crystal X-ray diffraction and discussion for complex **13**.*

The metal organic cluster complex **13** was synthesised from copper acetate and **H_2L1** in methanol with triethylamine used as a base to deprotonate the ligand. A slow evaporation crystallisation produced large green block crystals after two weeks which were isolated directly in 11% yield. The crystals were suitable for single crystal X-ray diffraction. More crystals formed from the filtrate the original crystals were taken from over time, however, the yield was enough to fully characterise the metal cluster.

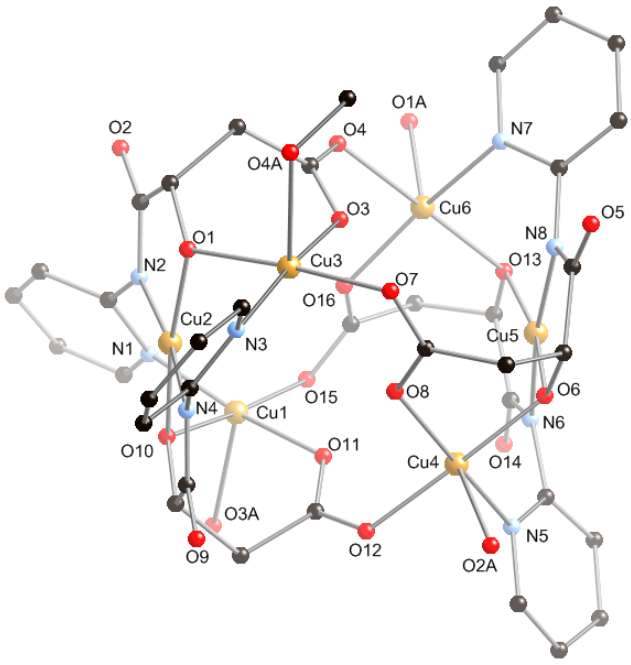

Figure 2.41 *Crystal structure of complex **13**. All solvent and hydrogen atoms omitted for clarity.*

Complex **13** crystallised in the C_2/c space group, refined with a R1 factor of 3.31% and is shown in Figure 2.41. The unit cell comprises eight complex **13** molecules and eight methanol solvent molecules. Complex **13** is a hexanuclear Cu(II) cluster with four **L1A** ligands. The structure of **L1A** is shown in Figure 2.42. Four copper metal ions are in square pyramidal geometry with either water molecules or methanol molecules as the axial ligands. In addition two copper atoms are in the square planar geometry and are bound exclusively by ligand donor atoms.

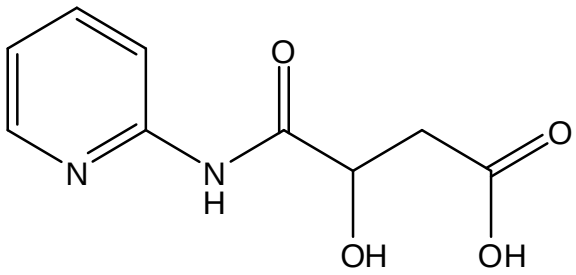

Figure 2.42 *The structure of* ***H_2L1A*** *oxidised from the* ***H_2L1*** *ligand.*

During the preparation of complex **13**, the ligand **H_2L1** was oxidised *in situ* to the **H_2L1A** ligand shown in Figure 2.42. Hydroxylation has occurred on the α-methylene adjacent to an amido group of the ligand. Complex **13** was prepared from $Cu(OAc)_2.H_2O$ and **H_2L1** in a methanol solution with triethylamine as a base while being stirred at 50 °C. The base was added to deprotonate the ligand at the carboxylic acid group to form a carboxylate group for coordination to the copper metal ions. A one-to-one ratio of metal salt to **H_2L1** ligand was used, and the resulting green solution was left to evaporate. After two weeks the green solution had formed dark green blocks of complex **13** in 11% yield. This equates to a 11% yield of the deprotonated form of the ligand **L1A**. Another solution with a three-to-two ratio of metal salt to **H_2L1** ligand was prepared, to match the ratio observed in the crystal structure of complex **13**, with one equivalent of triethylamine per ligand added. The solution turned green after 15 minutes of heating and stirring before a light green precipitate formed from a light blue solution. No crystals of complex **13** or the ligand were obtained.

Hydroxylation of an carbon atom α to the carbonyl of an amide is not unprecedented in the literature with one example of a molecule similar to ligand **H_2L1,** where α-hydroxylation has occurred through metal directed oxidation.[137] The metal directed hydroxylation involves a Cu(I) ion species which uses molecular oxygen as the oxidant,[137] is shown in Figure 2.43.

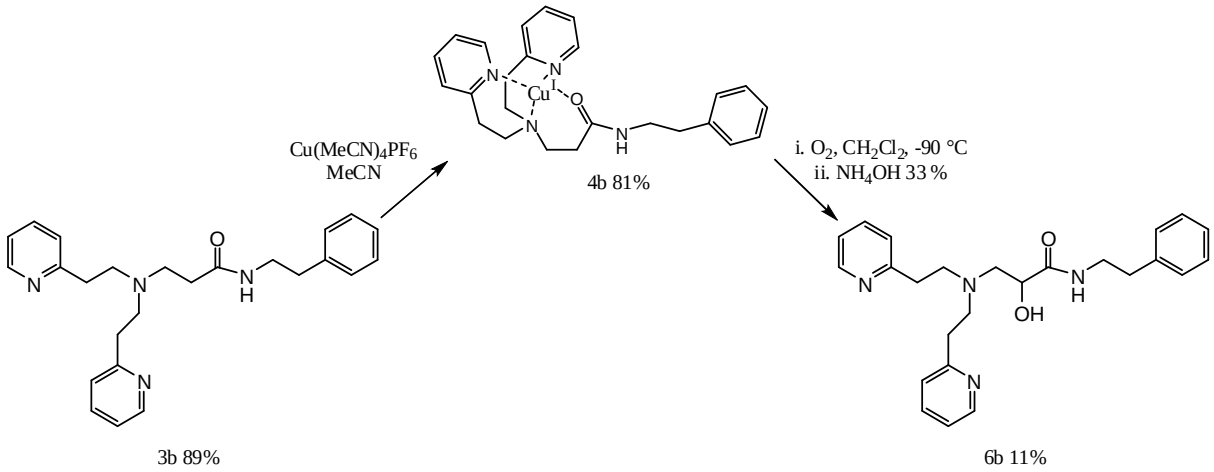

Figure 2.43 *Reaction scheme of the preparation of 6b, showing the metal directed oxidation of an α-methylene adjacent to an amide group.*[137]

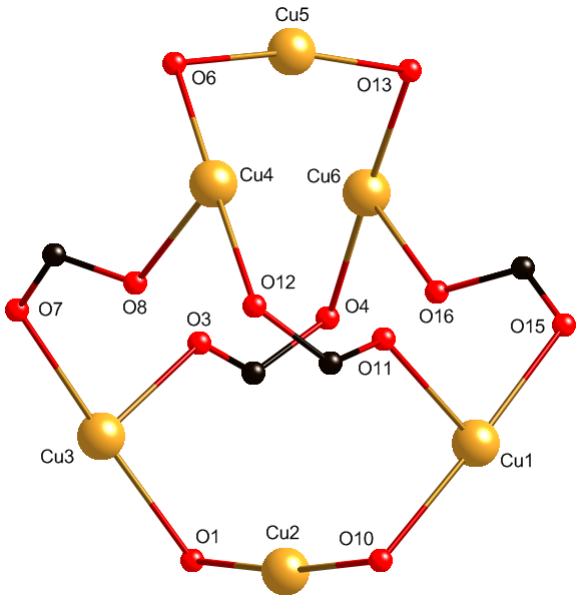

Figure 2.44 *The bridging oxygen and carbon atoms between the hexanuclear core of complex **13**. All other atoms and solvent molecules omitted for clarity.*

The hexanuclear core of complex **13** is made up for six non-equivalent copper metal ions Cu1-Cu6 shown in Figure 2.44. In Figure 2.44 three copper metal ions are bridged by two hydroxide oxygen atoms on two **L1A** ligands forming two dimers. These dimers are linked by the four carboxylate moieties on the four **L1A** ligands to form the cluster.

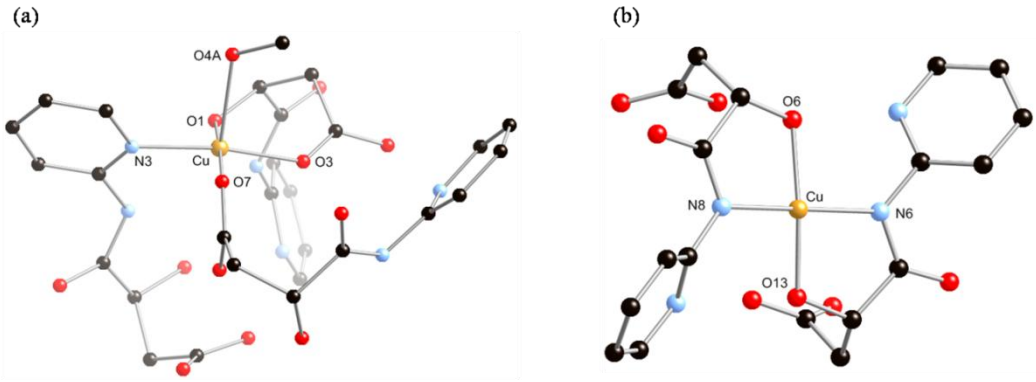

Figure 2.45 *(a) The square pyramidal coordination geometry of four copper metal ions, Cu1, Cu3, Cu4 and Cu6 in complex **13**. (b) The square planar coordination geometry of two copper metal ions, Cu2 and Cu5 in complex **13**. All other atoms and solvent molecules omitted for clarity.*

The two coordination geometry modes for the six copper metal ions are shown in Figure 2.45. Four copper metal ions; Cu1, Cu3, Cu4 and Cu6, have square pyramidal geometry where on Cu1, Cu4 and Cu6 the axial ligand is water. While the axial ligand on the copper metal ion Cu3 is a methanol molecule, which breaks the symmetry within the cluster. The coordination sphere on all four copper metal ions is completed by coordination to three **L1A** ligands through the pyridine nitrogen atom, the alkoxide and carboxylate group oxygen atoms on the same **L1A** ligand and via a bridging carboxylate group oxygen atom. Bond lengths in the four square pyramidal geometry copper metal ions to the oxygen atoms of the carboxylate groups in the **L1A** ligands range from 1.945(2) Å - 1.982(2) Å. While the bond lengths from copper metal ions to the nitrogen atoms, in the pyridine rings, range from 1.983(3) Å - 2.011(2) Å. The oxygen atom bonds lengths in the axial ligands to the copper metal ions range from 2.317(2) Å - 2.439(2) Å. The τ_5 value for the square pyramidal copper metal ions was calculated using Reedijk's method.[138] This is defined as (β-α)/60°, where β is the angle through the metal ion between donor atoms considered in the axial positions of the trigonal bipyramid (or a trans angle through the basal plane of a square pyramid), and α is the largest equatorial angle of the trigonal bipyramid (or the remaining trans angle in the basal plane), where a value of zero indicates a perfect square pyramidal geometry and a value of one represents trigonal bipyramidal geometry. All four copper metal ions with axial ligands are approximately square pyramidal geometry with the τ_5 values being 0.053, 0.074, 0.15 and 0.18 for Cu1, Cu3, Cu4 and Cu6, respectively.

The two copper metal ions, Cu2 and Cu5 have square planar geometry both of which have two **L1A** ligands chelating to them. Shown in Figure 2.45 is the coordination sphere of the copper metal ion is made up of two nitrogen atoms from separate **L1A** ligands coordinating to the Cu2 and Cu5 atoms. The coordination sphere is completed when the alkoxide oxygen atoms from the same **L1A** ligands coordinate. The two square planar copper metal ions have bond lengths to the alkoxide oxygen atoms, in the **L1A** ligand, in the range of 1.926(2) Å - 1.933(2) Å. While the amido nitrogen atoms to the Cu2 and Cu5 atoms have bond lengths in the range of 1.930(2) Å - 1.936(2) Å. The τ_4 values were

calculated for the two square planar geometry copper metal ions via the proposed τ_4 index equation by Houser[139] which is defined as $\tau_4 = 360 - (\beta + \alpha)/141°$. Where a value of zero is defined as a perfect square planar geometry and a value of one represents a perfect tetrahedral geometry. The τ_4 values 0.112 and 0.133 for Cu2 and Cu5, respectively, indicate they are approximately square planar.

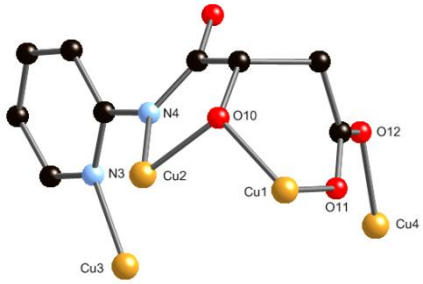

Figure 2.46 *Coordination mode of the **L1A** ligand in complex **13**. All hydrogen atoms omitted for clarity.*

There is one coordination mode for the **L1A** ligands in complex **13** and is shown in Figure 2.46. Each ligand coordinates to four of the copper metal ions in complex **13** three in the same dimer and one in the dimer bridged by the carboxylate group. The nitrogen atom N3 in the pyridine ring is coordinated to one copper metal ion Cu3 in Figure 2.46. Two copper atoms Cu2 and Cu1 are then bridged by the alkoxide oxygen O10 with Cu1 also coordinating to the oxygen atom O11 in the carboxylate group. In addition, the **L1A** ligand coordinates to a fourth copper metal ion Cu4 through the carboxylate group oxygen atom O12.

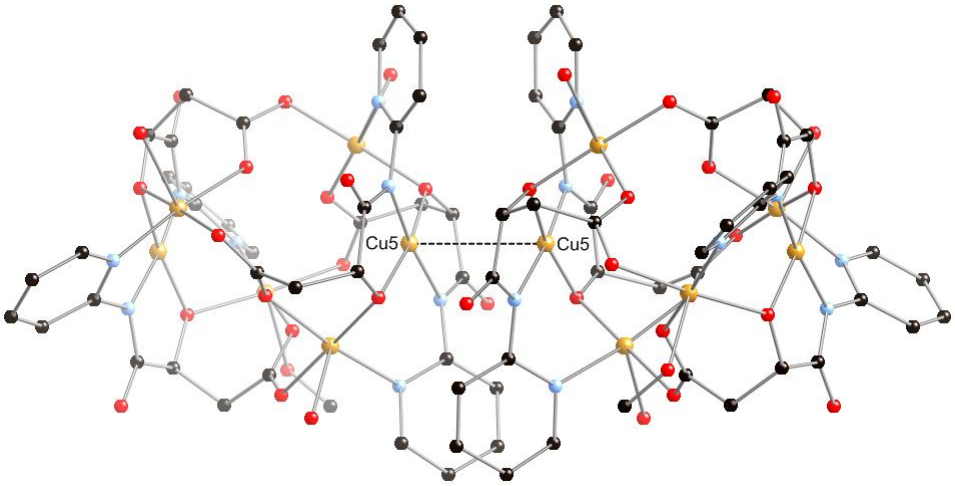

Figure 2.47 *The interaction between the two square planar Cu5 ions and examples of π–π stacking interactions in the crystal lattice of complex **13**.*

Complex **13** shows π–π stacking interactions within the crystal lattice. There are four intermolecular π–π stacking interactions between the pyridine rings on neighbouring complex **13** molecules. While all four are offset face to face π–π stacking interactions only two of them have the pyridine rings parallel to each other. The ring centroid to ring centroid distance of the pyridine ring

(N1-C4-C5-C3-C1-C2) on a neighbouring complex **13** molecules is 3.763(3) Å, while the ring centroid to ring centroid distance for the interaction between the pyridine ring atoms on neighbouring complex **13** molecules (N3-C10-C11-C14-C12-C13) is 3.416(2) Å. The dashed black line between two Cu5 atoms in neighbouring complex **13** molecules indicates a short interaction between the two metal ions. The distance between the two Cu5 atoms is 3.6826(8) Å and occurs on the same end of the complex molecule as the π–π stacking interactions indicated above. The π–π stacking interaction between the two ring centroids of the pyridine ring atoms (N5-C23-C22-C20-C19-C21) is 3.751(2) Å and has an angle of 3.99(14)°. In addition the distance between the two ring centroids of the pyridine ring atoms (N7-C32-C31-C29-C28-C30) is 3.725(2) Å with an angle of 11.51(14)°. Both the π–π stacking interactions and the Cu5–Cu5 have a synergistic effect. The Cu5-Cu5 interaction as well as π–π examples are shown in Figure 2.47.

2.2.9.4 *Thermogravimetric analysis of the metal organic cluster complex **13**.*

Complex **13** had its thermal behaviour analysed by thermogravimetric analysis (TGA) shown in Figure 2.48. A weight percentage loss of 10.75% is seen over 37 °C < T < 149 °C. This is consistent with the non-coordinated methanol molecule, coordinated methanol molecule, three coordinated water molecules, which was calculated at 8.88%. The anhydrous complex is stable until 228 °C. Complex **13** fully decomposes by 700 °C.

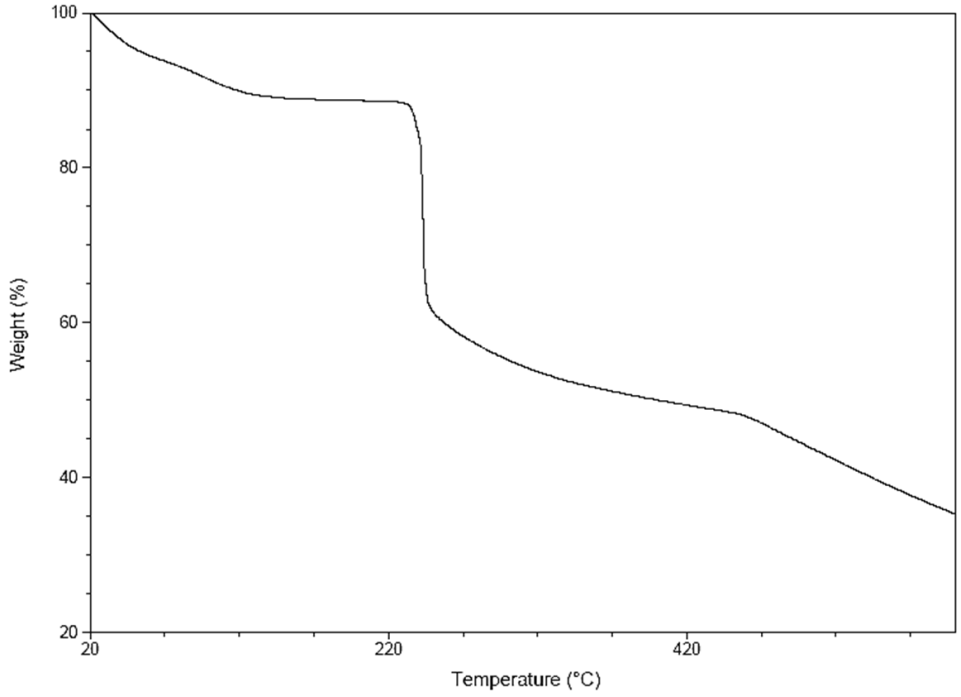

Figure 2.48 *Thermo gravimetric analysis (TGA) plots for complex **13**.*

2.2.9.5 *Magnetic characterisation of complex **13**.*

Magnetic susceptibility measurements were carried out on complex **13** as shown in Figure 2.49. Complex **13** has a $\chi_M T$ 2.5 cm^3 mol^{-1} K at 300 K, which increases slowly with decreasing temperature. The expected $\chi_M T$ value for six Cu(II) ions is 2.49 cm^3 mol^{-1} K with g = 2.10. Below 50 K there is a sharp increase to reach a maximum of 6.1 cm^3 mol^{-1} K at 4K before rapidly decreasing to 4.9 cm^3 mol^{-1} K at 2 K . This behaviour indicates dominant ferromagnetic interactions within complex **13** with a S = 3 ground spin state. The magnetisation (M) isotherms shown in Figure 2.51 confirm there are dominant ferromagnetic interactions where the 2K data saturates at M = 6 Nβ which is expected for an isolated S = 3 ground state.

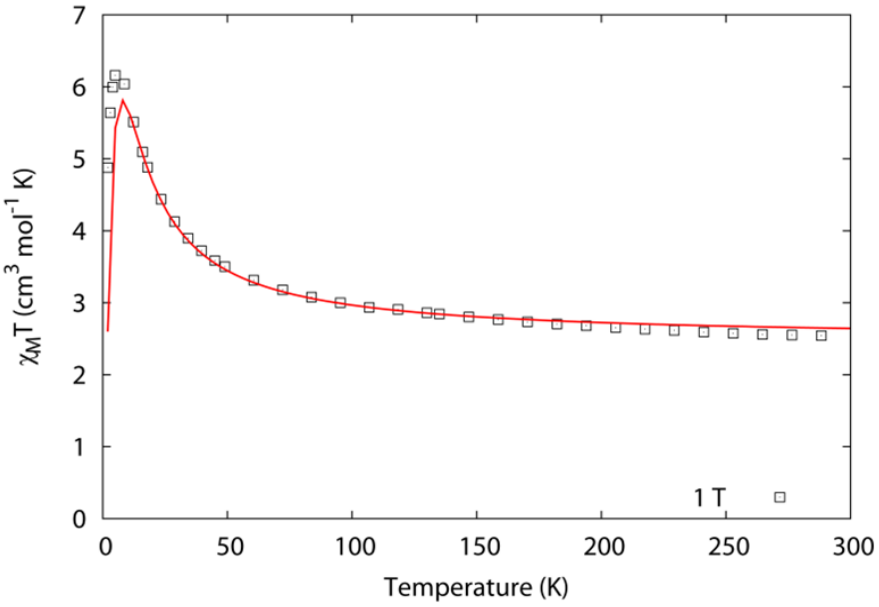

Figure 2.49 *The plot of $\chi_M T$ vs. T with an applied dc field of 1 T for complex **13**. Fitted data are represented as the red line while the actual data are represented by the hollow squares.*

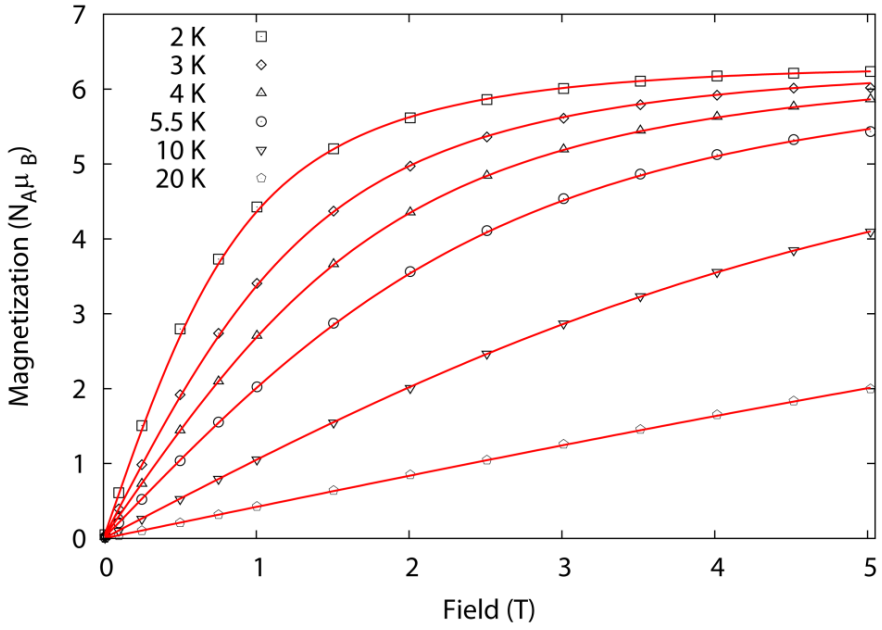

Figure 2.50 *The magnetisation (M) isotherm plots of complex **13**. The temperatures 2K (top) 3K, 4K, 5.6K, 10K and 20K (bottom) are plotted for complex **13**. Fitted data are represented by red lines while actual data are represented by hollowed out shapes.*

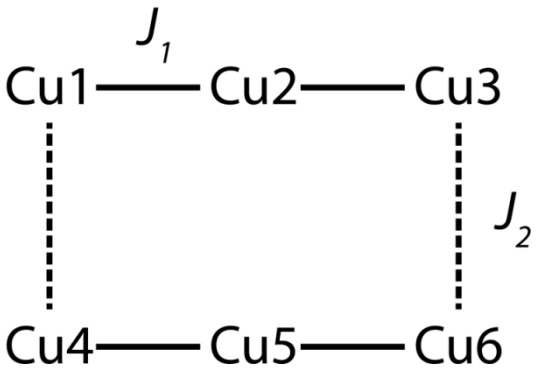

Figure 2.51 *The coupling scheme for complex **13**.*

The data for the magnetic susceptibility and magnetisation of complex **13** was fitted using the program *PHI*[140] using the $-2JS_1.S_2$ formalism to calculated the J values shown in Figure 2.51. Figure 2.51 shows the schematic representation of the Cu(II) ions in complex **13** where the values for J_1 and J_2 are 15.1 cm^{-1} and 5.18 cm^{-1} respectively with g = 2.10. All fitted data are shown in Figures 2.49 and 2.50 by the red lines.

In the literature there are many examples of copper clusters with antiferromagnetic interactions.[141-143] There are also examples of multinuclear copper clusters with dominant ferromagnetic interactions in the literature.[82, 144] The hexanuclear Cu(II) ion cluster by Jiang was prepared with glycine ligands. It shows a $\chi_M T$ value of 3.3 cm^3 mol^{-1} K at 300K which is above the 2.25 cm^3 mol^{-1} K value expected for six spin-only Cu(II) ions. The value is constant down to 70K

where it rises rapidly to 4.5 cm^3 mol^{-1} at 5K.[144] This behaviour is consistent with dominant ferromagnetic interactions. A hexanuclear copper cluster by Kruger was prepared with 2,2'-bipyridine and copper hydroxide also shows dominant ferromagnetic interactions. At 300K the $\chi_M T$ value is 4.8 cm^3 mol^{-1} K and gradually increases with decreasing temperature. A sharp rise in the $\chi_M T$ value to 6.77 cm^3 mol^{-1} K occurs at 3.5K, which is consistent with S = 3 ground state for six Cu(II) ions.[82]

2.2.9.6 *Single crystal X-ray diffraction discussion for complex **14**.*

The metal organic cluster, complex **14** was synthesised from iron perchlorate with **H_2L1** in a methanol solution and triethylamine as a base to deprotonate the **H_2L1** ligands. The solution was allowed to stand and evaporate. After two weeks brown plate crystals of complex **14** formed in 21% yield and were isolated through filtration. It was observed that more crystals formed in the filtrate, however, the yield of crystals obtained was enough to fully characterise the complex. The crystals were suitable for single crystal X-ray diffraction.

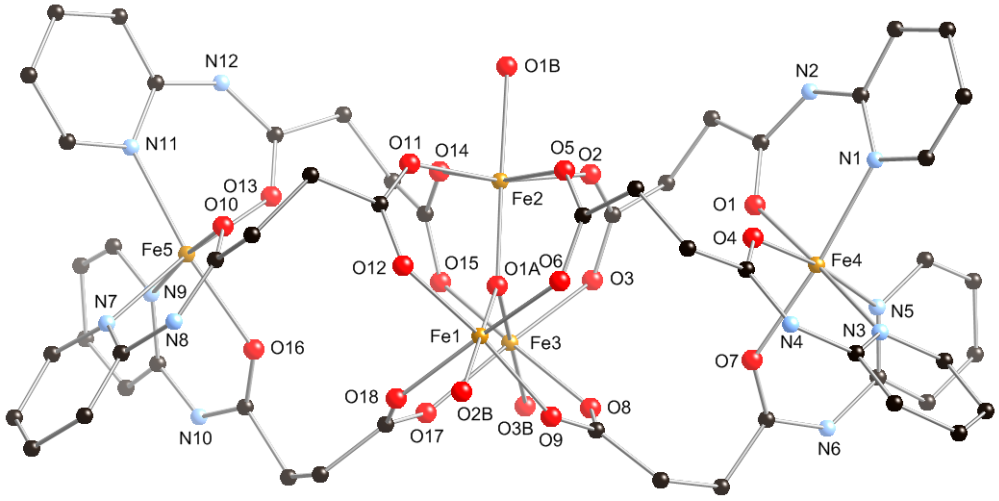

Figure 2.52 *Crystal structure of the metal organic cluster complex **14**. All anions, solvents and hydrogen atoms omitted for clarity.*

Complex **14**, shown in Figure 2.52 crystallised in the $P2_1/c$ space group and refined with a R1 factor of 10.10% before SQUEEZE. The unit cell contains four complex **14** molecules, ten perchlorate anions, eight acetonitrile solvent molecules and eight water solvent molecules. The crystal structure contained void space containing disordered solvent molecules which could not be modelled in the structure. The SQUEEZE[145] function in PLATON[146] was used to calculate the electron density within the void space. The electron density equated to one acetonitrile solvent molecule and two water solvent molecules extra per cluster in the unit cell. This brings the count of solvent molecules to twelve acetonitrile solvent molecules and sixteen water solvent molecules and bought the R1 factor down to 9.96% after SQUEEZE[145]. The perchlorate anions are also disordered throughout the crystal

structure. Complex **14** has five non-equivalent iron metal ions and six **HL1** ligands chelating to them. In addition there is a μ_3-O oxygen atom which coordinates to three of the iron metal ions which make up the iron triangle cluster at the centre of complex **14**. Both halves of complex **14**, from the axial iron metal ions to the metal ions in the triangular centre have the opposite handedness and therefore the complex is overall a mesocate. Complex **14** is a pentanuclear complex made up of five non-equivalent iron metal ions in two valence states. The two axial iron metal ions Fe4 and Fe5 are Fe(II) metal ions while the three iron metal ions in the central triangle are Fe(III) metal ions. Complex **14** is a unique metal cluster; however, there are examples of five iron metal clusters in the literature.[84, 147-149]

The five iron metal ions are in two coordination modes shown in Figure 2.52. Both the Fe(II) and Fe(III) metal ions have pseudo octahedral geometry. The coordination sphere of the iron metal ions in the axial positions of complex **14** is made up of three nitrogen atoms and three oxygen atoms from the pyridine rings and amido group respectively. Overall three **HL1** ligands coordinate to each of the metal ions Fe4 and Fe5. Bond lengths for the pyridine nitrogen atoms to iron metal ions range from 2.168(2) - 2.226(2) Å. While the amido oxygen atoms to iron metal ion bond lengths range from 2.0478(18) -2.1097(15) Å. The three remaining iron metal ions, Fe1, Fe2 and Fe3 are in the central triangle of the cluster. Each metal ion coordinates to four **HL1** ligands through the carboxylate group oxygen atoms. The coordination sphere of each iron metal ion is completed with the coordination to a water molecule and a μ_3-O oxygen atom. The bond lengths of the iron metal ions to the carboxylate group oxygen atoms range from 1.9808(15) - 2.0357(14) Å. Bond lengths between the μ_3-O and water oxygen atoms have ranges of 1.8928(12) - 1.9037(15) Å and 2.0798(16) - 2.0857(15) Å respectively.

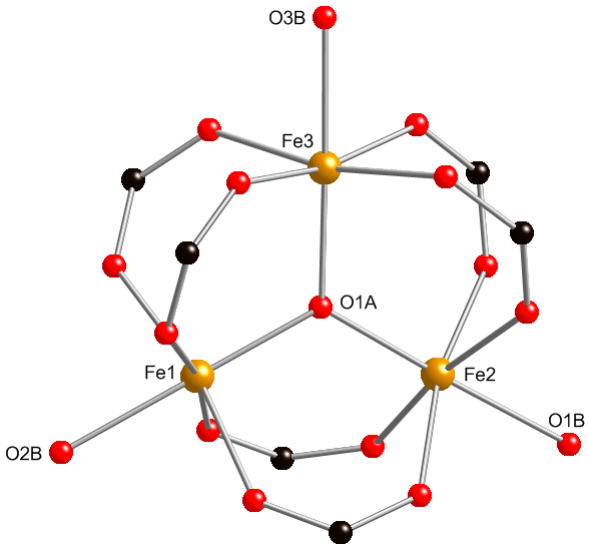

Figure 2.53 *Iron triangular core of with the three Fe(III) metal ions in complex **14**. All other atoms and hydrogen atoms omitted for clarity.*

Shown in Figure 2.53 is the triangular iron metal core at the centre of complex **14**. The core is made up of three Fe(III) metal ions, Fe1, Fe2 and Fe3, bridging carboxylate groups from six **HL1** ligands, one μ3-O oxygen atom, O1A, and three water ligands. The μ_3-O oxygen atom O1A is in the -

2 valence state and bridges all three metal ions in the iron triangle core. Each iron metal ion also has a water molecule, O1B, O2B and O3B, coordinated to it. Each metal ion has four oxygen atoms coordinated to it from the carboxylate groups of two **HL1** ligands. This bridging mode of the carboxylate groups forms the iron triangle cluster in complex **14**. This iron triangle core is well known and has been thoroughly studied in the literature.[150-151]

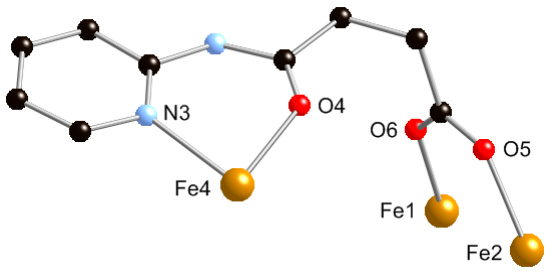

Figure 2.54 *Coordination mode of the **HL1** ligand in the metal organic cluster complex **14**. All anions, solvent and hydrogen atoms omitted for clarity.*

Shown in Figure 2.54 is the binding mode of the **HL1** ligand in complex **14**. Like the metal cluster complex **12**, **H_2L1** has deprotonated at the carboxylic acid group to form a carboxylate group. Six **HL1** ligands in complex **14** coordinate to three non-equivalent iron metal ions. All **HL1** ligands chelate to an axial Fe(II) metal ion through the nitrogen atom in the pyridine ring and the oxygen atom O4 in the amido group shown in Figure 2.54. The carboxylate groups on six **HL1** ligands bridge two non-equivalent Fe(III) metal ions through the oxygen atoms shown in Figure 2.53.

The metal cluster complex **14** was also prepared with iron perchlorate and **H_2L1** in an acetonitrile solution with triethylamine and crystallised with a vapour diffusion with toluene as the anti solvent. The Complex crystallised in the $P\overline{1}$ space group and was solved with an R factor of 6.87%. The unit cell comprises two metal cluster complex molecules, ten perchlorate anions, eleven water solvent molecules, two acetonitrile solvent molecules and two toluene solvent molecules which is on a special position that is a centre of inversion and is disordered over two orientations. The hydrogen atoms on the toluene were not included in the refinement of the toluene molecule.

2.2.9.7 *Magnetic characterisation of metal cluster complex **14**.*

Magnetic susceptibility measurements were performed on complex **14** and shown in Figures 2.55 and 2.56. Complex **14** has a $\chi_M T$ value of 10.1 cm^3 mol^{-1} K at 300K. This agrees with the expected value of 10.5 cm^3 mol^{-1} K for three Fe(III) ions with S = 5/2, and two non-coupled high spin Fe(II) metal ions with S = 2. This suggests the presence of antiferromagnetic interactions. The $\chi_M T$ value gradually decreases with decreasing temperature to 7 cm^3 mol^{-1} K at 20K before rapidly decreasing to 1.9 cm^3 mol^{-1} K at 2K. This is indicative of complex **14** having dominant

antiferromagnetic interactions. The magnetisation (M) isotherm plots shown in Figure 2.55 were measured using dc fields ranging from 0 to 50,000 Oe (5 T) and temperatures ranging from 2 to 20K. As shown the M values of are far from being saturated. This confirms dominant antiferromagnetic interactions are present in complex **14** and suggests a small non-zero spin ground state for the complex.

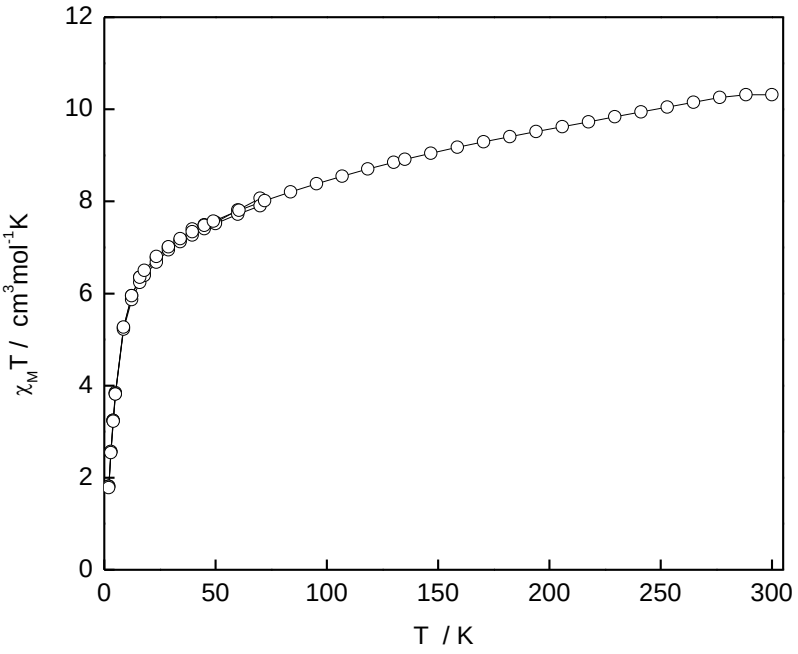

Figure 2.55 *The $\chi_M T$ vs. T plot with an applied dc field of 1 T for complex **14**.*

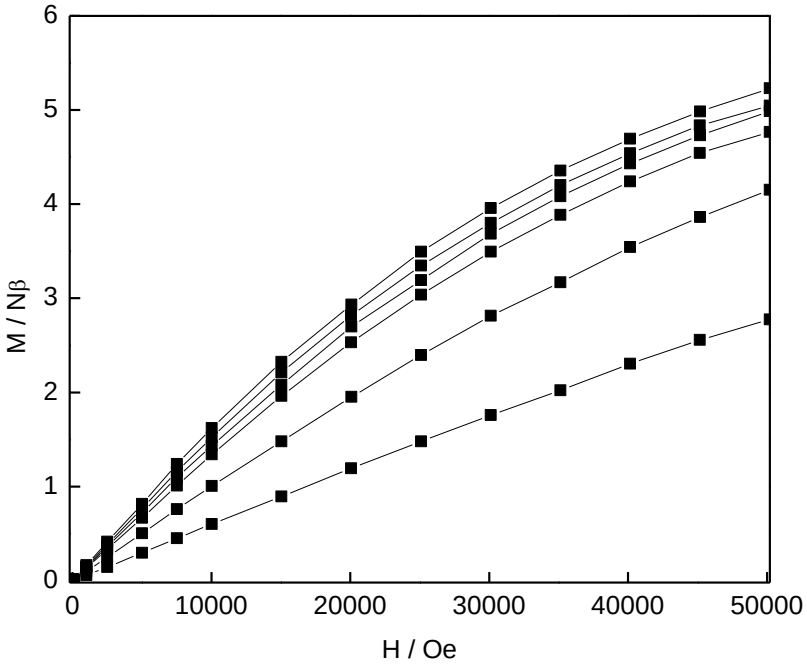

Figure 2.56 *The magnetisation (M) isotherm plots of complex **14**. The temperatures 2K (top) 3K, 4K, 5.6K, 10K and 20K (bottom) are plotted for complex **14**.*

Antiferromagnetic interactions in iron complexes is common.[84, 147-149] The iron triangle centre of complex **14** is also reported by itself and shows dominant antiferromagnetic interactions.[150-151]

2.2.10 *Summary of multinuclear metal clusters, complexes **12** - **14**.*

Three metal clusters were prepared from cobalt perchlorate, copper acetate and iron perchlorate with the **H_2L1** ligand with methanol and acetonitrile solutions in slow evaporation cyrstallisations. Complex **12** is an octanuclear Co(II) ion metal cluster with eight **HL1** ligands coordinated in two coordination modes. A hexanuclear Cu(II) metal cluster or complex **13** was prepared with the **H_2L1** ligand which underwent an *in situ* oxidation to the **H_2L1A** ligand. Here the α methylene carbon to an amido moiety was oxidised. Four of these ligands were present in the cluster with only one coordination mode to four metal ions. Two Cu(II) ion geometries were shown with the ligand and these were square pyramidal and square planar geometries. The **HL1A** ligand showed different coordination through the amido moiety in complex **13** compared to the others. It coordinated through the nitrogen atom instead of the oxygen atom that coordinated in complexes **12** and **14**. Iron perchlorate was used with the **H_2L1** ligand to prepare the metal cluster complex **14**. Complex **14** showed π–π stacking interactions between pyridine rings on neighbouring complexes and a metal-

metal interaction between two neighbouring complexes. Complex **14** was a pentanuclear metal cluster with six **HL1** ligands which were in one coordination mode to three iron metal ions. There were two Fe(II) ions in axial positions and three Fe(III) ions which formed and iron triangle motif.

All metal clusters were sent to Monash University for magnetic characterisation. Both complex **12** and **14** showed dominant antiferromagnetic interactions while complex **13** showed dominant ferromagnetic interactions. Data from Complex **13** was fitted with the program *PHI*[140] to calculate the coupling between the Cu(II) ions. This gave values of J_1 = 15.1 cm^{-1} and J_2 = 5.18 cm^{-1} and g = 2.10 for complex **13**.

2.2.11 *Conclusions*

Using the **H_2L1** ligand with 1st row transition metals produced 14 mononuclear and multinuclear complexes. The following conclusions based off results in this thesis were reached.

- The **H_2L2** and **H_2L3** ligands did not produce any mononuclear or multinuclear complexes because this chelation through the pyridine nitrogen and the amido oxygen atoms was not possible.
- All complexes showed similar coordination of the ligand through the pyridine nitrogen atom the amido oxygen atom and in one case the amido nitrogen atom.
- The **H_2L1** ligand proved to be a versatile ligand which produced a wide range of complexes
- Vapour diffusion crystallisation techniques and light solvothermal techniques generated mononuclear complexes with a range of 1st row transition metals. The mononuclear complexes formed with the **H_2L1** ligand through the pyridyl and amido moieties. However, no coordination took place through the carboxylic acid groups of the **H_2L1** ligand.
- The mononuclear complexes required chelation through the pyridine nitrogen atom and the amido oxygen atom in order to form.
- The hydrogen bonding networks in the crystal lattice of the mononuclear complexes were either 1D chains or 3D networks.
- Using harsher solvothermal conditions increased the coordination mode of the **H_2L1** ligand, forming two isostructural 2D coordination polymers and one 1D coordination polymer.
- The **H_2L1** ligand in these coordination polymers did not only coordinate to 1st row transition metals through the pyridyl and amido moieties. Coordination also occurred through the deprotonated carboxylic acids as carboxylate groups.
- Larger discrete multinuclear complexes were formed with the **H_2L1** ligand using slow evaporation crystallisation methods and using a base, triethylamine, to deprotonate the carboxylic acids. Three metal clusters were prepared. Again, the same chelation through the pyridine nitrogen and the amido oxygen atom was seen in two of the metal clusters. The third

metal cluster showed one of the less common coordination modes of the pyridyl-amido moiety through the pyridine nitrogen and the amido nitrogen atoms. However chelation still played a role in the formation of this complex.

- Four coordination modes of the carboxylate funtional groups were shown in the complexes. These were the η^1, bridging μ_2-η^1, η^1 and bridging μ_2-η^2 modes and are shown in Figure 2.57.

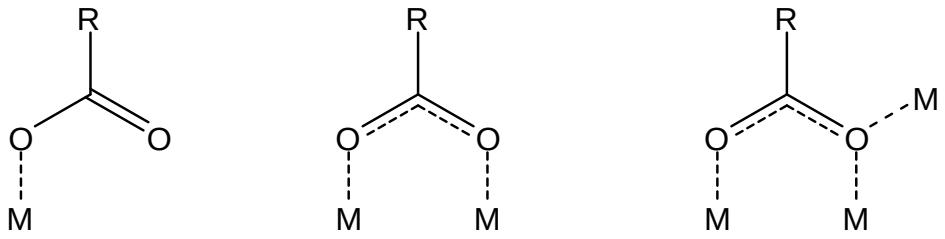

Figure 2.57 *Coordination modes of carboxylate groups seen in the complexes of the present research study*.

- The magnetic behaviour of the multinuclear metal clusters were characterised. The octanuclear cobalt metal cluster and pentanuclear iron metal cluster both had dominant antiferromagnetic interactions common for both types of transition metal clusters. The hexanuclear copper cluster showed dominant ferromagnetic interactions and the *J* coupling values between the Cu(II) ions were determined.

2.2.12 *Future work.*

Further work in altering the back bone of the **H_2L1** ligand could allow for more metal clusters to be prepared and little work has been done in the structural studies of these ligands. These alterations could include introducing a double bond between the methylene carbon atoms, placing a benzene ring across the methylene carbon atoms as well as placing extra carboxylic acid functional groups off these carbon atoms to further the coordination of the ligand to prepare even more multinuclear complexes with transition metals. Further complexes could be possible with the **H_2L1** ligand with other transition metals and the lanthanoid metals and the continued versatility of the ligand needs to be investigated. Further to this, using different solvents to those used in the present study could be employed to create more complexes with the **H_2L1** ligand. Investigations with different bases to deprotonate the carboxylic acid functional group to allow coordination to 1st row transition metals and other metal ions. Introducing a base into solvothermal preparations could also be investigated to get the carboxylic acid functional groups to coordinate to metal ions. Furthermore mixed metal complexes could also be synthesised with the **H_2L1** ligand to form multinuclear clusters or coordination polymers.

Chapter 3

Experimental

3.1 *Materials and Methods.*

3.1.1 *General information.*

Unless otherwise specified, all reagents and starting materials were of reagent grade, purchased from standard suppliers and used as received. Water was purified by reverse phase osmosis *in-house*. Where anhydrous solvents were required, the HPLC-grade solvent was either distilled from standard drying agents or dried by passing over a sealed column of activated alumina. Melting points were recorded on an Electrothermal melting point apparatus and are uncorrected. Elemental analysis was carried out by Campbell Microanalytical Laboratory, University of Otago. Except where otherwise specified, all reactions were carried out in air.

3.1.2 *Infrared Spectroscopy.*

All infrared spectra were recorded on Perkin-Elmer Spectrum One FTIR instrument operating in reflectance mode with samples prepared as KBr mulls, or in transmittance mode.

3.1.3 *Thermogravimetric Analysis.*

Thermogravimetric analyses were carried out on an Alphatech SDT Q600 TGA/DSC apparatus. All samples were heated on alumina crucibles under a nitrogen flow of 100 mL/min. Unless otherwise specified, all heating cycles consist of heating at 1 °C/min to 800 °C.

3.1.4 *Solvothermal Syntheses.*

All solvothermal reactions were carried out within Parr Instruments Teflon lined stainless steel acid digestion bombs, models 4744 (23 mL capacity) and 4749 (45 mL capacity), which were heated using the specified parameters in a Carbolite PF60 programmable oven with a Eurotherm 3508 temperature controller. Unless otherwise specified, initial heating rates for each cycle were 200 °C/hr. Prior to each use, the vessels were cleaned by heating 10 mL of 10% nitric acid solution to 180 °C, allowed to dwell at this temperature for 12 hours, and cooled to room temperature, following which the Teflon inserts were rinsed several times, refilled with water and subjected to the same heating cycle. Vessels cleaned by this method were not found to impact any detectable pH change to a further loading of water on heating.

3.1.5 *Nuclear Magnetic Resonance.*

All spectra were recorded on a Varian INOVA 500 instrument, operating at 500 MHz, for ^{1}H and 125 MHz, for ^{13}C. All samples were dissolved in commercially available deuterated solvents d_6-DMSO, $CDCl_3$, CD_3CN or D_2O. Spectra were referenced to the residual solvent peaks and/or TMS. 1D-nOesy, COSY, HSQC and HMBC experiments were employed where required, using standard Varian pulse sequences. The following abbreviations are used: s: singlet, d: doublet, dd: doublet of doublets, t: triplet, at: apparent triplet, dt: doublet of triplets.

3.1.6 *Mass Spectrometry.*

Mass spectra were recorded by Dr Marie Squire and Dr Meike Holzenkaempfer on a Bruker MaXis 4G spectrometer, both of which were operated in high resolution positive ion electrospray mode. Samples were dissolved and diluted to the required concentration of 10 µg/mL in HPLC grade acetonitrile or methanol.

3.1.7 *Magnetic Susceptibilities.*

The magnetic susceptibilities were measured using a Quantum Design Squid Magnetometer, PPMS 5, ac and dc field of 1 T, with the samples (*ca.*10 mg) contained in gelatin capsules held at the centre of a drinking straw that was fixed at the end of the sample rod. Diamagnetic corrections were obtained using Pascal's constants. Samples were sent to Monash University and the magnetic susceptibilities were run by Boujemaa Moubaraki and the data fitted by Professor Keith Murray and Nicholas Chilton.

3.1.8 *X-Ray Crystallography.*

Crystallographic refinement data, important bond lengths and bond angles are presented in Appendix **I**, **II**. X-ray crystallographic data collection and refinement were carried out with either a Bruker APEXII instrument, using graphite-monochromated Mo Kα (λ = 0.71073 Å) radiation, or an Oxford-Agilent Supernova instrument with focused mircosource Cu Kα (λ = 1.5418 Å) and Mo Kα (λ = 0.71073 Å) radiation and ATLAS CCD area detector. All structures were solved using direct methods with SHELXS[152] and refined on F^2 using all data full matrix least-squares procedures with SHELXL-97[153] within OLEX-2.[154] Non-hydrogen atoms were refined with anisotropic displacement parameters. Hydrogen atoms were included in calculated positions, or were manually assigned from

residual electron density where appropriate, isotropic displacement parameters 1.2 times the isotropic equivalent of their carrier atoms. The functions minimized were $\Sigma w(F^2_o - F^2_c)$, with $w = [\sigma^2(F^2_o) + aP_2 + bP]^{-1}$, Where $P = [\max(F_o)^2 + 2F^2_c]/3$. Graphical representations of crystallographic data were prepared using the CrystalMaker and OLEX-2 packages.[154] Crystallographic data for all compounds is included in .cif format as electronic supplementary information.

X-Ray Powder Diffraction data were collected using an Oxford-Agilent Supernova instrument using Cu Kα (λ = 1.5418 Å) radiation and an ATLAS CCD area detector. Samples were prepared by grinding *ca.*5 mg of analyte with a minimum quantity of Paratone-N oil and applying a sample of approximately 0.5 mm diameter to a thin glass fibre mounted on a goniometer head, which was mounted directly in the beam path. Diffraction data was recorded using four averaged 360° scans in δ with 150 second exposure time per rotation frame. The diffraction data were integrated radially and a background correction manually applied.

3.1.8.1 *X-ray powder diffraction of complexes **1** - **14***

Complexes **2**, **5**, **9**, **10**, **12**, **13** and **14** all were found to be in the same phase when X-ray powder diffractions were run on them. Complexes **1**, **3** and **4** had X-ray powder diffraction and appeared to be in two phases, however, the other phase was not isolated. In addition complexes **6**, **7** and **8** did not have X-ray powder diffractions run on them due to not having enough of each complex. Complex **11** decomposed upon grinding in preparation for X-ray powder diffraction.

3.2. Synthesis of **H_2L1**, **H_2L2** and **H_2L3**.

3.2.1 *Synthesis of N-(2-pyridyl)-4-amino-4-oxobutanoic acid (**H_2L1**).*

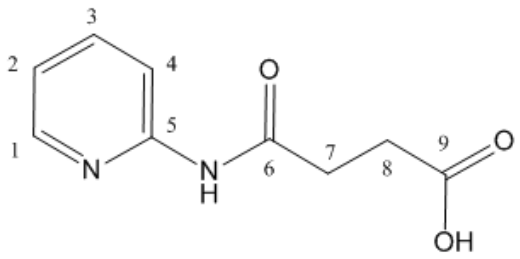

Succinic anhydride (2.73 g, 2.72 mmol) and 2-aminopyridine (2.57 g, 2.73 mmol) were dissolved in 150 mL of ethyl acetate and heated to reflux temperature. After 24 hours a white precipitate was filtered and washed with 50 mL of hot ethyl acetate. A minimum amount of methanol was used to recrystallise the white precipitate which afforded 2.08 g of **H_2L1** as colourless needle crystals suitable for single crystal X-ray diffraction. Yield 39%. m.p. 180 - 182 °C; δ_H(500 MHz, CD_3OD) 2.66 (at, *J* 6.1 Hz, 12.7 Hz, 2H, H_8), 2.72 (at, *J* 6.1 Hz, 12.9 Hz, 2H, H_7), 7.08 (t, *J* 6.0 Hz, 1.0 Hz, 1H, H_2), 7.74 (dt, *J* 8.0 Hz, 1.9 Hz, 1H, H_3), 8.06 (d, *J* 8.2 Hz, 1H, H_4), 8.26 (d, *J* 6.0 Hz, 1.0 Hz, 1H, H_1); δ_C(125 MHz, CD_3OD) 28 (CH_2, C_7), 31 (CH_2, C_8), 114 (CH, C_4), 119 (CH, C_2), 138 (CH, C_3), 148 (CH, C_1), 152 (C, C_5), 172 (C, C_6), 175 (C, C_9); ESMS: (CH_3OH, ES+) m/z; Calculated for $C_9H_{10}N_2O_3$ $[M+H]^+$:

195.0764 Found: 195.0766 [M+H]; IR; υ_{max}(KBr)/cm^{-1}; 634s, 745m, 784s, 845m, 916w, 963m, 1006s, 1168s, 1248s, 1313m, 1357m, 1438m, 1590m, 1696s, 2475m, 3071m

3.2.2 *Synthesis of N-(3-pyridyl)-4-amino)-4-oxobutanoic acid (**H_2L2**).*

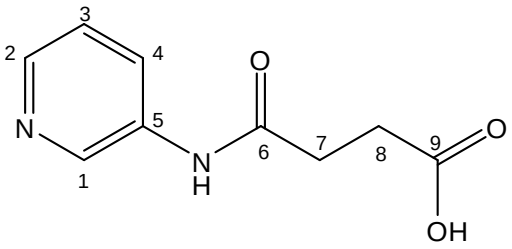

Succinic anhydride (2.73 g, 2.72 mmol) and 3-aminopyridine (2.57 g, 2.73 mmol) were dissolved in 150 mL of ethyl acetate and heated at reflux. After 24 hours the resulting precipitate was filtered and washed with 50 mL of hot ethyl acetate. A minimum amount of 50:50 acetonitrile to methanol solution was used to recrystallise the precipitate which afforded 1.803 g of **H_2L2** as colourless block crystals suitable for single crystal X-ray diffraction. Yield 34%. m.p. 198 - 200 °C; δ_H (500MHz, d_6-DMSO) 2.53 (at, *J* 13.0 Hz, 6.1 Hz, 2H, H_8) 2.59 (at, *J* 13.0 Hz, 6.1 Hz, 2H, H_7) 7.32 (dd, *J* 8.3 Hz, 4.6 Hz, 1H, H_3) 8.01 (d, *J* 8.3 Hz, 1H, H_4) 8.23 (d, *J* 3.4 Hz, 1H, H_2) 8.71 (s, 1H, H_1); δ_C(125 MHz, d_6-DMSO) 29 (CH_2, C_8) 31 (CH_2, C_7) 124 (CH, C_3) 126 (CH, C_4) 136 (C, C_5) 140 (CH, C_1) 144 (CH, C_2) 171 (C, C_6) 174 (C, C_9); ESMS: (CH_3OH, ES+) m/z; Calculated for $C_9H_{10}N_2O_3$ $[M+H]^+$: 195.0764 Found: 195.0764 [M+H]; IR: υ_{max}(KBr)/cm^{-1}; 655m, 706s, 753s, 808s, 908m, 944m, 1047m, 1255m, 1368w, 1490m, 1689s, 2366w.

3.2.3. *Synthesis of N-(4-pyridyl)-4-amino)-4-oxobutanoic acid (**H_2L3**).*

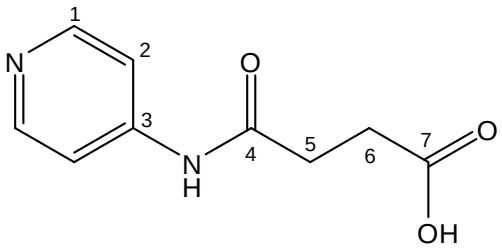

Succinic anhydride (1.0 g, 1.0 mmol) and 4-aminopyridine (0.94 g, 1.0 mmol) were added to 40 mL of dry THF and heated to reflux temperature under an inert atmosphere of N_2 for 24 hours. The resulting precipitate was washed with 10 mL of water and 10mL of ether and dried which afforded 0.264 g of white precipitate of **H_2L3**. Colourless block crystals suitable for single X-ray diffraction were grown by recrystallisation of the white precipitate with the minimum amount of methanol. Yield: 14%. m.p. 220 - 221 °C; δ_H(500MHz, d_6-DMSO) 2.50 (at, *J* 6.1 Hz, 12.7 Hz, 2H, H_6) 2.57 (at, *J* 12.8 Hz 6.2 Hz, 2H, H_5) 7.51 (d, *J* 6.0 Hz, 2H, H_1) 8.37 (d, *J* 6.0 Hz, 2H, H_2); δ_C(125MHz, d_6-DMSO) 29 (CH_2, C_5) 31 (CH_2, C_6) 113 (2CH, C_2) 146 (C, C_3) 151 (2CH, C_1) 172 (C, C_4) 175 (C, C_7); ESMS: (CH_3OH, ES+) m/z; Calculated for $C_9H_{10}N_2O_3$ $[M+H]^+$: 195.0764 Found: 195.0767 [M+H]; IR: υ_{max}(KBr)/cm^{-1}; 602m, 842s, 1157s, 1508s, 1706s, 3084m.

3.3 *General synthesis of discrete complexes by bench top methods.*

To **H_2L1** (20 mg, 0.10 mmol) in one of three solvents, which were acetonitrile, nitromethane and acetone, was added the appropriate metal perchlorate salt. The solution was stirred and heated at 50 °C for 2 hours, after this time 0.5 mL aliquots of the solution were placed in a 1 mL vial and the appropriate precipitating solvent diffused into the solution.

3.3.1 *Synthesis of $[Co(HL1)_2(MeCN)_2].(ClO_4)_2$* ***1***.

$[Co(HL1)_2(CH_3CN)_2].(ClO_4)_2$ was prepared according to the general procedure with $Co(ClO_4)_2.6H_2O$ (37 mg, 0.10 mmol) in 10 mL acetonitrile and diisopropyl ether used as the anti solvent. Orange block crystals formed after two weeks in 11% yield; CHN calculated for $CoC_{20}H_{27}N_5O_{16}Cl_2$ C, 33.21; H, 3.76; N, 9.68%. Found C, 32.88; H, 3.73; N, 9.50%. IR: υ_{max}(KBr)/cm^{-1}; 587w, 651m, 789s, 869m, 1015m, 1044m, 1188s, 1383s, 1420s, 1544s, 1623s, 1665s, 1709s, 3053w br.

3.3.2 *Synthesis of $[Ni(HL1)_2(H_2O)_2].(ClO_4)_2$* ***2***.

$[Ni(HL1)_2(H_2O)_2].(ClO_4)_2$ was prepared according to the general procedure with $Ni(ClO_4)_2.6H_2O$ (38 mg, 0.10 mmol) in 5 mL of nitromethane and diisopropyl ether as the anti solvent. Blue block crystals formed after 3 weeks in 14% yield; CHN calculated for $NiC_{36}H_{52}N_8O_{34}Cl_4$ C, 30.88; H, 3.74; N, 8.00%. Found C, 30.88; H, 3.51; N, 7.98%. IR: υ_{max}(KBr)/cm^{-1}; 518m, 625s, 781s, 1086s, 1272m, 1425m, 1486s, 1543s, 1626s, 1665s, 1714s, 3312w br.

3.3.3 *Synthesis of $[Co(HL1)_2(H_2O)_2].2ClO_4.MeNO_2$* ***3***.

$[Co(HL1)_2(H_2O)_2].2ClO_4.MeNO_2$ was prepared according to the general procedure with $Co(ClO_4)_2.6H_2O$ (37 mg, 0.10 mmol) in 10 mL of acetonitrile and benzene as the anti solvent. Purple block crystals formed after 1 week in 24% yield; CHN calculated for $CoC_{18}H_{33}N_4O_{20.5}Cl_2$ C, 28.30; H, 4.36; N, 7.34%. Found C, 27.80; H, 3.49; N, 7.30%; IR: υ_{max}(KBr)/cm^{-1}; 544m, 625s, 783s, 1095s, 1219m, 1283m, 1377m, 1484s, 1534s, 1625s, 1669s, 2475w br.

3.3.4 *Synthesis of [Cu(HL1)$_2$(ClO$_4$)$_2$].(CH$_3$)$_2$CO* ***4****.*

[Cu(HL1)$_2$(ClO$_4$)$_2$].(CH$_3$)$_2$CO was prepared according to the general procedure with Cu(ClO$_4$)$_2$.6H$_2$O (38 mg, 0.10 mmol) in 10 mL of acetone and diethyl ether as the anti solvent. Large blue needle crystals formed over night in 13% yield; CHN calculated for $CuC_{18}H_{20}N_4O_{14}Cl_2$ C, 33.22; H, 3.10; N 8.61%. Found C, 33.13; H, 3.13; N, 8.54%. IR: υ_{max}(KBr)/cm^{-1}; 627s, 871m, 1092s, 1241m, 1426m br, 1481s, 1541s, 1623s, 1650s, 1726s, 2932w br.

3.4 *General synthesis of discrete complexes by solvothermal techniques.*

To **H$_2$L1** (20 mg, 0.10 mmol) in 5 mL of acetonitrile was added the appropriate metal salt. The solution was stirred for 5 minutes and then added to a 45 mL Teflon lined stainless steel acid digestion bomb which was then heated at the prescribed temperature for a select amount of time before being cooled to room temperature at a certain temperature rate per hour. All solvothermal discrete complexes were prepared using this general procedure unless otherwise specified.

3.4.1 *Synthesis of [Ni(HL1)$_2$(MeCN)$_2$].NO$_3$* ***5****.*

[Ni(HL1)$_2$(MeCN)$_2$].NO$_3$ was prepared according to the general discrete complexes solvothermal procedure with Ni(NO$_3$)$_2$.6H$_2$O (15 mg, 0.10 mmol) and heated at 100 °C for 36 hours with a cooling rate of 2 °C per hour. Small blue block crystals formed in 43% yield; CHN calculated for $NiC_{22}H_{26}N_8O_{12}$ C, 40.45; H, 4.01; N, 17.20%. Found C, 40.20; H, 3.96; N, 16.9%. IR: υ_{max}(KBr)/cm^{-1}; 577m, 645m, 713m, 1019m, 1319m br, 1481s, 1542s, 1622s, 1661s, 1725s, 2292s, 2941w br.

3.4.2 *Synthesis of [Ni(HL1)$_2$(H$_2$O)$_2$].2H$_2$O* ***6****.*

[Ni(HL1)$_2$(H2O)$_2$].2H$_2$O was prepared according to the general discrete complexes solvothermal procedure for poly-[Ni(HL1)(H$_2$O)(NO$_3$)] or complex **10** described below. Green crystals of complex **10** were dissolved in water to form complex **6** and small blue block crystals formed in 50% yield; CHN calculated for $NiC_{18}H_{22}N_4O_8$ C, 44.90; H, 4.61; N, 11.60%. Found C, 45.00; H, 4.58; N, 11.70%. IR: υ_{max}(KBr)/cm^{-1}; 784m, 860m, 955s, 998m, 1022 m, 1163s, 1183s, 1250s, 1288m, 1313m, 1420s, 1481s, 1541s, 1622s, 1675s, 2921w br.

3.4.3 *Synthesis of [Co(HL1)$_2$(MeCN)$_2$].NO$_3$* ***7****.*

[Co(HL1)$_2$(MeCN)$_2$].NO$_3$ was prepared according to the general discrete complexes solvothermal procedure with Co(NO$_3$)$_2$.6H$_2$O (30 mg, 0.10 mmol) and heated at 100 °C for 36 hours with a cooling rate of 2 °C per hour. The pink solution that formed was allowed to sit for a day and orange block crystals formed in 10% yield; CHN calculated for $CoC_{22}H_{32}N_8O_{14}$ C, 38.10; H, 4.67; N, 16.21%. Found C, 38.50; H, 3.94; N, 16.00%. IR: υ_{max}(KBr)/cm^{-1}; 627s, 782s, 939m br, 1083s, 1242m, 1272m, 1430m, 1483s, 1541s, 1624s, 1664s, 1712s, 3282m br.

3.4.4 *Synthesis of [Co(HL1)$_2$Cl$_2$].H$_2$O* ***8****.*

[Co(HL1)$_2$Cl$_2$].H$_2$O was prepared according to the general discrete complexes solvothermal procedure with CoCl$_2$.6H$_2$O (25 mg, 0.10 mmol) and heated to 100 °C for 24 hours with a cooling rate of 4 °C per hour. A blue solution formed which was slowly evaporated over 5 days. Small purple block crystals formed in 30% yield; CHN calculated for $CoC_{18}H_{24}N_4O_8Cl_2$, C, 39.00; H, 4.37; N, 10.10%. Found C, 38.78; H, 4.14; N 10.10%. IR: υ_{max}(KBr)/cm^{-1}; 606m, 650s, 785s, 975s, 1018m, 1062m, 1155s, 1186s, 1287s, 1372s, 1417s, 1478s, 1538s, 1622s, 1664s, 1721s, 2914w br, 3316s.

3.5 *General synthesis of 1D and 2D coordination polymers.*

To **H$_2$L1** (20 mg, 0.10 mmol) in acetonitrile was added the appropriate metal nitrate or chloride salt. The solution was stirred for 5 minutes and then placed in a 45 mL Teflon lined stainless steel acid digestion bomb and heated at the prescribed temperature for a set amount of time before going through a controlled cooling cycle. All coordination polymers were prepared according to this procedure unless otherwise specified.

3.5.1 *Synthesis of poly-[Co(HL1)(H$_2$O)(NO$_3$)]* ***9****.*

Poly-[Co(HL1)(H$_2$O) (NO$_3$)] was prepared according to the general coordination polymers procedure with Co(NO$_3$)$_2$.6H$_2$O (30 mg, 0.10 mmol) in 5 mL acetonitrile solution and heated at 100 °C for 36 hours with a cooling cycle of 2 °C per hour. Small pink rod crystals formed which were then filtered, dried under air and formed in 17% yield. m.p. >300 °C; CHN calculated for $Co_2C_{18}H_{20}N_6O_{13}$ C, 33.45; H, 3.12; N, 13.00%. Found C, 33.62; H, 2.94; N, 13.04%. IR: υ_{max}(KBr)/cm^{-1}; 590s, 681s, 773m, 1018m, 1053s, 1162s, 1206s, 1421m, 1485s, 1540s, 1610m, 1676s, 2967w br.

3.5.2 *Synthesis of poly-[Ni(HL1)(H_2O)(NO_3)]* ***10***.

Poly-[Ni(HL1)(H_2O)(NO_3)] was prepared according to the general coordination polymers procedure with $Ni(NO_3)_2.6H_2O$ (30 mg, 0.10 mmol), 3 mL of acetonitrile and heated at 100 °C for 36 hours with a cooling cycle of 2 °C per hour. Green rod crystals formed which were filtered, washed with water, dried in air and formed in 21% yield. m.p. > 300 °C; CHN calculated for $Ni_2C_{18}H_{20}N_6O_{13}$ C, 33.45; H, 3.12; N, 13.00%. Found C, 33.36; H, 3.10; N, 13.09%. IR: υ_{max}(KBr)/cm^{-1}: 592s, 878m, 1163s, 1208s, 1325s, 1486s, 1540s, 1607m, 1676s, 2928s br.

3.5.3 *Synthesis of poly-[Co_2(HL1)(H_2O)$_4Cl_2$].2H_2O* ***11***.

Poly-[Co_2(HL1)(H_2O)$_4Cl_2$].2H_2O was prepared according to the general coordination polymers procedure with $CoCl_2.6H_2O$ (25 mg, 0.10 mmol) with the addition of 1 mL of water and heated at 100 °C for 48 hours with a cooling cycle of 4 °C per hour. Purple block crystals were dried under air and formed in 10% yield. m.p. >300 °C; CHN calculated for $Co_2C_{18}H_{30}N_4O_{12}$ C, 31.60; H, 4.43; N, 8.13%. Found C, 31.70; H, 4.35; N, 8.13%. IR: υ_{max}(KBr)/cm^{-1}; 532m, 776m, 980m, 1155s, 1249s, 1372s, 1476s, 1540s, 1619m, 1658m, 3298w br.

3.6 *General synthesis of clusters.*

To **H_2L1** (130 mg, 0.67 mmol) in 30 mL of methanol was added the appropriate metal perchlorate salt or metal acetate salt. To this stirred solution 1 mL of a (0.5 mL to 5 mL of triethylamine to methanol) solution was added dropwise and the solution was heated at 50 °C for 12 hours. The solution was allowed to slowly evaporate over time. All clusters were prepared according to the general procedure unless otherwise specified.

3.6.1 *Synthesis of [Co_8(HL1)$_8$(O)(OH)$_4$(MeOH)$_3$(H_2O)].3ClO_4.5MeOH.2H_2O* ***12***.

[Co_8(HL1)$_8$(O)(OH)$_4$(MeOH)$_3$(H_2O)].3ClO_4.5MeOH.2H_2O was prepared according to the general procedure with $Co(ClO_4)_2.6H_2O$ (245 mg, 0.67 mmol). Pink block crystals formed after 1 week in 1% yield; CHN calculated for $Co_8C_{70}H_{87}N_{16}O_{52}Cl_3$ C, 32.80; H, 3.42; N. 8.75%; Found C, 32.50; H, 3.84; N, 8.29%. IR: υ_{max}(KBr)/cm^{-1}; 512m, 626m, 783m, 1106s, 1240m, 1311s, 1438s, 1479s, 1540s, 1581m, 1602m, 1674s, 3318w br.

3.6.2 *Synthesis of [$Cu_6(L1A)_4(MeOH)(H_2O)_3$].MeOH* ***13***.

[$Cu_6(HL1A)_4(MeOH)(H_2O)_3$].MeOH was prepared according to the general procedure with $Cu(OAc)_2.H_2O$ (133 mg, 0.67 mmol). Large dark green block crystals formed after 2 weeks they were isolated via filtration and formed in 11% yield. m.p. >300 °C; CHN calculated for $Cu_6C_{36}H_{34}N_8O_{19}$ C, 34.21; H, 2.71; N 8.87%. Found C, 33.80; H, 2.97; N, 8.63%. IR: υ_{max}(KBr)/cm^{-1}; 527m, 581m, 657s, 746m, 773s, 886s, 916s, 969s, 1042m, 1091s, 1196s, 1297s, 1389s, 1455s, 1480s, 1569s, 2831s, 3340w br.

3.6.3 *Synthesis of [$Fe_5(HL1)_6(O)(H_2O)_3$].5(ClO_4).3MeCN.4H_2O* ***14***.

[$Fe_5(HL1)_6(O)(H_2O)_3$].5(ClO_4).3MeCN.4H_2O was prepared according to the general procedure with $Fe(ClO_4)_2.6H_2O$ (249 mg, 0.67 mmol) and a 1 mL (0.5 mL to 5 mL of triethylamine to acetonitrile, 0.75 mmol) solution. Brown plate crystals formed after 2 weeks in 21% yield; CHN calculated for $Fe_5C_{54}H_{66}N_{12}O_{46}Cl_5$ C, 31.20; H, 3.21; N 8.10%. Found C, 31.30; H, 3.38; N, 8.08%. IR: υ_{max}(KBr)/cm^{-1}; 518m, 628m, 788s, 884m, 1095s, 1219s, 1319s, 1478s, 1540s, 1601s, 1677s, 3322w br.

Appendix I

Crystallographic Refinement Data.

*Table A1.1 Crystallographic refinement data for ligands **H_2L1**, **H_2L1** and **H_2L3***

Identification code	**H_2L1**	**H_2L2**	**H_2L3**
Empirical formula	$C_9H_{10}N_2O_3$	$C_9H_{10}N_2O_3$	$C_9H_{10}N_2O_3$
Formula weight	194.19	194.19	194.19
Temperature/K	113(2)	113(2)	113(2)
Crystal system	monoclinic	monoclinic	triclinic
Space group	$P2_1/n$	$P2_1/n$	P-1
a/Å	12.7827(6)	12.3620(6)	4.8325(3)
b/Å	5.0507(2)	5.1950(2)	9.3912(5)
c/Å	13.8509(7)	13.8975(7)	9.7985(6)
α/°	90	90	103.463(4)
β/°	92.809(3)	99.347(2)	96.815(4)
γ/°	90	90	95.784(4)
Volume/$Å^3$	893.16(7)	880.66(7)	425.60(4)
Z	4	4	2
$\rho_{calc}mg/mm^3$	1.444	1.465	1.515
m/mm^{-1}	0.11	0.112	0.116
F(000)	408	408	204
Crystal size/mm^3	0.31 × 0.18 × 0.15	0.41 × 0.15 × 0.12	0.39 × 0.19 × 0.12
2Θ range for data collection	5.88 to 52.88°	4.82 to 50.1°	5.42 to 50.1°
Index ranges	$-15 \le h \le 16$, $-6 \le k \le 6$, $-17 \le l \le 17$	$-14 \le h \le 14$, $-6 \le k \le 6$, $-16 \le l \le 16$	$-5 \le h \le 5$, $-11 \le k \le 11$, $-11 \le l \le 11$
Reflections collected	16166	16111	8040
Independent reflections	1840[R(int) = 0.0415]	1556[R(int) = 0.0384]	1507[R(int) = 0.0364]
Data/restraints/parameters	1840/2/133	1556/2/133	1507/3/136
Goodness-of-fit on F^2	1.229	1.072	1.048
Final R indexes [I>=2σ (I)]	$R_1 = 0.0513$, $wR_2 = 0.1073$	$R_1 = 0.0286$, $wR_2 = 0.0685$	$R_1 = 0.0326$, $wR_2 = 0.0773$
Final R indexes [all data]	$R_1 = 0.0679$, $wR_2 = 0.1141$	$R_1 = 0.0355$, $wR_2 = 0.0723$	$R_1 = 0.0436$, $wR_2 = 0.0836$
Largest diff. peak/hole / e $Å^{-3}$	0.21/-0.22	0.17/-0.18	0.16/-0.22

*Table A1.2 Crystallographic refinement data for complexes **1**, **2** and **3**.*

Identification code	**Complex 1**	**Complex 2**	**Complex 3**
Empirical formula	$C_{22}H_{26}Cl_2CoN_6O_{14}$	$C_{36}H_{48}Cl_4N_8Ni_2O_{32}$	$C_{20}H_{30}Cl_2CoN_6O_{20}$
Formula weight	728.32	1364.04	804.33
Temperature/K	113(2)	113(2)	120.01(10)
Crystal system	monoclinic	triclinic	triclinic
Space group	$P2_1/c$	P-1	P-1
a/Å	9.3899(9)	9.4365(3)	8.0538(4)
b/Å	10.1330(9)	10.4477(4)	8.9769(4)
c/Å	15.8329(15)	15.2492(5)	11.9490(5)
α/°	90	99.329(2)	89.235(4)
β/°	95.942(7)	104.754(2)	72.655(4)
γ/°	90	107.509(2)	83.275(4)
Volume/$Å^3$	1498.4(2)	1339.23(8)	818.73(6)
Z	2	1	1
$\rho_{calc}mg/mm^3$	1.614	1.691	1.631
m/mm^{-1}	0.829	1.008	6.451
F(000)	746	700	413
Crystal size/mm^3	0.22 × 0.15 × 0.1	0.61 × 0.32 × 0.11	0.28 × 0.2 × 0.11
2Θ range for data collection	4.78 to 50.1°	4.72 to 50.1°	7.76 to 130.94°
Index ranges	$-11 \le h \le 11$, $-12 \le k \le 12$, $-18 \le l \le 18$	$-11 \le h \le 11$, $-12 \le k \le 12$, $-18 \le l \le 18$	$-9 \le h \le 9$, $-10 \le k \le 10$, $-14 \le l \le 12$
Reflections collected	17322	24828	6061
Independent reflections	2650[R(int) = 0.0680]	4733[R(int) = 0.0351]	2831[R(int) = 0.0138]
Data/restraints/parameters	2650/2/212	4733/8/428	2831/4/236
Goodness-of-fit on F^2	1.114	1.112	1.087
Final R indexes [I>=2σ (I)]	$R_1 = 0.0578$, $wR_2 = 0.1388$	$R_1 = 0.0370$, $wR_2 = 0.0887$	$R_1 = 0.0255$, $wR_2 = 0.0697$
Final R indexes [all data]	$R_1 = 0.1054$, $wR_2 = 0.1831$	$R_1 = 0.0403$, $wR_2 = 0.0905$	$R_1 = 0.0255$, $wR_2 = 0.0697$
Largest diff. peak/hole / e $Å^{-3}$	1.01/-0.65	0.52/-0.69	0.27/-0.41

*Table A1.3 Crystallographic refinement data for complexes **4**, **5** and **6**.*

Identification code	**Complex 4**	**Complex 5**	**Complex 6**
Empirical formula	$C_{24}H_{32}Cl_2CuN_4O_{16}$	$C_{22}H_{26}N_8NiO_{12}$	$C_{18}H_{26}N_4NiO_{10}$
Formula weight	766.98	653.22	517.12
Temperature/K	120.01(10)	120.01(10)	278.17(10)
Crystal system	monoclinic	monoclinic	monoclinic
Space group	$P2_1/c$	$P2_1/c$	$P2_1/n$
a/Å	7.88139(14)	8.4839(2)	7.9156(4)
b/Å	9.86777(17)	10.0302(3)	8.8082(5)
c/Å	20.1534(4)	15.9235(4)	15.3392(8)
α/°	90	90	90
β/°	96.6528(18)	92.435(2)	94.508(5)
γ/°	90	90	90
Volume/Å^3	1556.81(5)	1353.78(6)	1066.17(10)
Z	2	2	2
ρ_{calc}mg/mm^3	1.636	1.602	1.6107
m/mm^{-1}	3.3	1.741	1.899
F(000)	790	676	535.9
Crystal size/mm^3	0.23 × 0.22 × 0.19	0.31 × 0.21 × 0.11	0.146 × 0.105 × 0.058
2Θ range for data collection	8.84 to 138°	10.42 to 141°	11.58 to 133.98°
Index ranges	$-9 \le h \le 9$, $-11 \le k \le 11$, $-24 \le l \le 22$	$-10 \le h \le 8$, $-12 \le k \le 7$, $-19 \le l \le 19$	$-9 \le h \le 8$, $-6 \le k \le 10$, $-18 \le l \le 17$
Reflections collected	14690	4672	3790
Independent reflections	2896[R(int) = 0.0202]	2565[R(int) = 0.0119]	1898[R(int) = 0.0495]
Data/restraints/parameters	2896/0/222	2565/3/243	1898/1/165
Goodness-of-fit on F^2	1.069	1.078	0.995
Final R indexes [I>=2σ (I)]	R_1 = 0.0275, wR_2 = 0.0682	R_1 = 0.0480, wR_2 = 0.1273	R_1 = 0.0412, wR_2 = N/A
Final R indexes [all data]	R_1 = 0.0282, wR_2 = 0.0687	R_1 = 0.0505, wR_2 = 0.1298	R_1 = 0.0585, wR_2 = 0.1057
Largest diff. peak/hole / e Å^{-3}	0.39/-0.46	0.84/-0.30	0.77/-0.64

*Table A1.4 Crystallographic refinement data for complexes **7**, **8** and **9**.*

Identification code	**Complex 7**	**Complex 8**	**Complex 9**
Empirical formula	$C_{22}H_{28}CoN_8O_{12}$	$C_{18}H_{24}Cl_2CoN_4O_8$	$C_{18}H_{20}Co_1N_6O_{13}$
Formula weight	655.45	554.24	646.26
Temperature/K	120.01(10)	120.01(10)	120.01(10)
Crystal system	monoclinic	triclinic	monoclinic
Space group	$P2_1/c$	P-1	C2/c
a/Å	8.5007(3)	7.4606(7)	15.4827(5)
b/Å	10.0364(4)	7.6909(8)	9.1457(2)
c/Å	15.9762(6)	11.3322(8)	19.0037(7)
α/°	90	75.948(8)	90
β/°	92.498(3)	76.937(7)	115.903(4)
γ/°	90	67.008(9)	90
Volume/$Å^3$	1361.73(9)	574.36(9)	2420.60(12)
Z	2	1	4
$\rho_{calc}mg/mm^3$	1.599	1.602	1.773
m/mm^{-1}	5.644	8.468	11.472
F(000)	678	285	1312
Crystal size/mm^3	0.29 × 0.23 × 0.21	0.19 × 0.12 × 0.1	0.23 × 0.21 × 0.11
2Θ range for data collection	10.42 to 140.98°	8.14 to 137.88°	10.34 to 142.9°
Index ranges	$-10 \le h \le 7$, $-12 \le k \le 9$, $-19 \le l \le 18$	$-7 \le h \le 9$, $-8 \le k \le 9$, $-9 \le l \le 13$	$-18 \le h \le 18$, $-10 \le k \le 11$, $-21 \le l \le 23$
Reflections collected	4785	3360	6953
Independent reflections	2581[R(int) = 0.0196]	2110[R(int) = 0.0201]	2329[R(int) = 0.0228]
Data/restraints/parameters	2581/3/243	2110/3/163	2329/2/183
Goodness-of-fit on F^2	1.143	1.063	1.051
Final R indexes [I>=2σ (I)]	$R_1 = 0.0525$, $wR_2 = 0.1254$	$R_1 = 0.0313$, $wR_2 = 0.0821$	$R_1 = 0.0244$, $wR_2 = 0.0610$
Final R indexes [all data]	$R_1 = 0.0550$, $wR_2 = 0.1269$	$R_1 = 0.0314$, $wR_2 = 0.0824$	$R_1 = 0.0268$, $wR_2 = 0.0623$
Largest diff. peak/hole / e $Å^{-3}$	0.44/-0.39	0.37/-0.57	0.24/-0.32

*Table A1.5 Crystallographic refinement data for complexes **10**, **11** and **12**.*

Identification code	**Complex 10**	**Complex 11**	**Complex 12**
Empirical formula	$C_{18}H_{20}N_6Ni_2O_{13}$	$C_{18}H_{30}Cl_2Co_2N_4O_{12}$	$C_{79.5}H_{113.3}Cl_3Co_8N_{16}O_{52}$
Formula weight	645.82	683.22	2702.95
Temperature/K	120.01(10)	120.01(10)	120.01(10)
Crystal system	monoclinic	triclinic	monoclinic
Space group	C2/c	P-1	C2/c
a/Å	15.4053(19)	7.8790(6)	25.9059(4)
b/Å	9.0877(10)	8.1783(6)	14.9866(2)
c/Å	18.948(2)	11.6082(9)	27.3422(4)
α/°	90	78.004(6)	90
β/°	116.228(15)	80.974(6)	91.2539(15)
γ/°	90	61.659(7)	90
Volume/Å^3	2379.5(5)	642.49(8)	10612.8(3)
Z	4	1	4
ρ_{calc}mg/mm^3	1.803	1.766	1.692
m/mm^{-1}	2.713	12.647	1.398
F(000)	1320	350	5541
Crystal size/mm^3	0.38 × 0.21 × 0.17	0.21 × 0.15 × 0.11	0.149 × 0.113 × 0.09
2Θ range for data collection	11.56 to 130.98°	7.8 to 140.98°	5.44 to 50.1°
Index ranges	-18 ≤ h ≤ 13, -10 ≤ k ≤ 10, -22 ≤ l ≤ 22	-9 ≤ h ≤ 9, -9 ≤ k ≤ 7, -14 ≤ l ≤ 11	-23 ≤ h ≤ 30, -17 ≤ k ≤ 13, -25 ≤ l ≤ 32
Reflections collected	4351	3906	20972
Independent reflections	2052[R(int) = 0.0308]	2413[R(int) = 0.0229]	9392[R(int) = 0.0220]
Data/restraints/parameters	2052/2/183	2413/7/186	9392/12/765
Goodness-of-fit on F^2	1.035	1.034	1.068
Final R indexes [I>=2σ (I)]	R_1 = 0.0369, wR_2 = 0.0885	R_1 = 0.0272, wR_2 = 0.0676	R_1 = 0.0536, wR_2 = 0.1148
Final R indexes [all data]	R_1 = 0.0476, wR_2 = 0.0948	R_1 = 0.0298, wR_2 = 0.0695	R_1 = 0.0641, wR_2 = 0.1208
Largest diff. peak/hole / e Å^{-3}	0.54/-0.46	0.33/-0.33	1.94/-1.61

*Table A1.5 Crystallographic refinement data for complexes **13** and **14**.*

Identification code	**Complex 13**	**Complex 14**
Empirical formula	$C_{38}H_{42}Cu_6N_8O_{21}$	$C_{60}H_{75}Cl_5Fe_5N_{15}O_{46}$
Formula weight	1328.04	2198.8
Temperature/K	120.01(10)	120.02(10)
Crystal system	monoclinic	monoclinic
Space group	C2/c	$P2_1/c$
a/Å	41.7229(8)	16.2556(2)
b/Å	13.7165(3)	22.8571(4)
c/Å	15.3592(3)	25.5874(4)
α/°	90	90
β/°	91.5503(18)	102.0441(15)
γ/°	90	90
Volume/$Å^3$	8786.7(3)	9297.9(2)
Z	8	4
$\rho_{calc}mg/mm^3$	2.008	1.529
m/mm^{-1}	4.009	8.284
F(000)	5344	4364
Crystal size/mm^3	0.17 × 0.1 × 0.06	0.14 × 0.07 × 0.03
2Θ range for data collection	6.78 to 144.96°	5.56 to 133.98°
Index ranges	$-50 \le h \le 51$, $-16 \le k \le 15$, $-18 \le l \le 18$	$-19 \le h \le 19$, $-22 \le k \le 27$, $-30 \le l \le 30$
Reflections collected	17949	56674
Independent reflections	8599[R(int) = 0.0283]	16567[R(int) = 0.0518]
Data/restraints/parameters	8599/8/685	16567/26/1184
Goodness-of-fit on F^2	1.031	1.165
Final R indexes [I>=2σ (I)]	$R_1 = 0.0339$, $wR_2 = 0.0884$	$R_1 = 0.0995$, $wR_2 = 0.2938$
Final R indexes [all data]	$R_1 = 0.0414$, $wR_2 = 0.0943$	$R_1 = 0.1327$, $wR_2 = 0.3179$
Largest diff. peak/hole / e $Å^{-3}$	0.92/-0.57	2.74/-1.49

Appendix II

Important Bond lengths and bond angles for complexes 1-14

Table A2.1 *Selected bond lengths (Å) and angles (°) from structures complex **1**.*

1						**Symmetry Codes**
Co1-O1^{i}	2.075(4)	O1^{1}-Co1-O1	180.00(19)	N31-Co1-N3	179.999(1)	i = -*x*,1-*y*,1-*z*
Co1-O1	2.075(4)	O1^{1}-Co1-N3^{1}	87.55(16)	N31-Co1-N11	90.24(18)	
Co1-N3^{i}	2.120(5)	O1-Co1-N3^{1}	92.45(16)	N3-Co1-N11	89.76(18)	
Co1-N3	2.120(5)	O1^{1}-Co1-N3	92.45(16)	N3-Co1-N1	90.24(18)	
Co1-N1^{i}	2.137(5)	O1-Co1-N3	87.55(16)	O1-Co1-N1	84.77(16)	
Co1-N1	2.137(5)	O1^{1}-Co1-N1^{1}	84.76(16)	N31-Co1-N1	89.76(18)	
		O1-Co1-N1	95.24(16)	N11-Co1-N1	179.999(1)	
		O1-Co1-N1^{1}	95.24(16)			

Table A2.2 *Selected bond lengths (Å) and angles (°) from structures complex **2**.*

2						**Symmetry Codes**
Ni1-N1	2.095(2)	N1^{i}-Ni1-N1	180	O5-Ni2-O5^{ii}	180	i = -*x*,-*y*,1-*z*;
Ni1-N1^{i}	2.095(2)	O1^{i}-Ni1-N1^{i}	87.00(8)	O5^{ii}-Ni2-O8^{ii}	88.29(8)	ii = 2-*x*,1-*y*,-*z*
Ni1-O1^{i}	2.0182(18)	O1-Ni1-N1^{i}	93.00(8)	O5-Ni2-O8^{ii}	91.71(8)	
Ni1-O1	2.0182(18)	O1^{i}-Ni1-N1	93.00(8)	O5-Ni2-O8	88.29(8)	
Ni1-O4^{i}	2.064(2)	O1-Ni1-N1	87.00(8)	O5^{ii}-Ni2-O8	91.71(8)	
Ni1-O4	2.064(2)	O1^{i}-Ni1-O1	180	O5-Ni2-N3^{ii}	87.02(8)	
Ni2-O5^{ii}	2.0059(17)	O1^{i}-Ni1-O4	87.72(9)	O5^{ii}-Ni2-N3^{ii}	92.98(8)	
Ni2-O5	2.0059(17)	O1-Ni1-O4	92.28(9)	O5^{ii}-Ni2-N3	87.02(8)	
Ni2-O8^{ii}	2.069(2)	O1^{i}-Ni1-O4^{i}	92.28(9)	O5-Ni2-N3	92.98(8)	
Ni2-O8	2.069(2)	O1-Ni1-O4^{i}	87.72(9)	O8-Ni2-O8^{ii}	180	
Ni2-N3^{ii}	2.094(2)	O4-Ni1-N1	90.77(9)	O8-Ni2-N3^{ii}	89.49(9)	
Ni2-N3^{ii}	2.094(2)	O4^{i}-Ni1-N1	89.23(9)	O8^{ii}-Ni2-N3^{ii}	90.51(9)	
		O4^{i}-Ni1-N1^{i}	90.77(9)	O8-Ni2-N3	90.51(9)	
		O4-Ni1-N1^{i}	89.22(9)	O8^{ii}-Ni2-N3	89.49(9)	
		O4-Ni1-O4^{i}	179.999(1)	N3-Ni2-N3^{ii}	180	

Table A2.3 *Selected bond lengths (Å) and angles (°) from structures complex **3**.*

3						**Symmetry Codes**
Co1-O1	2.0713(11)	$O1^{i}$-Co1-O1	180	O1-Co1-O4	92.53(5)	i = 1-*x*,1-*y*,1-*z*
Co1-$O1^{i}$	2.0713(11)	$O1^{i}$-Co1-N1	93.14(5)	$N1^{i}$-Co1-N1	180	
Co1-N1	2.1068(13)	O1-Co1-N1	86.86(5)	N1-Co1-O4	90.04(5)	
Co1-$N1^{i}$	2.1067(13)	$O1^{i}$-Co1-$N1^{i}$	86.86(5)	$N1^{i}$-Co1-O4	89.96(5)	
Co1-O4	2.1339(12)	O1-Co1-$N1^{i}$	93.14(5)	N1-Co1-41	89.96(5)	
Co1-$O4^{i}$	2.1339(12)	O1-Co1-$O4^{i}$	87.47(5)	$N1^{i}$-Co1-$O4^{i}$	90.04(5)	
		$O1^{i}$-Co1-O4	87.47(5)	$O4^{i}$-Co1-O4	180	
		$O1^{i}$-Co1-$O4^{i}$	92.53(5)			

Table A2.4 *Selected bond lengths (Å) and angles (°) from structures complex **4**.*

4				**Symmetry Codes**
Cu1-$O1^{i}$	1.9317(11)	$O1^{i}$-Cu1-O1	180	i = -*x*,-*y*,1-*z*
Cu1-$O1^{i}$	1.9317(11)	O1-Cu1-$N1^{i}$	90.83(5)	
Cu1-$N1^{i}$	2.0420(13)	$O1^{i}$-Cu1-$N1^{i}$	89.17(5)	
Cu1-$N1^{i}$	2.0421(13)	$O1^{i}$-Cu1-$N1^{i}$	90.83(5)	
		O1-Cu1-$N1^{i}$	89.17(5)	
		$N1^{i}$-Cu-N1	180	

Table A2.5 *Selected bond lengths (Å) and angles (°) from structures complex **5**.*

5						**Symmetry Codes**
Ni1-O1	2.0483(4)	$O1^{i}$-Ni1-O1	180	$O1^{i}$-Ni1-N3	88.38(2)	i = 1-*x*,1-*y*,1-*z*
Ni1-$O1^{i}$	2.0483(4)	O1-Ni1-$N1^{i}$	86.34(2)	$N1^{i}$-Ni1-N1	180	
Ni1-N1	2.0786(6)	$O1^{i}$-Ni1-N1	86.34(2)	$N3^{i}$-Ni1-$N1^{i}$	90.17(2)	
Ni1-$N1^{i}$	2.0786(6)	$O1^{i}$-Ni1-$N1^{i}$	93.66(2)	N3-Ni1-N11	89.83(2)	
Ni1-N3	2.0650(6)	O1-Ni1-$N1^{i}$	93.66(2)	N3-Ni1-N1	90.17(2)	
Ni1-$N3^{i}$	2.0650(6)	$O1^{i}$-Ni1-$N3^{i}$	91.62(2)	$N3^{i}$-Ni1-$N1^{i}$	89.83(2)	
		O1-Ni1-$N3^{i}$	88.38(2)	N3-Ni1-$N3^{i}$	180.00(3)	
		O1-Ni1-N3	91.62(2)			

Table A2.6 *Selected bond lengths (Å) and angles (°) from structures complex* ***6****.*

6						**Symmetry Codes**
Ni1-O1	2.0427(19)	$O1^{i}$-Ni1-O1	180	$N1^{i}$-Ni1-$O1^{i}$	86.58(8)	i = -*x*,-*y*,1-*z*
Ni1-$O1^{i}$	2.0427(19)	$O4^{i}$-Ni1-$O1^{i}$	91.30(8)	$N1^{i}$-Ni1-O1	93.42(8)	
Ni1-O4	2.078(2)	$O4^{i}$-Ni1-O1	88.70(8)	N1-Ni1-$O4^{i}$	86.96(9)	
Ni1-$O4^{i}$	2.078(2)	O4-Ni1-$O1^{i}$	88.70(8)	N1-Ni1-O4	93.04(9)	
Ni1-N1	2.064(2)	O4-Ni1-O1	91.30(8)	$N1^{i}$-Ni1-$O4^{i}$	93.04(9)	
Ni1-$N1^{i}$	2.064(2)	O4-Ni1-$O4^{i}$	180	$N1^{i}$-Ni1-O4	86.96(9)	
		N1-Ni1-$O1^{i}$	93.42(8)	$N1^{i}$-Ni1-N1	180	
		N1-Ni1-O1	86.58(8)			

Table A2.7 *Selected bond lengths (Å) and angles (°) from structures complex* ***7****.*

7						**Symmetry Codes**
Co1-$O1^{i}$	2.0668(6)	$O1^{i}$-Co1-O1	179.999(3)	O1-Co1-$N3^{i}$	87.53(3)	i = 2-*x*,2-*y*,1-*z*
Co1-O1	2.0669(6)	$O1^{i}$-Co1-$N1^{i}$	95.04(3)	$N1^{i}$-Co1-N1	179.999(1)	
Co1-$N1^{i}$	2.1152(7)	O1-Co1-$N1^{i}$	84.96(3)	N1-Co1-$N3^{i}$	90.01(3)	
Co1-N1	2.1153(8)	$O1^{i}$-Co1-N1	84.96(3)	$N1^{i}$-Co1-$N3^{i}$	89.99(3)	
Co1-$N3^{i}$	2.1202(8)	O1-Co1-N1	95.04(3)	$N1^{i}$-Co1-N3	90.01(3)	
Co1-N3	2.1202(8)	$O1^{i}$-Co1-$N3^{i}$	92.47(3)	N1-Co1-N3	89.99(3)	
		O1-Co1-N3	92.47(3)	$N3^{i}$-Co1-N3	180	
		$O1^{i}$-Co1-N3	87.53(3)			

Table A2.8 *Selected bond lengths (Å) and angles (°) from structures complex* ***8****.*

8						**Symmetry Codes**
Co1-Cl1	2.4793(4)	$Cl1^{i}$-Co1-Cl^{i}	180	$O1^{i}$-Co1-$N1^{i}$	85.98(4)	i = -*x*,1-*y*,1-*z*
Co1-$Cl1^{i}$	2.4793(4)	$O1^{i}$-Co1-Cl^{i}	90.03(3)	O1-Co1-N1	85.98(4)	
Co1-$O1^{i}$	2.0598(9)	O1-Co1-Cl^{i}	89.97(3)	N1-Co1-$Cl1^{i}$	88.75(3)	
Co1-O1	2.0598(9)	O1-Co1-$Cl1^{i}$	90.03(3)	$N1^{i}$-Co1-$Cl1^{i}$	91.25(3)	
Co1-N1	2.1365(10)	$O1^{i}$-Co1-$Cl1^{i}$	89.97(3)	N1-Co1-Cl1	91.25(3)	
Co1-$N1^{i}$	2.1365(10)	$O1^{i}$-Co1-O1	180	$N1^{i}$-Co1-Cl^{i}	88.75(3)	
		O1-Co1-$N1^{i}$	94.02(4)	N1-Co1-$N1^{i}$	180	
		$O1^{i}$-Co1-N1	94.02(4)			

Table A2.9 *Selected bond lengths (Å) and angles (°) from structures complex **9**.*

9						**Symmetry Codes**
Co1-O2	2.0358(13)	O2-Co1-O3	97.72(5)	O3-Co1-N1	96.11(5)	i = 1-*x*,+*y*,1/2-*z*
Co1-O3	2.0563(12)	O2-Co1-O5	173.31(5)	O1-Co1-O5	88.14(5)	
Co1-O5	2.1287(13)	O2-Co1-O1	87.14(5)	O1-Co1-O4	84.60(4)	
Co1-O1	2.1081(12)	O2-Co1-O4	95.13(5)	O4-Co1-O5	89.13(5)	
Co1-O4	2.1272(10)	O2-Co1-N1	92.87(5)	N1-Co1-O5	82.03(5)	
Co1-N1	2.1001(14)	O3-Co1-O5	87.16(5)	N1-Co1-O1	85.37(5)	
$Co1^{i}$-O4	2.1272(10)	O3-Co1-O1	174.83(5)	N1-Co1-O4	166.83(6)	
		O3-Co1-O4	93.17(4)	Co1-O4-$Co1^{i}$	109.86(8)	

Table A2.10 *Selected bond lengths (Å) and angles (°) from structures complex **10.***

10						**Symmetry Codes**
Ni1-O2	2.0127(15)	O2-Ni1-O4	94.76(5)	O3-Ni1-O1	175.31(7)	i = 1-*x*,+*y*,1/2-*z*
Ni1-O4	2.0651(12)	O2-Ni1-O3	96.11(6)	O3-Ni1-N1	94.85(6)	
Ni1-O3	2.0354(14)	O2-Ni1-O5	173.29(5)	O1-Ni1-O4	85.54(5)	
Ni1-O5	2.0872(16)	O2-Ni1-O1	87.94(6)	O1-Ni1-O5	88.49(6)	
Ni1-O1	2.0642(14)	O2-Ni1-N1	91.24(6)	N1-Ni1-O4	170.55(7)	
Ni1-N1	2.0526(15)	O4-Ni1-O5	90.62(6)	N1-Ni1-O5	82.92(6)	
$Ni1^{i}$-O4	2.0650(12)	O3-Ni1-O4	91.76(5)	N1-Ni1-O1	87.40(6)	
		O3-Ni1-O5	87.71(6)	$Ni1^{i}$-O4-Ni1	113.53(10)	

Table A2.11 *Selected bond lengths (Å) and angles (°) from structures complex **11**.*

11						**Symmetry Codes**
						i = -*x*,3-*y*,1-*z*;
$Co2-O2^{i}$	2.0685(14)	$O2^{i}$-Co2-O2	180.00(7)	$Cl3^{ii}$-Co1-Cl3	179.999(2)	ii = 1-*x*,1-*y*,2-*z*
Co2-O2	2.0685(14)	$O2^{i}$-Co2-$O5^{i}$	90.19(6)	O1-Co1-Cl3	91.51(4)	
$Co2-O5^{i}$	2.0833(15)	O2-Co2-$O5^{i}$	89.81(6)	$O1^{ii}$-Co1-Cl3	88.49(4)	
Co2-O5	2.0833(15)	$O2^{i}$-Co2-O5	89.81(6)	$O1^{ii}$-Co1-$Cl3^{ii}$	91.51(4)	
Co2-O4	2.1257(14)	O2-Co2-O5	90.19(6)	O1-Co1-$Cl3^{ii}$	88.49(4)	
$Co2-O4^{i}$	2.1257(14)	O2-Co2-O4	92.65(5)	O1-Co1-$O1^{ii}$	180.00(6)	
$Co1-Cl3^{ii}$	2.4654(5)	$O2^{i}$-Co2-O4	87.35(5)	$O1^{ii}$-Co1-$N1^{ii}$	84.47(6)	
Co1-Cl3	2.4654(5)	O2-Co2-$O4^{i}$	87.35(5)	O1-Co1-N1	84.47(6)	
Co1-O1	2.0648(14)	$O2^{i}$-Co2-$O4^{i}$	92.65(5)	O1-Co1-$N1^{ii}$	95.53(6)	
$Co1-O1^{ii}$	2.0648(14)	$O5^{i}$-Co2-O5	180	$O1^{ii}$-Co1-N1	95.53(6)	
Co1-N1	2.1087(17)	$O5^{i}$-Co2-O4	85.42(6)	N1-Co1-$Cl3^{ii}$	89.03(4)	
$Co1-N1^{ii}$	2.1087(17)	O5-Co2-O4	94.58(6)	$N1^{ii}$-Co1-$Cl3^{ii}$	90.97(4)	
		$O5^{i}$-Co2-$O4^{i}$	94.58(6)	N1-Co1-Cl3	90.97(4)	
		O5-Co2-$O4^{i}$	85.42(6)	$N1^{ii}$-Co1-Cl3	89.03(4)	
		O4-Co2-$O4^{i}$	180	N1-Co1-$N1^{ii}$	180.00(6)	

Table A2.12 *Selected bond lengths (Å) and angles (°) from structures complex* ***12****.*

12						**Symmetry Codes**
Co2-O11	2.081(6)	O11-Co2-O2H	93.8(2)	O1-Co1-N1	86.3(3)	i = 1-*x*,+*y*,1/2-*z*
Co2-O5	2.054(6)	O11-Co2-O1H	98.6(2)	O12-Co1-O1H	94.7(3)	
Co2-O2H	2.093(5)	O11-Co2-O3	88.3(2)	O12-Co1-O3	92.1(2)	
Co2-O1H	2.119(6)	O11-Co2-O1A	177.3(2)	O12-Co1-O13	81.9(3)	
Co2-O3	2.123(6)	O5-Co2-O11	87.9(2)	O12-Co1-N1	92.5(3)	
Co2-O1A	2.1504(11)	O5-Co2-O2H	95.3(2)	O13-Co1-O3	93.5(2)	
Co3-O8	2.075(6)	O5-Co2-O1H	87.8(2)	O13-Co1-N1	91.9(3)	
Co3-O2	2.070(6)	O5-Co2-O3	166.0(2)	N1-Co1-O3	173.3(3)	
Co3-O2H	2.106(6)	O5-Co2-O1A	94.3(3)	O2H-Co1-O6	79.5(2)	
Co3-O6	2.131(6)	O2H-Co2-O1H	167.3(2)	O2H-Co4-O14	172.5(2)	
Co3-O1H^{i}	2.083(6)	O2H-Co2-O3	98.4(2)	O2H-Co4-N3	98.4(2)	
Co3-O1A	2.1788(12)	O2H-Co2-O1A	84.44(19)	O6-Co4-O14	94.2(2)	
Co1-O1H	2.055(6)	O1H-Co2-O3	79.5(2)	O4-Co4-O2H	96.4(2)	
Co1-O1H	2.039(6)	O1H-Co2-O1A	83.1(2)	O4-Co4-O6	91.8(2)	
Co1-O12	2.050(7)	O3-Co2-O1A	90.0(4)	O4-Co4-O14	87.9(2)	
Co1-O3	2.153(6)	O8-Co3-O2H	98.1(2)	O4-Co4-O9	168.3(2)	
Co1-O13	2.148(7)	O8-Co3-O6	88.9(2)	O4-Co4-N3	85.1(2)	
Co1-N1	2.151(8)	O8-Co3-O1H^{1}	94.9(2)	O9-Co4-O2H	95.3(2)	
Co4-O2H	2.079(6)	O8-Co3-O1A	176.1(3)	O9-Co4-O6	89.9(2)	
Co4-O6	2.137(6)	O2-Co3-O8	87.3(2)	O9-Co4-O14	80.4(2)	
Co4-O4	2.057(6)	O2-Co3-O2H	89.9(2)	O9-Co4-N3	93.7(3)	
Co4-O14	2.157(6)	O2-Co3-O6	167.7(2)	N3-Co4-O6	176.0(2)	
Co4-O9	2.075(6)	O2-Co3-O1H^{1}	95.9(2)	N3-Co4-O14	88.1(3)	
Co4-N3	2.135(7)	O2-Co3-O1A	96.3(3)	Co2-O2H-Co3	92.6(2)	
		O2H-Co3-O6	79.0(2)	Co4-O2H-Co2	137.8(3)	
		O2H-Co3-O1A	83.4(2)	Co4-O2H-Co3	96.5(2)	
		O6-Co3-O1A	87.9(3)	Co3-O6-Co4	94.0(2)	
		O1H^{1}-Co3-O2H	165.9(2)	Co3^{1}-O1H-Co2	94.6(2)	
		O1H^{1}-Co3-O6	96.0(2)	Co1-O1H-Co2	95.9(2)	
		O1H^{1}-Co3-O1A	83.22(19)	Co1-O1H-Co3^{1}	137.7(3)	
		O1H-Co1-O3	80.2(2)	Co2-O3-Co1	92.9(2)	
		O1H-Co1-O13	172.9(2)	Co2-O1A-Co2^{1}	178.2(6)	
		O1H-Co1-N1	94.5(3)	Co2-O1A-Co3	89.04(4)	
		O1-Co1-O1H	97.3(2)	Co2^{1}-O1A-Co3	91.05(4)	
		O1-Co1-O12	168.0(3)	Co2-O1A-Co3^{1}	91.05(4)	
		O1-Co1-O3	90.2(2)	Co2^{1}-O1A-Co3^{1}	89.04(4)	
		O1-Co1-O13	86.2(3)	Co3-O1A-Co3^{1}	174.8(6)	

Table A2.13 *Selected bond lengths (Å) and angles (°) from structures complex* ***13****.*

13						**Symmetry Codes**
Cu1-O10	1.964(2)	O10-Cu1-O15	174.91(9)	O12-Cu4-O2A	83.71(8)	
Cu1-O11	1.958(2)	O10-Cu1-N1	88.07(9)	O12-Cu4-O8	88.44(9)	
Cu1-O15	1.966(2)	O10-Cu1-O3A	98.61(8)	O12-Cu4-N5	91.27(9)	
Cu1-N1	2.011(2)	O11-Cu1-O10	90.83(8)	N5-Cu4-O2A	93.65(9)	
Cu1-O3A	2.439(2)	O11-Cu1-O15	89.16(9)	O16-Cu6-N7	166.99(9)	
Cu5-O6	1.9279(19)	O11-Cu1-N1	171.68(10)	O16-Cu6-O1A	99.35(9)	
Cu5-O13	1.933(2)	O11-Cu1-O3A	95.19(8)	O13-Cu6-O16	91.02(8)	
Cu5-N6	1.930(2)	O15-Cu1-N1	91.21(9)	O13-Cu6-O5	178.05(9)	
Cu5-N8	1.936(2)	O15-Cu1-O3A	86.45(8)	O13-Cu6-N7	90.01(9)	
Cu2-O10	1.932(2)	N1-Cu1-O3A	93.14(9)	O13-Cu6-O1A	97.88(9)	
Cu2-O1	1.926(2)	O6-Cu5-O13	168.72(8)	O5-Cu6-O16	88.07(9)	
Cu2-N2	1.936(2)	O6-Cu5-N6	94.68(9)	O5-Cu6-N7	91.26(9)	
Cu2-N4	1.936(2)	O6-Cu5-N8	85.85(9)	O5-Cu6-O1A	80.57(9)	
Cu4-O2A	2.317(2)	O13-Cu5-N8	95.51(9)	N7-Cu6-O1A	93.35(10)	
Cu4-O8	1.978(2)	N6-Cu5-O13	85.48(9)	O1-Cu3-O7	175.32(9)	
Cu4-O6	1.9527(19)	N6-Cu5-N8	172.27(10)	O1-Cu3-N3	88.47(9)	
Cu4-O12	1.956(2)	O10-Cu2-N2	94.80(9)	O1-Cu3-O4A	97.01(10)	
Cu4-N5	2.003(2)	O10-Cu2-N4	85.83(9)	O7-Cu3-N3	90.51(9)	
Cu6-O16	1.977(2)	O1-Cu2-O10	172.14(8)	O7-Cu3-O4A	87.63(10)	
Cu6-O13	1.945(2)	O1-Cu2-N2	85.61(9)	O4-Cu3-O1	90.53(9)	
Cu6-O5	1.960(2)	O1-Cu2-N4	94.85(10)	O4-Cu3-O7	89.76(9)	
Cu6-N7	2.008(2)	N2-Cu2-N4	172.03(10)	O4-Cu3-N3	170.95(10)	
Cu6-O1A	2.402(2)	O8-Cu4-O2A	97.15(9)	O4-Cu3-O4A	93.55(9)	
Cu3-O1	1.973(2)	O8-Cu4-N5	169.10(9)	N3-Cu3-O4A	95.50(10)	
Cu3-O7	1.982(2)	O6-Cu4-O2A	98.16(8)	Cu2-O10-Cu1	102.34(9)	
Cu3-O4	1.936(2)	O6-Cu4-O8	90.90(8)	Cu2-O1-Cu3	103.59(9)	
Cu3-N3	1.983(3)	O6-Cu4-O12	178.09(9)	Cu5-O6-Cu4	104.36(9)	
Cu3-O4A	2.360(2)	O6-Cu4-N5	89.03(9)	Cu5-O13-Cu6	103.54(9)	

Table A2.14 *Selected bond lengths (Å) and angles (°) from structures complex **14**.*

14						**Symmetry Codes**
Fe1-O1A	1.8968(15)	O1A-Fe1-O12	95.61(6)	O15-Fe3-O8	168.61(7)	
Fe1-O12	1.9951(16)	O1A-Fe1-O2B	179.42(6)	O8-Fe3-O3B	84.16(6)	
Fe1-O2B	2.0827(15)	O1A-Fe1-O6	93.61(6)	O17-Fe3-O3	168.23(7)	
Fe1-O6	2.0130(16)	O1A-Fe1-O18	95.63(6)	O17-Fe3-O15	88.79(6)	
Fe1-O18	2.0001(15)	O1A-Fe1-O9	96.26(6)	O17-Fe3-O3B	84.91(6)	
Fe1-O9	1.9808(15)	O12-Fe1-O2B	84.54(6)	O17-Fe3-O8	95.29(6)	
Fe2-O1A	1.8928(12)	O12-Fe1-O6	91.35(7)	O7-Fe4-N1	174.34(7)	
Fe2-O1B	2.0857(15)	O12-Fe1-O18	87.37(6)	O7-Fe3-N3	85.89(7)	
Fe2-O2	2.0164(16)	O6-Fe1-O2B	85.83(6)	O7-Fe3-N5	83.30(7)	
Fe2-O5	2.0272(16)	O18-Fe1-O2B	84.93(6)	O1-Fe4-O7	92.01(6)	
Fe2-O11	2.0095(16)	O18-Fe1-O6	170.75(6)	O1-Fe4-O4	96.19(7)	
Fe2-O14	2.0229(16)	O9-Fe1-O12	168.09(6)	O1-Fe4-N1	82.86(7)	
Fe3-O1A	1.9037(15)	O9-Fe1-O2B	83.60(6)	O1-Fe4-N3	177.89(7)	
Fe3-O3	2.0112(15)	O9-Fe1-O6	88.78(6)	O1-Fe4-N5	86.17(7)	
Fe3-O15	2.0102(15)	O9-Fe1-O18	90.58(6)	O4-Fe4-O7	89.59(6)	
Fe3-O3B	2.0798(16)	O1A-Fe2-O1B	177.99(7)	O4-Fe4-N1	88.59(7)	
Fe3-O8	2.0357(14)	O1A-Fe2-O2	96.10(6)	O4-Fe4-N3	83.88(7)	
Fe3-O17	2.0089(15)	O1A-Fe2-O5	95.57(6)	O4-Fe4-N5	172.59(7)	
Fe4-O7	2.1097(15)	O1A-Fe2-O11	96.47(6)	N1-Fe4-N3	99.24(8)	
Fe4-O1	2.0749(16)	O1A-Fe2-O14	94.80(6)	N1-Fe4-N5	98.68(8)	
Fe4-O4	2.0798(17)	O2-Fe2-O1B	82.03(6)	N5-Fe4-N3	93.51(8)	
Fe4-N1	2.186(2)	O2-Fe2-O5	90.35(6)	O13-Fe5-O16	88.98(7)	
Fe4-N3	2.226(2)	O2-Fe2-O14	87.52(6)	O13-Fe5-O10	92.67(7)	
Fe4-N5	2.206(2)	O5-Fe2-O1B	85.19(6)	O13-Fe5-N9	89.40(8)	
Fe5-O13	2.0478(18)	O11-Fe2-O1B	85.38(6)	O13-Fe5-N11	82.39(8)	
Fe5-O16	2.1040(16)	O11-Fe2-O2	167.34(6)	O13-Fe5-N7	173.50(8)	
Fe5-O10	2.0960(19)	O11-Fe2-O5	89.95(7)	O16-Fe5-N9	83.67(7)	
Fe5-N9	2.201(2)	O11-Fe2-O14	89.91(7)	O16-Fe5-N11	171.37(8)	
Fe5-N11	2.168(2)	O14-Fe2-O1B	84.42(6)	O16-Fe5-N7	85.76(8)	
Fe5-N7	2.195(2)	O14-Fe2-O5	169.58(6)	O10-Fe5-O16	91.44(7)	
		O1A-Fe3-O3	96.68(6)	O10-Fe5-N9	174.66(7)	
		O1A-Fe3-O15	95.88(6)	O10-Fe5-N11	88.71(8)	
		O1A-Fe3-O3B	178.45(6)	O10-Fe5-N7	83.66(8)	
		O1A-Fe3-O8	94.38(6)	N11-Fe5-N9	96.44(8)	
		O1A-Fe3-O17	94.71(6)	N11-Fe5-N7	102.83(9)	
		O3-Fe3-O3B	83.78(6)	N7-Fe5-N9	93.80(9)	
		O3-Fe3-O8	86.80(6)	Fe1-O1A-Fe3	118.67(6)	
		O15-Fe3-O3	87.11(6)	Fe2-O1A-Fe1	120.40(8)	
		O15-Fe3-O3B	85.62(6)	Fe2-O1A-Fe3	120.93(8)	

References

[1] J. M. Lehn, *Angew. Chem. Int. Ed.* **1988**, *27*, 89-112.

[2] J. M. Lehn, *Angew. Chem. Int. Ed.* **1990**, *29*, 1304-1319.

[3] S. R. Batten, S. M. Neville, D. R. Turner, *Coordination Polymers. Design, Analysis and Application*, The Royal Society of Chemistry, **2009**.

[4] J. S. Siegel, *Science* **1996**, *271*, 949-949.

[5] Image credit: http://en.wikipedia.org/wiki/File:Molecular_Knot_RecTravChimPays-Bas_427_1993_commons.jpg, accessed 29/10/2012

[6] C. O. Dietrichbuchecker, J. P. Sauvage, *Angew. Chem. Int. Ed.* **1989**, *28*, 189-192.

[7] E. C. Constable, *Angew. Chem. Int. Ed.* **1991**, *30*.

[8] G. R. Desiraju, *Angew. Chem. Int. Ed.* **1995**, *34*, 2311-2327.

[9] M. Simard, D. Su, J. D. Wuest, *J. Am. Chem. Soc.* **1991**, *113*, 4696-4698.

[10] T. Steiner, *Angew. Chem. Int. Ed.* **2002**, *41*, 48-76.

[11] J. J. Dannenberg, *J. Am. Chem. Soc.* **1998**, *120*, 5604-5604.

[12] P. Metrangolo, H. Neukirch, T. Pilati, G. Resnati, *Acc. Chem. Res.* **2005**, *38*, 386-395.

[13] C. Janiak, *J. Chem. Soc., Dalton Trans.* **2000**, 3885-3896.

[14] Q. Chu, D. C. Swenson, L. R. MacGillivray, *Angew. Chem. Int. Ed.* **2005**, *44*, 3569-3572.

[15] H. Schmidbaur, A. Schier, *Chem. Soc. Rev.* **2008**, *37*, 1931-1951.

[16] C. M. Che, M. C. Tse, M. C. W. Chan, K. K. Cheung, D. L. Phillips, K. H. Leung, *J. Am. Chem. Soc.* **2000**, *122*, 2464-2468.

[17] G. R. Desiraju, *Acc. Chem. Res.* **1991**, *24*, 290-296.

[18] I. Dance, M. Scudder, *Chem. Eur. J.* **1996**, *2*, 481-486.

[19] C. Horn, B. Ali, I. Dance, M. Scudder, D. Craig, *CrystEngComm* **2000**, *2*, 6.

[20] V. Russell, M. Scudder, I. Dance, *J. Chem. Soc., Dalton Trans.* **2001**, 789-799.

[21] Image credit http://www.chem.tamu.edu/rgroup/wheeler/research.php, accessed 29/10/2012

[22] M. Venturi, A. Credi, V. Balzani, *Coord. Chem. Rev.* **1999**, *185–186*, 233-256.

[23] J. Perez, L. Riera, *Chem. Soc. Rev.* **2008**, *37*, 2658-2667.

[24] P. J. Lusby, *Annu. Rep. Prog. Chem. Sect. A: Inorg. Chem.* **2012**, *108*, 292.

[25] J. Brown, *Philos. Trans.* **1724**, *33*, 17-24.

[26] K. Itaya, I. Uchida, V. D. Neff, *Acc. Chem. Res.* **1986**, *19*, 162-168.

[27] H. J. Buser, D. Schwarzenbach, W. Petter, A. Ludi, *Inorg. Chem.* **1977**, *16*, 2704-2710.

[28] H. S. Zhdanov, *Comptes Rendus De L Academie Des Sciences De L Urss* **1941**, *31*, 352-354.

[29] Y. Kinoshita, I. Matsubara, T. Higuchi, Y. Saito, *B. Chem. Soc. Jpn.* **1959**, *32*, 1221-1226.

[30] B. F. Hoskins, R. Robson, *J. Am. Chem. Soc.* **1989**, *111*, 5962-5964.

[31] B. F. Hoskins, R. Robson, *J. Am. Chem. Soc.* **1990**, *112*, 1546-1554.

[32] H. Li, M. Eddaoudi, M. O'Keeffe, O. M. Yaghi, *Nature* **1999**, *402*, 276-279.

[33] H. K. Chae, D. Y. Siberio-Perez, J. Kim, Y. Go, M. Eddaoudi, A. J. Matzger, M. O'Keeffe, O. M. Yaghi, *Nature* **2004**, *427*, 523-527.

[34] Image credit http://www.chem.tamu.edu/rgroup/wheeler/research.php, accessed 24/10/2012

[35] K. Uemura, S. Kitagawa, K. Fukui, K. Saito, *J. Am. Chem. Soc.* **2004**, *126*, 3817-3828.

[36] B. F. Abrahams, B. F. Hoskins, D. M. Michail, R. Robson, *Nature* **1994**, *369*, 727-729.

[37] M. Eddaoudi, H. L. Li, O. M. Yaghi, *J. Am. Chem. Soc.* **2000**, *122*, 1391-1397.

[38] K. Barthelet, J. Marrot, D. Riou, G. Ferey, *Angew. Chem. Int. Ed.* **2002**, *41*, 281-284.

[39] C. Serre, F. Millange, C. Thouvenot, M. Nogues, G. Marsolier, D. Louer, G. Ferey, *J. Am. Chem. Soc.* **2002**, *124*, 13519-13526.

[40] S. Subramanian, M. J. Zaworotko, *Angew. Chem. Int. Ed.* **1995**, *34*, 2127-2129.

[41] S. S. Y. Chui, S. M. F. Lo, J. P. H. Charmant, A. G. Orpen, I. D. Williams, *Science* **1999**, *283*, 1148-1150.

[42] M. Kondo, T. Okubo, A. Asami, S. Noro, T. Yoshitomi, S. Kitagawa, T. Ishii, H. Matsuzaka, K. Seki, *Angew. Chem. Int. Ed.* **1999**, *38*, 140-143.

[43] R. Kitaura, S. Kitagawa, Y. Kubota, T. C. Kobayashi, K. Kindo, Y. Mita, A. Matsuo, M. Kobayashi, H. C. Chang, T. C. Ozawa, M. Suzuki, M. Sakata, M. Takata, *Science* **2002**, *298*, 2358-2361.

[44] M. O'Keeffe, O. M. Yaghi, *Chem. Rev.* **2012**, *112*, 675-702.

[45] N. L. Rosi, M. Eddaoudi, J. Kim, M. O'Keeffe, O. M. Yaghi, *CrystEngComm* **2002**, *4*, 401-404.

[46] C. S. Hawes, *1,2-Diazoles: Versatile Tectons for Metallosupramolecular Assemblies*, PhD Thesis, University of Canterbury, **2012**.

[47] M. Albrecht, *Chem. Rev.* **2001**, *101*, 3457-3497.

[48] C. Piguet, G. Bernardinelli, G. Hopfgartner, *Chem. Rev.* **1997**, *97*, 2005-2062.

[49] M. Fujita, *Acc. Chem. Res.* **1999**, *32*, 53-61.

[50] T. J. Hubin, D. H. Busch, *Coord. Chem. Rev.* **2000**, *200*, 5-52.

[51] M. Weck, B. Mohr, J. P. Sauvage, R. H. Grubbs, *J. Org. Chem.* **1999**, *64*, 5463-5471.

[52] V. Balzani, A. Credi, M. Venturi, *Chem. Soc. Rev.* **2009**, *38*, 1542-1550.

[53] J. P. Collin, C. Dietrich-Buchecker, P. Gavina, M. C. Jimenez-Molero, J. P. Sauvage, *Acc. Chem. Res.* **2001**, *34*, 477-487.

[54] G. A. Breault, C. A. Hunter, P. C. Mayers, *Tetrahedron* **1999**, *55*, 5265-5293.

[55] O. Lukin, F. Vogtle, *Angew. Chem. Int. Ed.* **2005**, *44*, 1456-1477.

[56] F. Li, J. K. Clegg, L. F. Lindoy, R. B. Macquart, G. V. Meehan, *Nature Communications* **2011**, *2*.

[57] M. Fujita, *Chem. Soc. Rev.* **1998**, *27*, 417-425.

[58] M. B. Duriska, S. M. Neville, J. Z. Lu, S. S. Iremonger, J. F. Boas, C. J. Kepert, S. R. Batten, *Angew. Chem. Int. Ed.* **2009**, *48*, 8919-8922.

[59] Y. Inokuma, T. Arai, M. Fujita, *Nat. Chem.* **2010**, *2*, 780-783.

[60] F. Hof, S. L. Craig, C. Nuckolls, J. Rebek, *Angew. Chem. Int. Ed.* **2002**, *41*, 1488-1508.

[61] T. Kusukawa, M. Fujita, *J. Am. Chem. Soc.* **2002**, *124*, 13576-13582.

[62] G. E. Kostakis, S. P. Perlepes, V. A. Blatov, D. M. Proserpio, A. K. Powell, *Coord. Chem. Rev.* **2012**, *256*, 1246-1278.

[63] J. D. Rinehart, J. R. Long, *Chem. Sci.* **2011**, *2*, 2078-2085.

[64] D. G. R. Sessoli, J. Villain, *Molecular Nanomagnets, Vol. 1*, Oxford University Press, Oxford, UK, **2006**.

[65] R. Winpenny, G. Aromi, *Single-Molecule Magnets and Related Phenomena*, Springer, **2006**.

[66] R. Bagai, G. Christou, *Chem. Soc. Rev.* **2009**, *38*, 1011-1026.

[67] D. Gatteschi, R. Sessoli, *Angew. Chem. Int. Ed.* **2003**, *42*, 268-297.

[68] R. Bircher, G. Chaboussant, C. Dobe, H. U. Gudel, S. T. Ochsenbein, A. Sieber, O. Waldmann, *Adv. Funct. Mater.* **2006**, *16*, 209-220.

[69] R. Sessoli, H. L. Tsai, A. R. Schake, S. Y. Wang, J. B. Vincent, K. Folting, D. Gatteschi, G. Christou, D. N. Hendrickson, *J. Am. Chem. Soc.* **1993**, *115*, 1804-1816.

[70] R. Sessoli, D. Gatteschi, A. Caneschi, M. A. Novak, *Nature* **1993**, *365*, 141-143.

[71] B. Hasenknopf, J. M. Lehn, B. O. Kneisel, G. Baum, D. Fenske, *Angew. Chem. Int. Ed.* **1996**, *35*, 1838-1840.

[72] Image credit http://en.wikipedia.org/wiki/File:Supramolecular_Assembly_Lehn.jpg, accessed 25/10/2012

[73] T. Gunnlaugsson, M. Glynn, G. M. Tocci, P. E. Kruger, F. M. Pfeffer, *Coord. Chem. Rev.* **2006**, *250*, 3094-3117.

[74] P. D. Beer, P. A. Gale, *Angew. Chem. Int. Ed.* **2001**, *40*, 486-516.

[75] B. E. Collins, E. V. Anslyn, *Chem. Eur. J.* **2007**, *13*, 4700-4708.

[76] E. B. Veale, D. O. Frimannsson, M. Lawler, T. Gunnlaugsson, *Org. Lett.* **2009**, *11*, 4040-4043.

[77] P. Mal, B. Breiner, K. Rissanen, J. R. Nitschke, *Science* **2009**, *324*, 1697-1699.

[78] Image credit http://www.ch.cam.ac.uk/group/nitschke/research/cages, accessed 25/10/2012

[79] J. N. van Niekerk, F. R. L. Schoening, *Acta Crystallogr.* **1953**, *6*, 227-232.

[80] R. Maurice, K. Sivalingam, D. Ganyushin, N. Guihéry, C. de Graaf, F. Neese, *Inorg. Chem.* **2011**, *50*, 6229-6236.

[81] S. Akine, W. Dong, T. Nabeshima, *Inorg. Chem.* **2006**, *45*, 4677-4684.

[82] P. E. Kruger, G. D. Fallon, B. Moubaraki, K. J. Berry, K. S. Murray, *Inorg. Chem.* **1995**, *34*, 4808-4814.

[83] X. Bao, J. D. Leng, Z. S. Meng, Z. J. Lin, M. L. Tong, M. Nihei, H. Oshio, *Chem. Eur. J.* **2010**, *16*, 6169-6174.

[84] C. Boskovic, G. Labat, A. Neels, H. U. Gudel, *Dalton Trans.* **2003**, 3671-3672.

[85] A. F. Orchard, *Magnetochemistry*, Oxford University Press, Oxford, **2007**.

[86] A. W. Ferguson, *The Synthesis and Characterisation of Single Molecule Magnets*, PhD Thesis, University of Glasgow, **2007**.

[87] B. C. Guha, *Proc. R. Soc. London, Ser. A* **1951**, *206*, 353-373.

[88] B. Bleaney, K. D. Bowers, *Proc. R. Soc. London, Ser. A* **1952**, *214*, 451-465.

[89] M. Gerloch, J. H. Harding, *Proc. R. Soc. London, Ser. A* **1978**, *360*, 211-227.

[90] A. Ozarowski, *Inorg. Chem.* **2008**, *47*, 9760-9762.

[91] O. Kahn, *Molecular Magnetism*, John Wiley & Sons, **1993**.

[92] C. M. Fitchett, P. J. Steel, *Polyhedron* **2007**, *26*, 400-405.

[93] P. Iliopoulos, G. D. Fallon, K. S. Murray, *J. Chem. Soc., Dalton Trans.* **1986**, 437.

[94] W. B. Blanton, S. W. Gordon-Wylie, G. R. Clark, K. D. Jordan, J. T. Wood, U. Geiser, T. J. Collins, *J. Am. Chem. Soc.* **1999**, *121*, 3551-3552.

[95] V. Maurizot, G. Linti, I. Huc, *Chem. Commun.* **2004**, 924-925.

[96] K. Rudzka, M. M. Makowska-Grzyska, E. Szajna, A. M. Arif, L. M. Berreau, *Chem. Commun.* **2005**, 489-491.

[97] Y. Sun, Z. Zhang, X. Wang, X. Li, L. Weng, X. Zhou, *Dalton Trans.* **2010**, 221-226.

[98] H. Hou, Y. Wei, Y. Song, L. Mi, M. Tang, L. Li, Y. Fan, *Angew. Chem. Int. Ed.* **2005**, *44*, 6067-6074.

[99] M. Y. Huang, C. Y. Yeh, G. H. Lee, S. M. Peng, *Dalton Trans.* **2006**, 5683-5690.

[100] A. Mishra, A. Ali, S. Upreti, M. S. Whittingham, R. Gupta, *Inorg. Chem.* **2009**, *48*, 5234-5243.

[101] A. T. Vallina, H. Stoeckli-Evans, A. Neels, J. Ensling, S. Decurtins, *Inorg. Chem.* **2003**, *42*, 3374-3382.

[102] A. P. Singh, G. Kumar, R. Gupta, *Dalton Trans.* **2011**, *40*, 12454-12461.

[103] D. K. Kumar, A. Das, P. Dastidar, *CrystEngComm* **2007**, *9*, 548.

[104] F. Pan, J. Wu, H. Hou, Y. Fan, *Cryst. Growth Des.* **2010**, *10*, 3835-3837.

[105] F. Pointillart, T. Cauchy, Y. Le Gal, S. Golhen, O. Cador, L. Ouahab, *Inorg. Chem.* **2010**, *49*, 1947-1960.

[106] T. M. Ross, S. M. Neville, D. S. Innes, D. R. Turner, B. Moubaraki, K. S. Murray, *Dalton Trans.* **2010**, 149-159.

[107] Y. Gong, Y. Zhou, J. Li, R. Cao, J. Qin, *Dalton Trans.* **2010**, *39*, 9923-9928.

[108] S. Su, Z. Guo, G. Li, R. Deng, S. Song, C. Qin, C. Pan, H. Guo, F. Cao, S. Wang, H. Zhang, *Dalton Trans.* **2010**, *39*, 9123-9130.

[109] M.-L. Hu, A. Morsali, L. Aboutorabi, *Coord. Chem. Rev.* **2011**, *255*, 2821-2859.

[110] S. J. Wezenberg, G. Salassa, E. C. Escudero-Adan, J. Benet-Buchholz, A. W. Kleij, *Angew. Chem. Int. Ed.* **2011**, *50*, 713-716.

[111] C. Chen, Q. Zhang, J. Jiang, Q. Wang, C. Su, *Aust. J. Chem.* **2005**, *58*, 115-118.

[112] E. E. Moushi, T. C. Stamatatos, V. Nastopoulos, G. Christou, A. J. Tasiopoulos, *Polyhedron* **2009**, *28*, 1814-1817.

[113] D. Sun, R. Cao, W. Bi, J. Weng, M. Hong, Y. Liang, *Inorg. Chim. Acta* **2004**, *357*, 991-1001.

[114] X. J. Li, R. Cao, Y. Q. Sun, W. H. Bi, X. Li, Y. Q. Wang, *Eur. J. Inorg. Chem.* **2005**, 321-329.

[115] C.-F. Wang, *Acta Crystallogr. Sect. E: Struct. Rep. Online* **2009**, *65*, o1244.

[116] J. Wu, L. Tang, K. Chen, L. Yan, F. Li, Y. Wang, *J. Colloid Interface Sci.* **2007**, *307*, 280-287.

[117] N. V. Kolotova, A. V. Dolzhenko, V. O. Koz'minykh, V. P. Kotegov, A. T. Godina, *Pharm. Chem. J.* **1999**, *33*, 635-637.

[118] M. Habash, M. O. Taha, *Bioorg. Med. Chem.* **2011**, *19*, 4746-4771.

[119] A. Nisonoff, D. Pressman, *J. Am. Chem. Soc.* **1957**, *79*, 5565-5572.

[120] H. Kato, S. Satomura, Wako Pure Chem Ind Ltd, Japan . **1994**, p. 19 pp.

[121] H. Kato, N. Yamamoto, S. Satomura, T. Tanaka, Wako Pure Chem. Ind. Ltd., Japan . **1994**, p. 13 pp.

[122] J. Wu, L. Tang, K. Chen, L. Yan, F. Li, Y. Wang, *J. Colloid Interface Sci.* **2007**, *307*, 280-287.

[123] Y. J. Wang, L. Yan, L. M. Tang, J. Yu, *Chin. Chem. Lett.* **2007**, *18*, 1009-1012.

[124] B. S. Garg, V. Kumar, M. J. Reddy, *Transition Met. Chem.* **1993**, *18*, 364-368.

[125] B. S. Garg, M. J. Reddy, V. Kumar, *J. Coord. Chem.* **1993**, *29*, 33-43.

[126] B. S. Garg, V. Kumar, M. J. Reddy, *Indian J. Chem. A.* **1993**, *32A*, 726-729.

[127] B. S. Garg, V. Kumar, M. J. Reddy, *Indian J. Chem. A.* **1996**, *35A*, 598-600.

[128] B. S. Garg, R. K. Sharma, R. Shrestha, S. Mittal, M. Sarbhai, *Indian J. Chem. A.* **2002**, *41A*, 1625-1628.

[129] X. Shen, B. Kang, Y. Tong, X. Shi, Y. Li, X. Huang, *J. Coord. Chem.* **1998**, *46*, 105-114.

[130] D. H. Williams, I. Fleming, *Spectroscopic methods in organic chemistry*, McGraw-Hill, **1987**.

[131] J. Echeverria, E. Cremades, A. J. Amoroso, S. Alvarez, *Chem. Commun.* **2009**, 4242-4244.

[132] E. Teller, *Proceedings. Mathematical, Physical and Engineering Sciences* **1937**, *161*, 220-235.

[133] X.-N. Cheng, W. Xue, J.-B. Lin, X.-M. Chen, *Chem. Commun.* **2010**, *46*, 246-248.

[134] E. Fursova, O. Kuznetsova, V. Ovcharenko, G. Romanenko, V. Ikorskii, I. Eremenko, A. Sidorov, *Polyhedron* **2007**, *26*, 2079-2088.

[135] L. Wang, Y. Li, Y. Peng, Z. Q. Liang, J. H. Yu, R. R. Xu, *Dalton Trans.* **2012**, *41*, 6242-6246.

[136] N. Berg, S. M. Taylor, A. Prescimone, E. K. Brechin, L. F. Jones, *CrystEngComm* **2012**, *14*, 2732-2738.

[137] E. Amadei, E. H. Alilou, F. Eydoux, M. Pierrot, M. Reglier, B. Waegell, *J. Chem. Soc., Chem. Commun.* **1992**, 1782-1784.

[138] A. W. Addison, T. N. Rao, J. Reedijk, J. van Rijn, G. C. Verschoor, *J. Chem. Soc., Dalton Trans.* **1984**, 1349.

[139] L. Yang, D. R. Powell, R. P. Houser, *Dalton Trans.* **2007**, 955-964.

[140] N. F. Chilton, unpublished, **2012**.

[141] T. C. Stamatatos, G. C. Vlahopoulou, C. P. Raptopoulou, A. Terzis, A. Escuer, S. P. Perlepes, *Inorg. Chem.* **2009**, *48*, 4610-4612.

[142] X. L. Wang, Y. F. Wang, G. C. Liu, A. X. Tian, J. W. Zhang, H. Y. Lin, *Dalton Trans.* **2011**, *40*, 9299-9305.

[143] H. X. Yang, S. P. Guo, J. Tao, J. X. Lin, R. Cao, *Cryst. Growth Des.* **2009**, *9*, 4735-4744.

[144] X. Y. Jiang, X. Y. Wu, R. M. Yu, D. Q. Yuan, W. Z. Chen, *Inorg. Chem. Commun.* **2011**, *14*, 1546-1549.

[145] P. Vandersluis, A. L. Spek, *Acta Crystallogr., Sect. A*, **1990**, *46*, 194-201.

[146] A. L. Spek, *J. Appl. Crystallogr.* **2003**, *36*, 7-13.

[147] X. Bao, J. D. Leng, Z. S. Meng, Z. J. Lin, M. L. Tong, M. Nihei, H. Oshio, *Chem-Eur. J.* **2010**, *16*, 6169-6174.

[148] W. Schmitt, L. Zhang, C. E. Anson, A. K. Powell, *Dalton Trans.* **2010**, *39*, 10279-10285.

[149] J. Tabernor, L. F. Jones, S. L. Heath, C. Muryn, G. Aromi, J. Ribas, E. K. Brechin, D. Collison, *Dalton Trans.* **2004**, 975-976.

[150] V. Psycharis, C. P. Raptopoulou, A. K. Boudalis, Y. Sanakis, M. Fardis, G. Diamantopoulos, G. Papavassiliou, *Eur. J. Inorg. Chem.* **2006**, *2006*, 3710-3723.

[151] V. Rabe, W. Frey, A. Baro, S. Laschat, M. Bauer, H. Bertagnolli, S. Rajagopalan, T. Asthalter, E. Roduner, H. Dilger, T. Glaser, D. Schnieders, *Eur. J. Inorg. Chem.* **2009**, 4660-4674.

[152] G. M. Sheldrick, *Acta Crystallogr., Sect. A*, **2008**, *64*, 112-122.

[153] G. M. Sheldrick, SHELXL-97, Programs for X-ray Crystal Structure Refinement, 1997, p. University of Gottingen.

[154] O. V. Dolomanov, L. J. Bourhis, R. J. Gildea, J. A. K. Howard, H. Puschmann, *J. Appl. Crystallogr.* **2009**, *42*, 339-341.